HEAT CAPACITY MAPPING MISSION

NASA INVESTIGATION HCM-034

(E82-10300) THERMAL MAPPING, GEOTHERMAL SOURCE LOCATION, NATURAL EFFLUENTS AND PLANT STRESS IN THE MEDITERRANEAN COAST OF SPAIN Final Report, Sep. 1978 - Aug. 1980 (Instituto Geografico Nacional) 218 p
N82-24576
HC A10/MF A01
Unclas
G3/43 00300

THERMAL MAPPING, GEOTHERMAL SOURCE LOCATION, NATURAL EFFLUENTS AND PLANT STRESS IN THE MEDITERRANEAN COAST OF SPAIN

FINAL REPORT

MARCH 31, 1981

COORDINATOR: Antonio Martínez de Aragón
Instituto Geográfico Nacional
General Ibáñez de Ibero, 3
Madrid-3. Spain

PREPARED FOR: Goddard Space Flight Center
Greenbelt, Maryland 20771. USA

PRINCIPAL INVESTIGATOR: Dr. Ing. Rodolfo Núñez de las Cuevas
AGENCY: Instituto Geográfico Nacional
General Ibáñez de Ibero, 3. Madrid-3. E SPAIN

HEAT CAPACITY MAPPING MISSION

NASA INVESTIGATION HCM-034

THERMAL MAPPING, GEOTHERMAL SOURCE LOCATION, NATURAL EFFLUENTS AND PLANT STRESS IN THE MEDITERRANEAN COAST OF SPAIN

FINAL REPORT

MARCH 31, 1981

COORDINATOR: Antonio Martínez de Aragón
Instituto Geográfico Nacional
General Ibáñez de Ibero, 3
Madrid-3. Spain

PREPARED FOR: Goddard Space Flight Center
Greenbelt, Maryland 20771. USA

PRINCIPAL INVESTIGATOR: Dr. Ing. Rodolfo Núñez de las Cuevas
AGENCY: Instituto Geográfico Nacional
General Ibáñez de Ibero, 3. Madrid-3. SPAIN

TECHNICAL REPORT STANDARD TITLE PAGE

1 Report No. HCM-034 Final Report	3 Recipient's Catalog No.
4 Title and Subtitle: Thermal Mapping, Geothermal Source Location, Natural Effluents and Plant Stress in the Mediterranean Coast of Spain.	5 Report Date: March 31, 1931
7 Author(s): Coordinator: Antonio Martínez de Aragón Principal Invest: R. Núñez de las Cuevas, And All.	6 Performing Organization Code 8 Performing Organization Report No.
9 Performing Organization Name and Address: Instituto Geográfico Nacional, General Ibáñez de Ibero 3, Madrid-3.	10 Work Unit No. 11 Contract or Grant No. NASA Investigation HCM-034
12 Sponsoring Agency Name and Address: Goddard Space Flight Center, Missions Investigation Office, Heat Capacity Mapping Mission, Greenbelt, Maryland 20771 USA	13 Type of Report and Period Covered: Final Report. September 1973 to August 30 14 Sponsoring Agency Code

15 Supplementary Notes: Prepared in cooperation with UAM-IBM Scientific Center, Instituto de Edafología y Biología Vegetal (CSIC), Instituto Español de Oceanografía, Departamento de Física Fundamental (U.de Valencia) Departamento de Estratigrafía (U,C. de Madrid)Servicio de Fotogrametría

16 Abstract

This report presents the joint work of different groups, in their respective fields, with one common objective: the evaluation of HCMM data over a complex and well known area in Eastern Spain.This work has been performed for NASA/Goddard Space Flight Center, as NASA Investigation HCM-034.Areas covered in this Report are Image Analysis, Image Preprocessing and Processing, Thermology, Geology, Edaphology, Agriculture, Oceanography, Hydrology and Pattern Recognition.

The fields where HCMM data have proved most useful are the study of macrostructures in Geology and the analysis of marine currents, layers and areas (although in these latter fields, other satellites, such as Nimbus 7 provide more data).The upper scale to work with HCMM data as a whole, appears to be 1:2.000.000.

The results achieved are documented, including suggestions for improvements that will lead to better results in geographic areas similar to the one analyzed.Other less restrictive zones, contiguous to the test-area have been studied, thus allowing for the comparison of constraints and their origin (HCMR, orbit, or characteristics of the geographical area).

17 Key Words (Selected by Author(s)): HCMM Satellite Data Analysis, Image Analysis, Image Interpretation, Image Processing, Thermology, Geology, Oceanography, Edaphology, Agriculture, Hydrology, Pattern Recog.	18 Distribution Statement		
19 Security Classif. (of this report)	20 Security Classif. (of this page)	21 No. of Pages: 217	22 Price*

*For sale by the Clearinghouse for Federal Scientific and Technical Information, Springfield, Virginia 22151.

PREFACE

This report presents the joint work of different groups, in their respective fields, with one common objective: the evaluation of HCMM data over a complex and well known area in Eastern Spain.

This work has been performed for NASA/Goddard Space Flight Center, as NASA Investigation HCM-034.

Areas covered in this Report are Image Analysis, Image Preprocessing and Processing, Thermology (on this subject, a M.Sc. dissertation has been presented), Geology, Edaphology, Agriculture, Oceanography, Hydrology and Pattern Recognition.

The fields where HCMM data have proved most useful are the study of macrostructures in Geology; and the analysis of marine currents, layers and areas (although in these latter fields, other satellites, such as NImbus-7 provide more data).

The upper scale to work with HCMM data as a whole, appears to be 1:2.000.000.Since the basic information in Spain is given in scales of 1:1.000.000 or greater, fields like Land-Use analysis have not been considered of primary interest in this research.

The results achieved are documented, including suggestions for improvements that will lead to better results in geographic areas similar to the one analyzed.

Other less restrictive zones, contiguous to the test-area have been studied, thus allowing for the comparison of constraints and their origin (HCMR, orbit, or characterisctics of the geographical area).

Antonio Martínez de Aragón

HCMM-034 COORDINATOR

"THERMAL MAPPING, GEOTHERMAL SOURCE LOCATION, NATURAL EFFLUENTS AND PLANT STRESS IN THE MEDITERRANEAN COAST OF SPAIN"

FINAL REPORT

TABLE OF CONTENTS

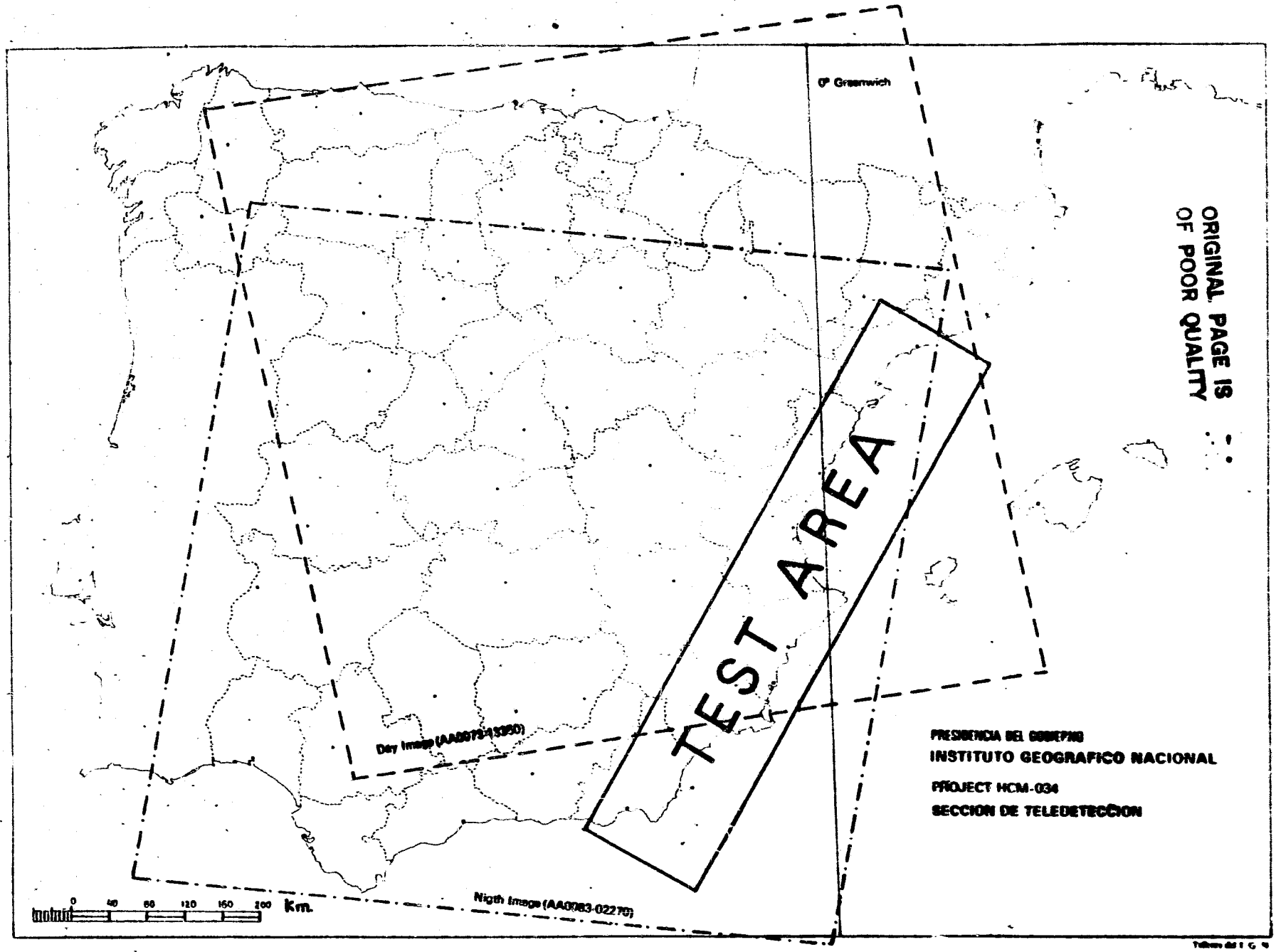

HCM-034

"THERMAL MAPPING, GEOTHERMAL SOURCE LOCATION, NATURAL EFFLUENTS AND PLANT STRESS IN THE MEDITERRANEAN COAST OF SPAIN".

LIST OF COINVESTIGATORS

INSTITUTO GEOGRAFICO NACIONAL

Sección de Teledetección
Gral. Ibáñez de Ibero 3
Madrid-3

- ANTONIO MARTINEZ DE ARAGON
- RAMON LOPEZ MUÑIZ
- RAMON BERMUDEZ DE CASTRO (under contract)

CENTRO DE INVESTIGACION UAM-IBM

Pabellón C-XVI
Universidad Autónoma de Madrid
Cantoblanco

- ALEJANDRO GARCIA
- FORTUNATO ORTI

FACULTAD DE CIENCIAS GEOLOGICAS

Departemento de Estratigrafía y Geología Histórica
Universidad Complutense
Ciudad Universitaria
Madrid-3

- PEDRO HERRANZ ARAUJO

INSTITUTO DE EDAFOLOGIA Y BIOLOGIA VEGETAL

Consejo Superior de Investigaciones Científicas
Serrano 115, dpd°.
Madrid-6

- JOSE LUIS LABRANDERO

INSTITUTO ESPAÑOL DE OCEANOGRAFIA

Alcalá 27
Madrid-14

- GREGORIO PARRILLA

FACULTAD DE CIENCIAS FISICAS

Departamento de Termología
Universidad de Valencia
Doctor Moliner 3
Burjasot (Valencia)

- JOAQUIN MELIA MIRALLES
- VICENTE CASELLES MIRALLES

SERVICIO DE FOTOGRAMETRIA Y FOTOINTERPRETACION

ETS Ingenieros Geógrafos
Universidad Politécnica de Madrid
Ciudad Universitaria
Madrid-3

- FERNANDO LOPEZ DE SAGREDO
- AMALIO DE JUANA

CENTRO DE ESTUDIOS HIDROGRAFICOS

Ministerio de Obras Públicas y Urbanismo
Paseo Vírgen del Puerto 3
Madrid-5

- JESUS PAREDES PERLADO

I N T R O D U C T I O N

A.- INTRODUCTION

- "Analysis of HCMM Data and its Noises"
  Antonio Martínez de Aragón
  Instituto Geográfico Nacional

ANALYSIS OF HCMM DATA AND ITS NOISES

Antonio Martínez de Aragón
Sección de Teledetección
Instituto Geográfico Nacional

INTRODUCTION

For project HCM-034 "Thermal Mapping, Geothermal Source Location, Natural Effluents and Plant Stress in the Mediterranean Coast of Spain", the Remote Sensing Department at the National Geographical Institute (IGN) acted as coinvestigator as well as coordinator of all the research effort performed with HCMM data delivered by NASA.

Here we will consider two different aspects of such data.
First, the data flow from NASA to IGN and the processes acting on these data prior to delivering them to the coinvestigators.
Second, a general analysis on the quality of the data and the factors that may have affected its degradation.

A.- HCMM DATA MANAGEMENT

Reception of HCMM data at IGN

The IGN received as Standing Order one (1) positive transparency of each HCMM image over the test area (Eastern Spain), with 30 % cloud cover or less; yet images with more than 60 % have been received.

The test area and the surface covered by typical day and night images are shown in page vi, test area location outline.
It should be noted that the South-East corner of the test area appeared in some cases in the lower frame.So, we have received a good collection of images from the Desert of Sahara.

The flow of data from NASA to IGN is detailed in Table 1.

TABLE 1.

HCM-034 DATA FLOW.

Positive Transparencies received at IGN from NASA IPF.

Year	Month	Number.	% (acumulated)	Notes
1978	Sept.	2(Sample)	0,4	
"	Oct.	0		
"	Nov.	6	1,7	
"	Dec.	0		
1979	Jan.	0		
"	Feb.	11	4,0	
"	March	8	5,8	
"	April	8	7,5	
"	May	12	10,0	First year's operation of the satellite(only data from thise period were sent to IGN).
"	June	16	13,4	
"	July	8	15,1	
"	August	14	18,1	First Progress Report
"	September	32	24,9	
"	October	31	31,6	
"	November	16	35,0	
"	December	4	35,8	Second Progress Report
1980	January	32	42,6	
"	February	39	51,0	
"	March	3	51,6	
"	April	3	52,2	Third Progress Report (Extension
"	May	53	63,5	NASA informs that all data have been shipped. Registered data may be ordered.
"	June	95	83,8	NASA extends HCMM-034 to March 1981 (5 months)
"	July	0		
"	August	0		Fourth Progress Report(extension
"	September	0		HCMM Satellite is retired
"	October	76	100	
Total		469		

Note. of the above positives, some are repeated; others are of low quality, "Non-Standard image", but no standard replacement was received.

The irregularities in the reception of the images are readily apparent.- Until September 1979 only 19 % of the images were received (The First Progress Report was due August, 31). In May and June 1981, 32 % of the images were received, when supposedly the research phase was over! As late as October 1980, 76 images were received.Thus, it was almost impossible to make use of 50 % of the data (those received after March 1980). The mean delay was one and a half year!

It should be said that the images received were not in the same order they were gathered, and until April 1980 only six 1979 images were received.

Images received are detailed in Table 2.Only the images that cover the test area have been included.Since about 100 images have been received two times or more, the totals from both tables are different.

- In Project HCM-034 it was planned to work with the CCT'S, so as to deliver to the coinvestigators, enhanced, filtered and processed data according to each one's specific needs.

  Since: a) there was such an extended delay in the reception of the standing order data (until September 1979 data didn't begin to be received regularly),

  b) time was needed to reproduce and analyze the images,

  c) the time that passed between the ordering of a CCT and its receipt exceeded 2 months, and

  d) originally the Draft Final Report was due July 1980,

  the above mentioned approach proved to be very time consuming, thus being reduced to a minimum.

- Anyway, 33 CCT'S were ordered from the images received before January 1980 (See Table 3), limit date in order to have time for the processing of the CCT'S and distribution of the resulting images and data on one hand, and to analyze them and include the results in the Draft Final Report (July 1980 without extension), on the other.

TABLE 2.

IMAGES RECEIVED AT IGN FOR HCM-034 PROJECT.

11-05-78	A0015-13500	(1,2)	
"	" 13510	(1,2)	
19-05-78	A0023-02100	(3)	
20-05-78	A0024-13200	(1,2)	
21-05-78	A0025-13380	(1,2)	
26-05-78	A0030-02400	(3)	
"	" 13310	(1,2)	
27-05-78	A0031-13510	(1,2)	
30-05-78	A0034-02140	(3)	
"	" 02144	(3)	
"	" 13090	(1,2)	
31-05-78	A0035-02330	(3)	
"	" "	(3)	
"	" 02320	(3)	
"	" 02310	(3)	
01-06-78	A0036-13440	(1,2)	C. N35-55/W002-38
"	" "	(1,2)	C. N38-35/W003-23
"	" 13444	(1)	
"	" 13460	(1,2)	
04-06-78	A0039-02090	(3)	
"	" 13020	(1,2)	
11-06-78	A0046-13310	(1,2)	
15-06-78	A0050-02140	(3)	
16-06-78	A0051-02320	(3)	
17-06-78	A0052-13430	(1,2)	
20-06-78	A0055-02070	(3)	C. N39-49/E002-30
"	" "	(3)	C. N40-48/E002-47
"	" "	(3)	C. N40-34/E002-43
"	" "	(3)	
"	" 02080	(3)	
"	" "	(3)	
"	" 02090	(3)	
"	" 01300	(1,2)	
"	" 02000	(3)	
21-06-78	A0056-02240	(3)	
22-06-78	A0057-13350	(1,2)	
"	" 13370	(1,2)	
26-06-78	A0061-02190	(3)	
"	" 13110	(1,2)	

FOLDOUT FRAME

ORIGINAL PAGE IS OF POOR QUALITY

16-06-78	A0051-02320	(3)	
17-06-78	A0052-13430	(1,2)	
20-06-78	A0055-02070	(3)	C. N39-49/E002-30
"	" "	(3)	C. N40-48/E002-47
"	" "	(3)	C. N40-34/E002-43
"	" "	(3)	
"	" 02080	(3)	
"	" "	(3)	
"	" 02090	(3)	
"	" 01300	(1,2)	
"	" 02000	(3)	
21-06-78	A0056-02240	(3)	
22-06-78	A0057-13350	(1,2)	
"	" 13370	(1,2)	
26-06-78	A0061-02190	(3)	
"	" 13110	(1,2)	
28-06-78	A0063-13400	(1,2)	
01-07-78	A0066-13050	(1,2)	
02-07-78	A0067-02280	(3)	
"	" 02300	(3)	
06-07-78	A0071-02040	(3)	
"	" 02060	(3)	
"	" 12590	(1,2)	
07-07-78	A0072-02230	(3)	
"	" 13150	(1,2)	
"	" 02240	(3)	
"	" 13170	(1,2)	
08-07-78	A0073-13330	(1,2)	
"	" 13350	(1,2)	
11-07-78	A0076-01570	(3)	
"	" 01590	(3)	C. N36-53/E003-10
"	" "	(3)	C. N34-16/E002-20
"	" 01680	(3)	
12-07-78	A0077-01760	(3)	
"	" 02180	(3)	

NOLDOUT FRAME 2

13-07-78	A0078-02340	(3)
16-07-78	A0081-01510	(3)
17-07-78	A0082-02090	(3)
"	A0082-13020	(1,2)
18-07-78	A0083-02270	(3)
22-07-78	A0087-02020	(3)
"	" 02030	(3)
23-07-78	A0088-02200	(3)
"	" 02220	(3)
27-07-78	A0092-01560	(3)
28-07-78	A0093-13060	(1,2)
"	" 13070	(1,2)
"	" 02130	(3)
29-07-78	A0094-13230	(1,2)
"	" 13250	(1,2)
30-07-78	A0095-13420	(1,2)
03-08-78	A0099-02240	(3)
08-08-78	A0104-13100	(1,2)
09-08-78	A0105-02360	(3)
"	" 02340	(3)
13-08-78	A0109-02100	(3)
"	" 02000	(3)
14-08-78	A0110-13210	(1,2)
"	" 02270	(3)
18-08-78	A0114-12570	(1,2)
19-08-78	A0115-02200	(3)
"	" 02220	(3)
20-08-78	A0116-13300	(1,2)
"	" 13320	(1,2)
23-08-78	A0119-01560	(3)
"	" 01540	(3)
24-08-78	A0120-13060	(1,2)
"	" 02120	(3)
"	" 02140	(3)
25-08-78	A0121-02310	(3)
"	A0121-13230	(1,2)
"	" 13240	(1,2)
26-08-78	A0122-13420	(1,2)
29-08-78	A0125-02070	(3)
30-08-78	A0126-13170	(1,2)
"	" 13180	(1,2)
"	" 02250	(3)
31-08-78	A0127-13340	(1,2)
"	" 13360	(1,2)
03-09-78	A0130-12550	(1)
"	" 12540	(1,2)
"	" 01590	(3)
04-09-78	A0131-13110	(1,2)
05-09-78	A0132-13280	(1,2)
08-09-78	A0135-01550	(3)
"	" 12490	(1,2)
09-09-78	A0136-02120	(3)
"	" 02140	(3)
"	" 13050	(1,2)
10-09-78	A0137-02310	(3)
"	" 13220	(1,2)
"	" 13240	(1,2)

14-09-78	A0141-12580	(1,2)	
"	" 13000	(1,2)	C. N42-15/E003-00
"	" "	(1,2)	C. N42-07/E003-02
"	" 02050	(3)	
"	" 02070	(3)	
15-09-78	A0142-02240	(3)	C.N39-53/W004-38
"	" "	(3)	C.N39-46/W004-40
"	" 13180	(1,2)	
19-09-78	A0146-02000	(3)	
21-09-78	A0148-13300	(1,2)	
"	" 13280	(1,2)	
24-09-78	A0151-12460	(1,2)	
25-09-78	A0152-02100	(3)	
"	" 02120	(3)	
26-09-78	A0153-13240	(1,2)	
"	A0153-13220	(1,2)	
29-09-78	A0156-01480	(3)	
30-09-78	A0157-02050	(3)	
"	" 02040	(3)	
"	" 02050	(3)	
05-10-78	A0162-12520	(1,2)	
10-10-78	A0167-12450	(1,2)	
11-10-78	A0168-13010	(1,2)	
"	" 13030	(1,2)	
"	" 02080	(3)	
12-10-78	A0169-13190	(1,2)	
16-10-78	A0173-12550	(1,2)	
18-10-78	A0175-13310	(1,2)	
22-10-78	A0179-13050	(1,2)	
"	" 13060	(1,2)	
27-10-78	A0184-12570	(3)	- Wrong annotation (it's day IR
"	" 12590	(1,2)	
"	" 12580	(1,2)	
"	" 12590	(3)	- " " " "
28-10-78	A0185-13160	(1,2)	
"	" 13180	(1,2)	
29-10-78	A0186-13330	(1,2)	
"	" 13340	(1,2)	
31-10-78	A0188-01390	(3)	
"	" 01410	(3)	
01-11-78	A0189-02000	(3)	
"	" 01580	(3)	
"	" 12500	(1,2)	
"	" 12520	(1,2)	
02-11-78	A0190-13090	(1,2)	
"	" 13080	(1,2)	
03-11-78	A0191-13250	(1,2)	
"	A0191-13270	(1,2)	
06-11-78	A0194-12450	(1,2)	
12-11-78	A0200-02010	(3)	
"	" 12540	(1,2)	
"	" 12550	(1,2)	

13-11-78	A0220-02190	(3)
"	02211	(3)
14-11-78	A0202-13300	(1,2)
"	" 13310	(1,2)
16-11-78	A0204-01360	(3)
"	" 01380	(3)
17-11-78	A0205-01570	(3)
"	A0205-01550	(3)
21-11-78	A0209-01310	(3)
22-11-78	A0210-01480	(3)
"	" 01500	(3)
23-11-78	A0211-02080	(3)
"	" 02090	(3)
"	" 02080	(3)
28-11-78	A0216-02020	(3)
29-11-78	A0217-02220	(3)
30-11-78	A0218-13290	(1,2)
08-12-78	A0226-01500	(3)
"	" 01520	(3)
09-12-78	A0227-12590	(1,2)
"	" 13010	(1,2)
10-12-78	A0228-13170	(1,2)
13-12-78	A0231-12350	(1,2)
14-12-78	A0232-12540	(1,2)
15-12-78	A0233-13100	(1,2)
25-12-78	A0243-12500	(1,2)
"	" 02040	(3)
26-12-78	A0244-13150	(1,2)
30-12-78	A0248-12500	(1,2)
31-12-78	A0249-13080	(1)
"	" 13080	(2)
14-01-79	A0263-01370	(3)
15-01-79	A0264-01550	(3)
"	" 01530	(3)
16-01-79	A0265-02110	(3)
"	" 02120	(3)
26-01-79	A0275-12520	(1,2)
"	" 01590	(3)
06-02-79	A0286-02060	(3)
16-02-79	A0296-12450	(1)
23-02-79	A0303-12130	(1,2)
27-02-79	A0307-12490	(1,2)
01-03-79	A0309-13240	(2)
"	" 13220	(1,2)
14-03-79	A0322-12270	(1,2)
15-03-79	A0323-12440	(1,2)
16-03-79	A0324-13020	(1,2)
"	" 13040	(1,2)
20-03-79	A0328-12390	(1,2)
21-03-79	A0329-12570	(1,2)
11-04-79	A0350-12450	(1,2)
"	" 12460	(1,2)
17-04-79	A0356-12580	(1,2)
21-04-79	A0360-12350	(1,2)
"	" 12370	(1,2)
23-04-79	A0362-13120	(1,2)

01-05-79	A0370-01310	(3)
"	" 12250	(1,2)
02-05-79	A0371-01500	(3)
07-05-79	A0376-01440	(3)

Total	114	Day images
	109	Night "

TABLE 3.

LIST OF HCMM IMAGES RECEIVED AS CCT'S AT IGN.

Date	Image	Bands	A	B
05-11-78	015 13510	1,2	*	
05-31-78	035 02330	3	*	
06-01-78	036 13440	1,2		
06-21-78	056 02240	3		
06-22-78	057 13370	1,2		
07-02-78	067 02300	3	*	
07-07-78	072 02240	3		
07-07-78	072 02330	3	*	*
07-07-78	072 13170	1,2	*	*
07-08-78	073 13350	1,2		
07-08-78	073 13330	1,2		
07-17-78	082 02090	3		
07-23-78	088 02200	3		
07-23-78	088 02220	3		
07-28-78	093 02130	3	*	*
07-28-78	093 13070	1,2	*	*
07-29-78	094 13250	1,2	*	
07-29-78	094 13230	1,2		
08-19-78	115 02200	3	*	*
08-19-78	115 13130	1,2	*	*
09-14-78	141 02050	3	*	*
09-14-78	141 02070	3		
09-14-78	141 13000	3	*	*
09-15-78	142 02240	3		
09-26-78	153 13220	1,2	*	
10-28-78	185 13160	1,2	*	
10-28-78	185 13180	1,2		
11-02-78	190 13090	1,2	*	
11-03-78	191 13270	1,2		
11-12-78	200 02010	3		
11-17-78	205 01550	3	*	
12-29-78	227 13010	1,2	*	
12-29-78	227 12590	1,2		

A: Covers most of the test area

B: Day-night coverage over the test area.

These CCT'S belong to images whose positives were received at IGN before January 1980 (35% of all the images received in - HCM-034 project).

Given the delay in the reception of positive transparencies, there was no time to order CCT'S of 1979, neither of some 1978 high quality images.

Interesting work was done on some of these images, which is reported here.

Also, thermal inertia and temperature difference digital data were received from NASA, corresponding to images 0072-13170 (1 & 2) and 0072-02230 (3).-

There were ordered, but not received because of problems at IPF, three more CCT'S (0184-12590- 1 & 2, 0141-02050-3, 0157-02050) and one registered data set (0073-13330- 1 & 2 - with 0072 - 02240 - 3).

Processing at Instituto Geográfico Nacional

Given the time constraints stated before, a new approach to the analysis and extraction of information from HCMM images was devised:

The new objective was to process the HCMM data in ways familiar and accesible to most Remote Sensing Applications Laboratories, and analyze the capability of HCMM to provide new information or complement the existing one in fields of general interest.

Consequently, sophisticated image-processing techniques were avoided as standard processing, and only selected images were considered.

Analog-processing techniques as well as manual interpretation were emphasized.

The contrast and the modulation of the positive transparencies provided by NASA was considered low (4 to 8, and around 7 respectively). So, from all positive transparencies received, an enhanced negative was obtained in a Log-Etronics Mark-IV C dodger; from each negative, also in the Log-Etronics, two enhanced positive paper copies were made of each image.These paper copies were analyzed, evaluating quality, cloud cover, test area coverage, interest,...

A selection of the best cloud-free images over the test area was reproduced photographically and sent to the coinvestigators, which also ordered, on an individual basis, images of particular interest for their specific needs.

Most of the images on CCT were enhanced.

Of the 4 day-night pairs over the test area received as CCT, only the one corresponding to July 7, was considered worth of further processing, given its high quality and lack of clouds.The night IR was registered to the day one, and temperature difference and thermal inertia images were computed and compared to the ones provided by NASA's Image Processing Facility.

The images delivered by NASA are geometrically corrected to Hot-line Oblique Mercator projection.The checks performed on the images gave good results, with regard to the resolution and scale of the images, so it was unnecessary to correct geometrically the data at IGN.HCMM images have proven to work well at scales of 1:2.000.000 and smaller.Magnification to a 1:1000.000 scale shows the pixels as 0,6 x 0,6 mm^2, which is too big for practical purposes.Since the scale of general maps in Spain is of 1:1.000.000 or greater, a rough generalization was necessary before comparing them with HCMM images.

B.- GENERAL ANALYSIS OF HCMM DATA

Here we will focus on the analysis of the quality of HCMM data and their sources of noise.

Meteorological Aspect

One striking fact was the abundance of clouds, fog mist, haze,... over the test area in the period of the project.

Clouds were dominant in most images since summer 1978.

Fog was very thick at night in coastal areas in summer and early autumn and also quite apparent in Central Spain at the same time.
This latter fog seemed to come from the Atlantic, through the main valleys.

Haze was noticeable over the sea even in some day-images (July 7, 1978; November 2, 1979) when comparing IR and visible data (see histograms, figs. 1, 2, 3).However this noon mist was scarcely visible on the photographic reproductions.

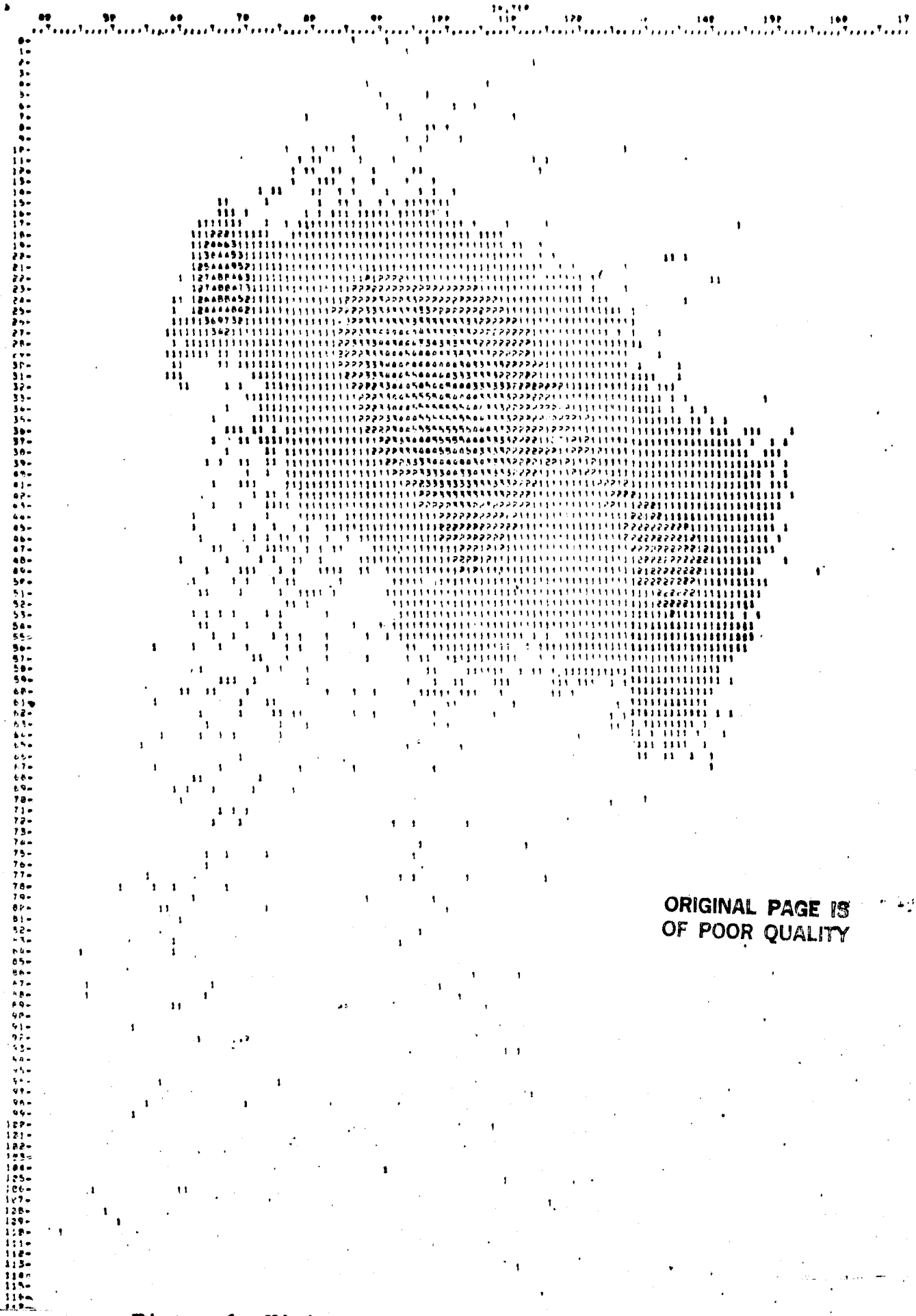

Figure 1. Histogram, Visible - Day IR bands. July 7, 1978

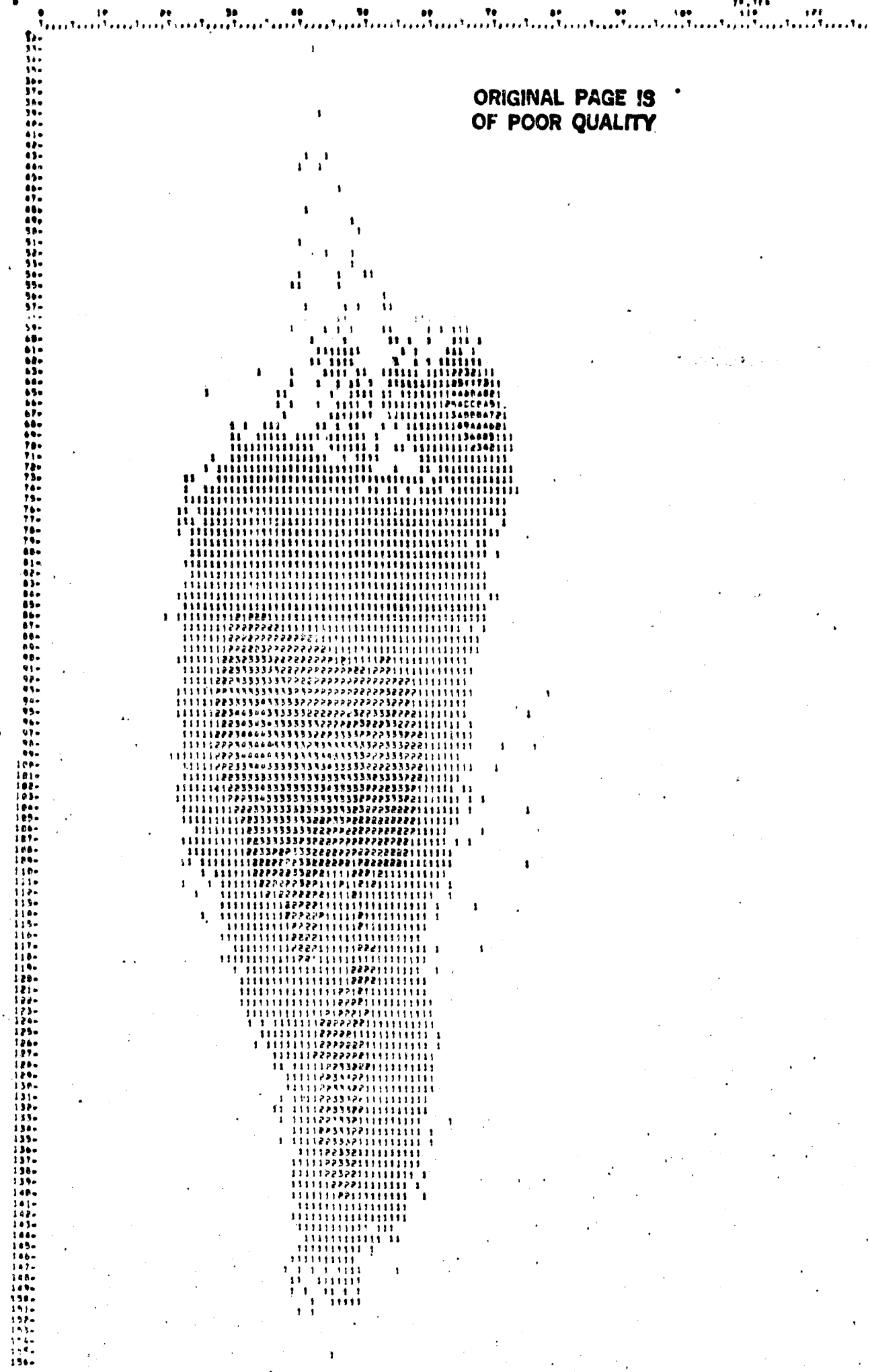

Figure 2. Histogram, Day - Night IR bands. July 7, 1978

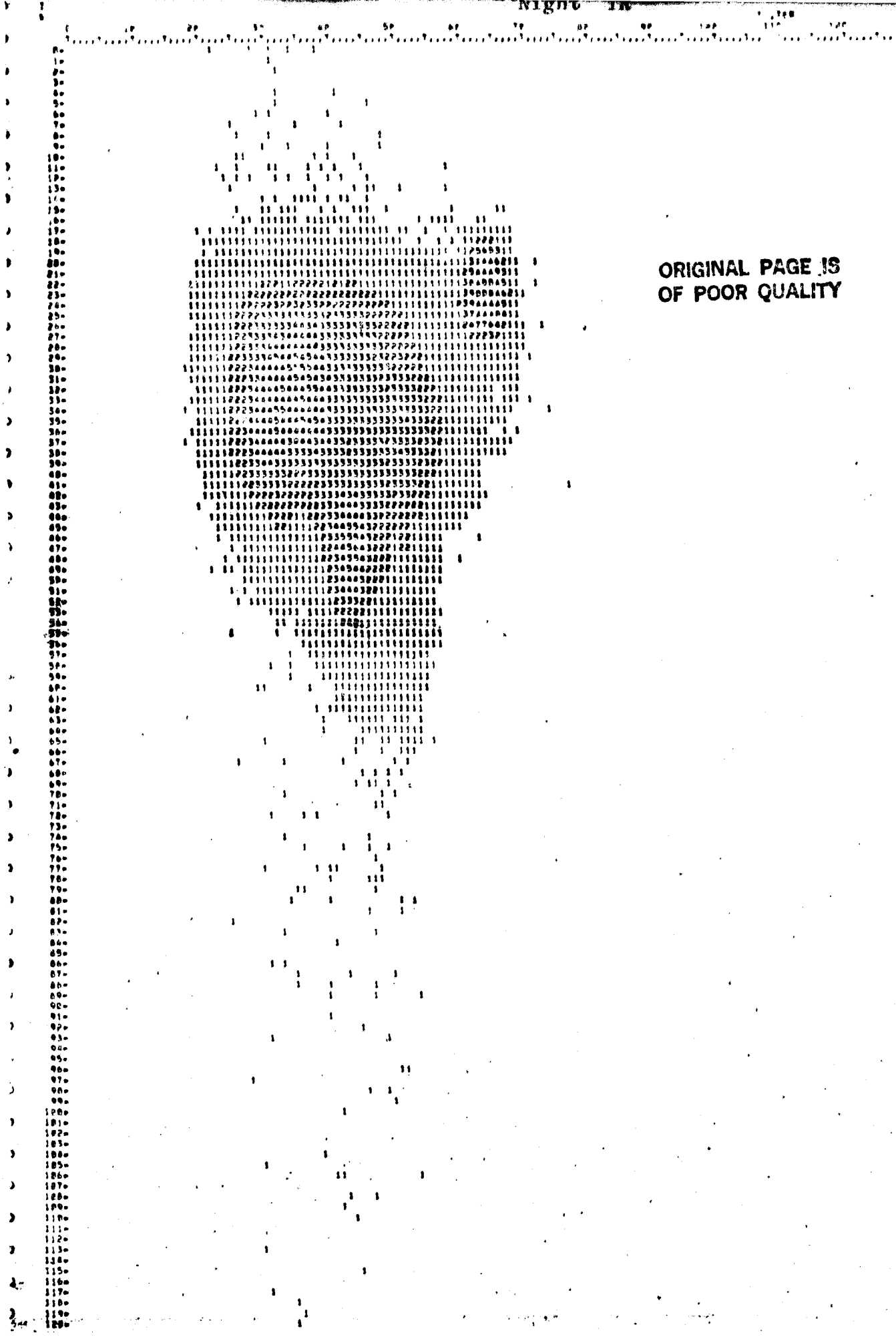

ORIGINAL PAGE IS
OF POOR QUALITY

Figure 3. Histogram, Visible - Night IR bands. July 7, 1978

HCMM data proved to be very valuable in following storms and their evolution, not only from the clouds, but also from differences in temperature of the soils, probably caused by rain (Images 184-12590, 190-13090, Fig.6).

From the histograms of several images, some kind of clouds may be differentiated automatically from their temperatures, correlated to their height, besides their shape and size.

Dynamic Range of the Original Data

The dynamic range of the images analyzed is very low. Most of the range is covered by clouds that show high dispersion, mainly in the visible (see histograms, Figs. 1, 2, 3).

The range of land feature is about 20 % of the total range in all bands and most images (In summer, day IR data have a real range of 35 %).

This makes the effective Signal Noise Ratio (SNR) worse. Thus the data are of scarce interest in automatic pattern recognition, since they are grouped with elongated bell-shaped distribution (only two clearly different clusters are seen in the histograms, besides the clouds, corresponding to water and vegetated land.

Here we should point out that although the Noise Equivalent Temperature Difference (NEΔT) of the HCMR is of 0,3°K, this is the nominal value at the satellite's altitude. Correcting this value from the atmospheric effects with Dr. Price's delivered and corrected RADTRA program (contract NASS-24272), it roughly corresponds to 0°K at ground level, in strong agreement with the observed range of ground values. A similar analysis was performed on the albedo data: comparing the Noise Equivalent Reflectance difference (NE$\Delta\rho$) of the HCMR to that of Landsat MSS, weighted so that the resulting value of the MSS is HCMR albedo, similar values result.

The ratio "Real range/total range" of 2 is apparently justified by the fact that the IR detector should be equally operative at noon (maximum) and midnight (minimum) temperatures, in deserti areas as well as polar ones; this should occur both in summer and in winter. But these extreme operating conditions are not as restrictive as they seem, as shows the experience with data from other satellites (NIMBUS, NOAA, DMSP).

Cuantification Effect

The low dynamic range together with the "uniform quantization" procedure adopted necessarily for the HCMR, makes quantization noise very likely to happen, and noise from other sources to be noticed, as may be seen in figures 7 and 8, and fig. 9 that compares HCMM and Landsat data of the same area.

This high-frequency random noise is also evident in the classification results shown in figure 10, as isolated points inside homogeneous areas.

Data Gathering and Transmission Problem

It seems that much of the noise present in the data, that affects so strongly its quality, has its origin in analog telemetry systems onboard the satellite.Since the data are transmitted in an analog form, and digitized and processed once received, the multiple perturbations that may affect the transmission in S-band alter the data without possibility of recovery.This situation is worse for the data in the visible channel, transmitted on subcarrier at a higher frequency, thus more sensitive to perturbations or losses in gain; but it is not exclusive of the visible channel as suggested in III-4.4 d) of "HCMM User's Guide",being also observed in the IR one, more neatly at night (Fig.11).

The other important problem that affected the data, mainly the night IR ones, was the degradation of the power system (namely the battery). Adequate management of the operations of HCMM satellite led to better night images in May 1979 than in June 1978.

Atmospheric Influence

An important source of what we may call "noise", meaning any disturbance that affects the data, hidding the information they convey, is the atmosphere.In areas with rough relief, the different local climates and wheather conditions affect the atmospheric parameters of interest in evaluating thermal transmittance and bias, in a way that any atmospheric sounding shows.-

As an example, the maximum and minimum temparatures in the main cities located in the registered July 7 subscene (see Figs. 14 to 17) are shown in Table 4.There are four inland cities, three colder (Teruel,Albacete and Calamocha)than coastal ones, and other warmer (Murcia,surrounded by irrigated farmland (huerta)).The differences in color doesn't correspond with differences in temperature.Also, "corridors" appear along valleys, two of them very apparent, that don't correspond with differences in land cover or lithology.They seem to be thermal corridors that connect inland areas to the coast.

TABLE 4

Temperatures (°C) July 7, 1978

City	Symbol	Maximum	Minimum
Valencia	VA	24	16
Castellón	CS	25	15
Tarragona	TA	28	13
Tortosa	TO	29	16
Alicante	AL	26	15
Murcia (*)	MU	30	18
Albacete	AB	29	9
Teruel	TE	25	6
Calamocha	CA	23	3

(*) (Not in the IR area)

Topographical Aspects

The thermal data are strongly influenced by the altitude over the sea of the area under analysis, as well as by its geomorphology.Both factors have micrometeorological implications, and also affect the characteristics of the atmosphere above that area.

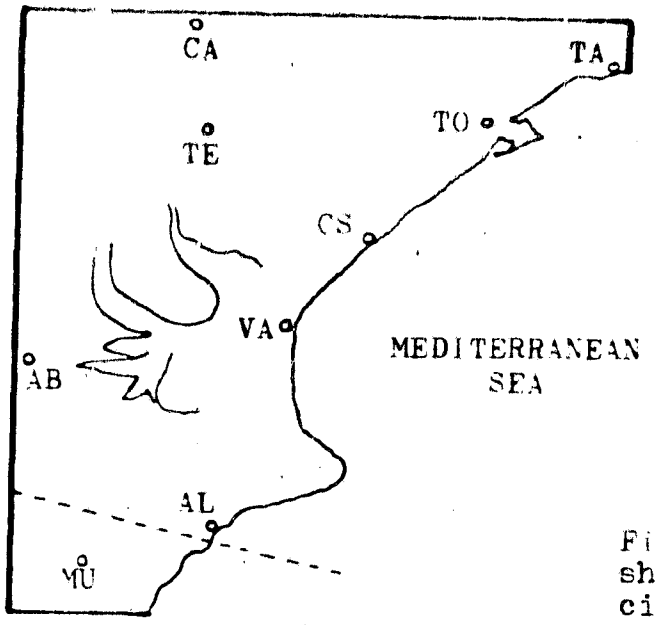

Fig. 16:

Fig. 14(see page) overlay, showing shoreline and main cities.

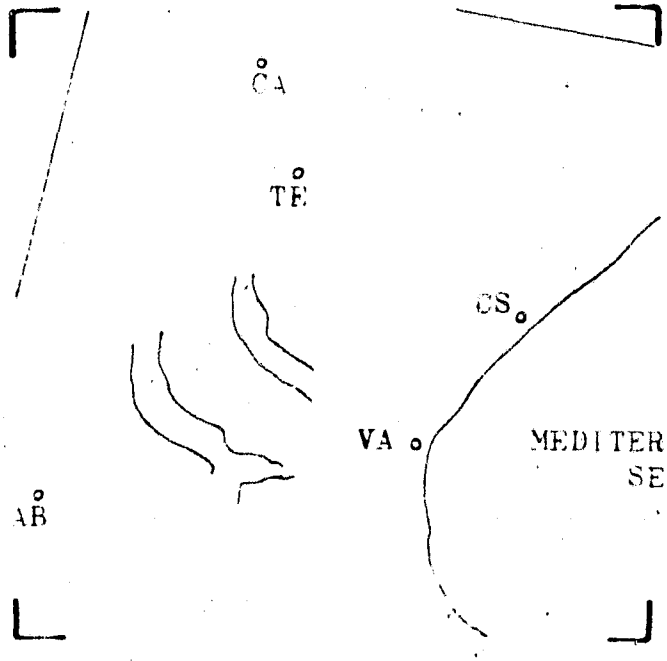

Fig. 17 :

Fig. 15 (see page)overlay showing shoreline and main cities.

In some images this influence appears very neatly, marking different ground levels (see Fig. 18), that obscure the nature of the land-cover or the soils in the area.

Low Frequency Noise

Another troublesome effect was the high period (low frequency) noise present in the images.
The most apparent are the strong differences in the average value of consecutive lines in the infrared images, mainly since the launch.This noise seems to have originated in the calibration system of the Heat Capacity Mapping Radiometer (HCMR).

In some images, see Fig. 5, the striping is not along scan lines, but perpendicular to the orbit! This may be caused only in the processing of the data at NASA'S IPF.

It seems that the "zero level" is not recovered when a new line starts, so the output of the IR detector has a "bias" on some lines, that also influences the multiplexer output.

This problem is random (not 10 lines wide as stated in III-4,4b of "HCMM User's Guide"). Except in some images (141-13000-1 &2, see Fig 13) there is no apparent pattern in the noise, that changes from image to image.Anyway, it seems to be changing slowly, but sharply, in each image. Since there is only one IR detector, the correction of this problem in the data is difficult.A simple approach was tried with acceptable results (See "Digital Processing of HCMM images" in this Report), but more sophisticated methods should be used (moving average, line averages ajusted to a high-order polinominal"...)

Statistical Analysis of a Sample HCMM Image

Registered subscene of images 072-02230 and 072-13170 (July 7, 1978) centered in Valencia (see Figs. 12) was transformed to its principal components.This same subscene is the one whose histograms are shown in Figs 1, 2 and 3). The results are as follows:

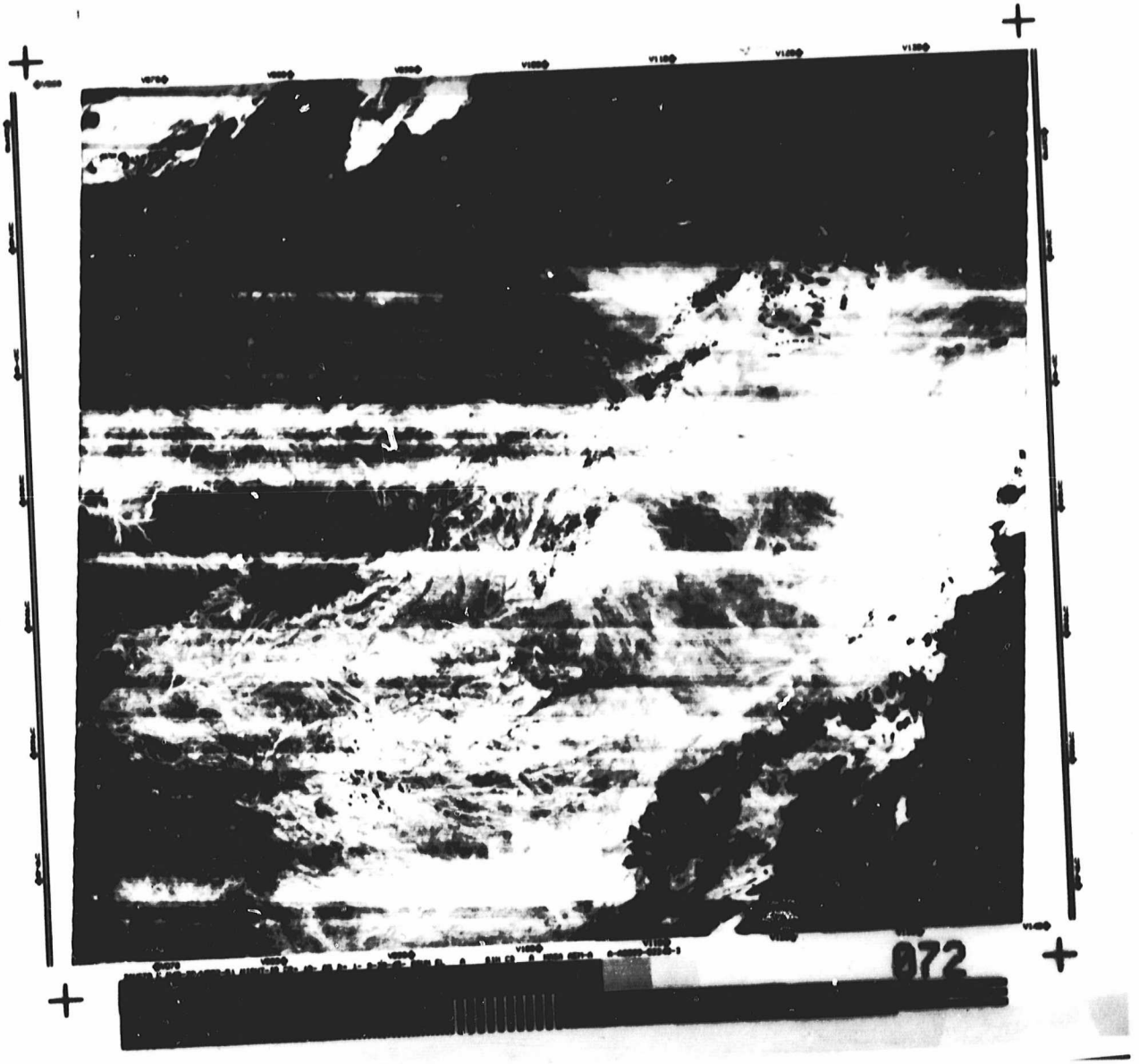

Figure 5. Along-track stripping. Suggested IPF anomaly

TABLE 5

Band	1 (Albedo)	2 (Day IR)	3(Night IR)
Mean	79,6	87,5	31,5
Standard deviation	43,2	26,4	11,3
Coefficient of Variation	0,54	0,30	0,36
Variance-Covariance Matrix:			
	1871	-245	-117
	-245	698	261
	-117	261	129
Eigenvalues	1936	735	27
% variance explained	71,8	27,2	1,0
Correlation-Matrix:			
	1,0	-0,22	-0,24
	-0,21	1,0	0,87
	-0,24	0,87	1,0
Eigenvalues	1,974	0,895	0,131
% variance explained	65,8	29,8	4,4

Eigenvectors are shown in figure 4.

The Correlation-Matrix was preferred to the Variance-Covariance one, given the differences between the means and coefficients of variation of each originated band.

The use of the principal components on the image 190-13090 subscene gave better results on the classification of its land-covers than the original bands (see"Numerical Analysis of HCMM Data" in this Report). The main difference rests upon the different kinds of vegetation (Forests, irrigated land, dry farming,...) that lie along the first principal component axis.

This approach is very useful in classification by means of look-up table.

E I G E N V E C T O R S
July 7, 1978. Registered night-day Subscene

CORRELATION MATRIX.	VARIANCE-COVARIANCE MATRIX

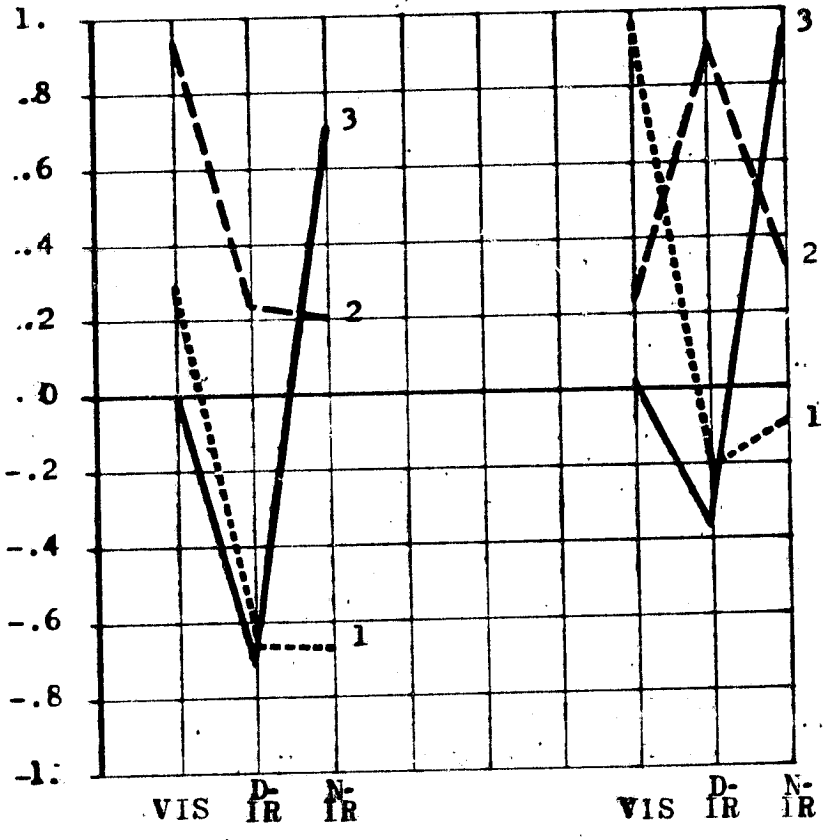

Figure 4.

CONCLUSIONS

In this paper we have analyzed the different kinds of noises that seem to affect HCMM data and have strongly influenced Project HCM-034:

- Data distribution delays, that forced us to select non-optimal images (low quality, clouds,...) to work with (Table 6).
  These delays forced us to change the planning and schedule.

  From an intensive digital processing of most images followed by detailed analysis, we should switch to a broad enhancement of the data, (data that in some cases were not adequate; in some cases originals of a very good quality, that didn't need any processing, were received months later), followed by a general analysis of its applications and usefulness in fields of general interest.

  Images were evaluated in terms of their information content in an user-oriented approach. The users disciplines were broadly chosen, as well as their analysis, over areas in which good and recent ground-truth information exists.

- Relief and ground elevation, that reduces the temperature of ground as well as that of the atmospheric layer in contact with it.

- Atmospheric influence, for quantitative analysis, forces to restrict the zones of analysis to small and homogeneous geographic areas, and recommends the sounding of the atmosphere to correct the data.

  The atmosphere influence also "degrades" the characteristics of the HCMR, increasing the NEΔT for the IR channel to 0°K.

- HCMM telemmetry characteristics, makes the transmission and recording of data very noisy, thus worsening the quality of the data, that may have been, according to the HCMR specifications (specially in the visible-near IR channel), much better.

- HCMM power failure, that made operation at night hazardous, until the regularization of the data gathering process, with problems in the resulting data.

TABLE 6

MOST USED HCMM IMAGES

36-13440 - 1 and 2

67-02300 - 3

72-02230 - 3

72-3170 - 1 and 2

99-02240 - 3

141-02050 - 3

141-13000 - 1 and 2

184-12590 - 1 and 2 (wrongly annotated 3 instead of 2)

185-13160 - 1 and 2

190-13090 - 1 and 2

- NASA'S Image Processing Facility update, very late for this Project, was in part the cause of the delays stated in first term, and it seems that also of some kinds of noises in the data not well understood yet (stripping ...)

After the experience attained in the Project and the information on the data really available, it's now when we may restart our research, with guarantees of completion in time, and when we can follow our original plan of works.

List of Figures

In order to avoid unnecessary duplication of HCMM images, those reproduced in other parts of this Report and referred to here, are listed below:

Fig.6. Image 184-12590.
See "Applications of HCMM Images in Geology", Fig.7, pg.151
See also the quotation to Fig.8 below.Pg.183

Fig.7. Subimage from 067-02300-3
See "Digital Processing of HCMM Satellite Data"
Fig.10 and 11, pg.67

Fig.8. Subimage from 190-13090-1 & 2 , pg.183
See "Applications of the HCMM Satellite Data to the Study of the Subterranean Water Discharges on the Mediterranean Sea", Fig.1 and 2

Fig.9 See "Digital Preprocessing of HCMM Images". Fig. 11, page 46

Fig.10. See "Numerical Analysis of HCMM Data"
Photographs 3, 4 and 5. Page 199 and 200

Fig.11 Subimage from 067-02300-3
See "Digital Processing of HCMM Satellite Data"
Phot. 5 and 6. Page 64 and 65

Fig.12. Registered Subscene from images 72-02230-3 and 72-13170- 1 & 2
See "Results of the Interpretation of HCMM Images Applied to Soils"
Fig. 1, 2 and 3. Page 165. 167 and 170

Fig.13. Figs 6a and 6b in same Report quoted for Fig.6. Pg. 147 and 148

Fig.14. See "Digital Processing of HCMM Images". Fig.1. Pg.72

Fig.15. See "Digital Preprocessing of HCMM Imagery" Fig.9. Pg.46

Fig.18. See "Digital Processing of HCMM Satellite Data"
Fig. 4, 10 and 11. Page 61 and 67

I M A G E P R O C E S S I N G

B.- IMAGE PROCESSING

- "Digital Preprocessing of HCMM Imagery"
  Alejandro García & Fortunato Ortí
  Centro de Investigación UAM-IBM

- "Digital Processing of HCMM Satellite Data"
  (Reproduced from the First Progress Report)
  Ramón López Muñiz
  Instituto Geográfico Nacional

- "Digital Processing of HCMM Images"
  Ramón López Muñiz
  Instituto Geográfico Nacional

DIGITAL PREPROCESSING OF HCMM IMAGERY

A.García
F.Ortí
UAM-IBM Scientific Center

1. INTRODUCTION

Images acquired by scanners on board aircraft or spacecraft platforms have some distortions, geometric and radiometric, which have to be corrected to ease the task of referencing the image to existing ground information (geometric corrections), and to have the best possible image data (radiometric corrections).

Also, if use is going to be made of multitemporal data, as it is the case with day and night HCMM images, some way of directly sumperimposing images of the same area taken at different times is desirable, because the direct registration of two images would generally be more accurate than the indirect registration achieved through referencing both images to a common grid.

Due to the involvement of the Scientific Center in different aspects of digital image processing in general, and in LANDSAT image processing in particular (see for example references [1], [2] and [3]) a software package already existed to perform most of the desired image manipulations, and with some slight modifications could be made suitable to be used in the present study.

This paper describes the method followed to register day and night HCMM images and the similar process of registering HCMM to MSS-LANDSAT images.

Results for two day-night pairs are presented, together with the registration of one of them to a precision corrected LANDSAT image. Also, from one of the day-night pairs, a temperature difference image was created and from it an apparent thermal inertia image was obtained.

Despite of the fact that in some facilities (e.g. NASA Goddard Center, USA; Lannion, France) the same kind of processing was going to be done in a routine basis, our rational for getting involved with this problem

was that while those facilities would have to go towards standard products and would have to limit human intervention to a minimum, we could afford to process smaller areas, with more human interaction and in a more research like basis.

2. DESCRIPTION OF THE IMAGE TO IMAGE REGISTRATION PROCESS.

To register an image (input) to another one (reference) two things are needed: the geometric transformation, or mapping functions, relating one image to the other and an interpolation rule to actually transform or resample the input image.

For all registrations reported in this paper, the assumption is made that the mapping functions can be well approximated by two bivariate polynomials of first or second degree, whose coefficients are determined by a set of homologous points (ground control points or GCP's) using a standard least-squares method.

Two comments about the actual implementation of the polynomial coefficients computation follows:

a) When fitting two sets of points, outliers are detected by looking at the residual errors; if the residual error is judged to be too large, the corresponding point is rejected and the polynomial coefficients recomputed.

   After the first registration experiment performed with two HCMM images reported below, it was felt that the rejection of the outliers should be more objective. Thus a modification was made to the program to automatically reject those points with residuals larger than 2.5 times the standard deviation of the residuals in any of the two directions vertical or horizontal.

b) After the fit has been performed, the error in the coefficients can be estimated and this error propagated to any point in the image.

   In our program we compute this propagated error in both directions in 25 points uniformly distributed over the image. Though these propagated errors should be taken with care, because of the underlying assumption that the transformation functions are well

represented by polynomials of a certain degree, they should give an idea of the quality of the achieved registration in different regions of the image.

With respect to the resampling algorithms, only to say that we have the possibility of using nearest-neighbor, bilinear or cubic convolution; as a rule, for substantial enlargements the cubic convolution algorithm has been used. For details about these resampling rules the reader is referred to reference [4].

The point remaining to be discussed is how the GCP set is obtained. Although the method varied slightly depending on the images to be registered, basically was as follows:

1. A few GCP's are manually located in the input and reference images. From them a linear transformation is computed and the input image is resampled giving an intermediate image roughly registered to the reference one.

2. A set of points is selected in the reference image and added to the manually chosen. This selection is made automatically placing a specified number of points uniformly distributed over the image, with the possibility of adding more manually. Around each one of them a small window or chip of 20x20 pixel size is extracted.

   Similarly, around each homologous point in the intermediate image a search area of a certain specified size (minimum 20x20, maximum 100x100) is extracted.

3. The cross-correlation coefficient between the window and search areas is computed for all possible positions of the window within the search area, and its maximum absolute value is taken as marking the position of matching. If this maximum exceeds a given threshold, the matching is considered to be succesful and the corresponding GCP is kept to be used later in the polynomial coefficients computation. (see reference [5] for an account of matching methods).

4. With the set of GCP's provided by the cross-correlation matching the transformation between the intermediate and the reference images is computed. Using it, the intermediate image can be resampled again or the transformation relating the input and the reference images can be found and used to resample the input image.

A clear waste of processing time is involved in this procedure, as the input image is resampled twice: once to get the intermediate image and again when making the final resampling. This may be avoided by resampling only the search areas extracted from the input image, according to the transformation derived from a small set of manually chosen GCP's. However, in our case it was felt that for the limited amount of processing to be performed with these images it was not worthwhile to implement the necessary modifications.

3. RESULTS

The method just described was used to register two day-night image pairs and one of them, already registered, was superimposed to a precision corrected LANDSAT image.

At the beginning of this study no day and night images of the same date were available, so to test the programs and to learn de problems associated with HCMM imagery two images of different dates were chosen for processing, one corresponding to the night of July 2, 1978 (AA0067023003) and the other the day image taken on October 28, 1978 (AA0185131601,2).

3.1. Registration of the HCMM images AA0185131601,2 and AA0067023003 (different date)

As a first step the night image was rotated by an angle twice the one formed by the North and the satellite track direction computed at a latitud of 40°N from the nominal orbit inclination. The reason for this step was to have both, day and night, images with approximately the same orientation to increase the cross-correlation coefficient between window and search areas used later on to locate homologous points in the images.

Then, a set of GCP's was found by an operator and a first order transformation computed from it. This transformation served to locate the search areas in the rotated image for a set of points chosen in the day image. The cross-correlation matching program was run with window and search areas sizes of 20x20 and 40x40 pixels respectively, and using a cross-correlation coefficient threshold of 0.6.

In Fig. 1 a two-dimensional frequency plot for the window-search pairs is shown, in which the absolute value of the cross-correlation coefficient is represented in the horizontal axis and the horizontal displacement given to the window to obtain the maximum correlation coefficient (measured with respect to the position computed by the first order transformation) is represented in the vertical axis. Two points merit some comments:

a) The relatively high values for the cross-correlation coefficient are due to the fact that many of the windows (features in the day image) were chosen by an operator along the coast-line, and for those window-search pairs large negative value of the cross-correlation coefficient are expected.

b) Even for these high correlation coefficients the dispersion appears to be large. It is interesting to compare the frequency plot shown in Fig. 1 for HCMM images with one obtained for two LANDSAT images taken in April and June of the same year and corresponding to a rural area in Western Spain (unpublished work). The frequency plot corresponding to the LANDSAT images using MSS band 7 is shown in Fig. 2 and it can be clearly seen the small dispersion present on it, even though the vertical axis is the sum of the absolute values of the displacements in the horizontal and vertical directions rather than the values of one of these displacements, used in Fig. 1.

With the GCP's given by the cross-correlation process, and some of the ones found by the operator (the ones discarded by lack of correlation) two transformations were computed: one using a pair of first degree polynomials, and the other using a pair of second degree polynomials.

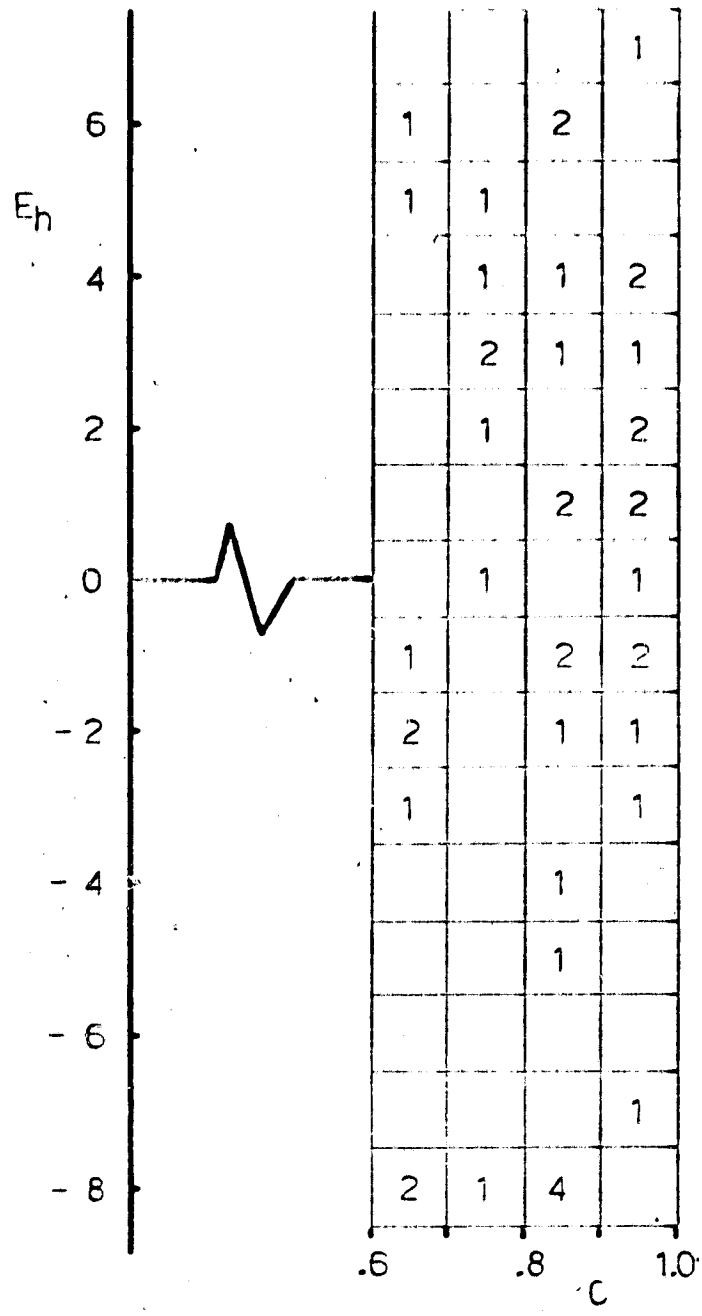

Fig. 1. Two dimensional frequency plot for the correlation matching pr[illegible]s for the HCMM images AA0185131601,2 and AA0067023003. E_h is the displacement given to the window to match the corresponding subimage in the search area in the horizontal direction. C is the cross-correlation coefficient.

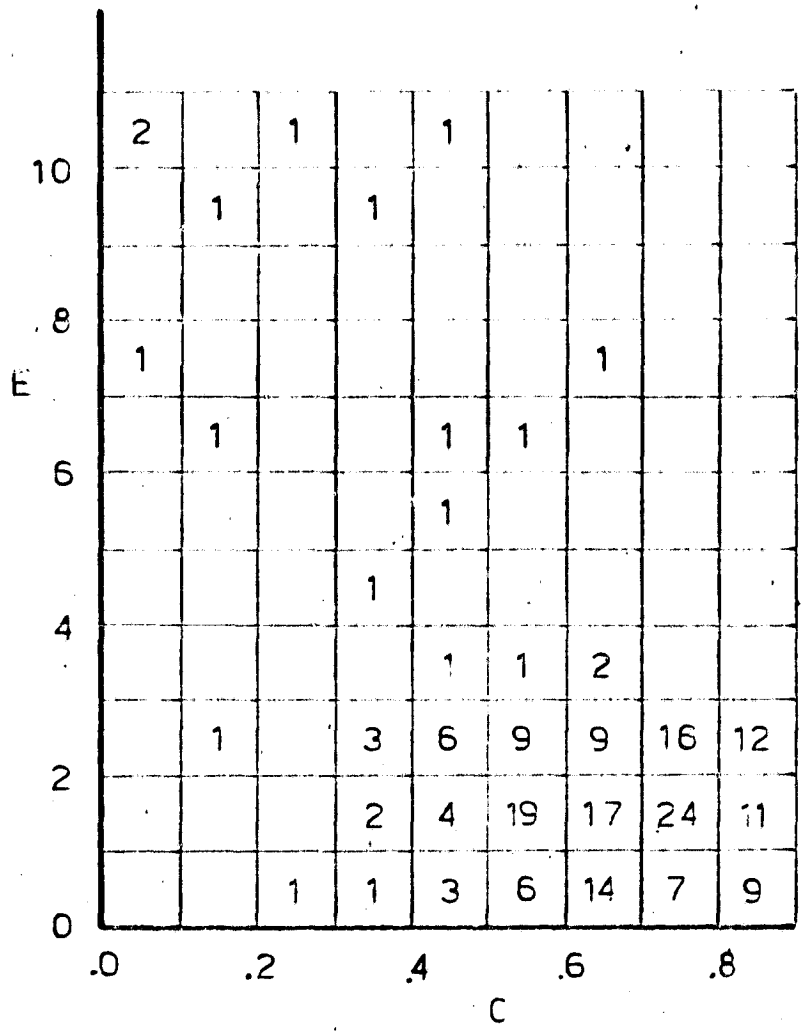

Fig. 2. Two dimensional frequency plot for the correlation matching process for two LANDSAT images (taken on April and June). E is the sum of the absolute values of the horizontal and vertical displacements given to the window to obtain the maximum correlation coefficient, C.

Table 1. Summary of least squares fits (1st and 2nd degree polynomials) for the HCMM images AA0185131601,2 and AA0067023003

Size of the image: 920 lines x 1500 pixels.

Points used in the fit and their situation on the image (points in 25 zones of the image)

1st degree	2nd degree
0 0 0 0 4	0 0 0 0 4
5 1 0 0 8	5 1 0 0 7
0 3 0 11 3	0 3 1 9 3
2 0 0 0 0	2 0 0 0 0
0 1 5 1 0	0 1 5 1 0
Total 44 GPC's	Total 42 GCP's

Estimated standard deviations for the location error

1st degree	2nd degree
σ_{PIX} = 2.44 pixels	σ_{PIX} = 1.67 pixels
σ_{LIN} = 1.50 pixels	σ_{LIN} = 1.25 pixels

Output to input transformation (2nd degree)

(v and u are pixel and line of input image; y, x are pixel and line of output)

$$v = 108.6 + .1448x + .2166\times10^{-5}\, x^2 + .9490\, y + .7120\times10^{-5}\, xy + .2415\times10^{-4}\, y^2$$

$$u = 519.3 + .9898x + .6406\times10^{-5}\, x^2 - .1519\, y - .4143\times10^{-5}\, xy + .3829\times10^{-6}\, y^2$$

Estimated standard deviations of the registration errors in 25 points of the image

VERTICAL DIRECTION	HORIZONTAL DIRECTION
2.0 1.6 1.6 1.2 0.8	2.6 2.2 2.1 1.6 1.0
1.1 0.7 0.9 0.5 0.8	1.5 1.0 1.1 0.6 1.1
0.9 0.4 0.5 0.3 1.4	1.3 0.5 0.7 0.5 1.8
1.3 0.6 0.4 0.6 1.9	1.7 0.8 0.5 0.8 2.6
1.7 1.0 0.7 1.1 2.6	2.3 1.3 0.9 1.5 3.4

Table 1 gives a summary of the results of the least-squares fit.

It can be noted that, for the size of the image chosen, the non-linear terms of the transformation are significant, suggesting that a first degree transformation is not adequate. Comparison of the estimated locations errors also points towards the same fact.

With these two transformations the rotated night image was resampled. Fig. 3 is a false color composite of the visible, day thermal infrarred and night thermal infrarred bands obtained by assigning them to the blue, green and red guns of a color TV monitor respectively. The night band transformed by a second degree transformation is the one used in the display. This display explains the reason of having the GCP distribution shown in Table 1: clouds and sea hampered having points in the first and forth fifths of the image.

An assessment of the registration quality achieved by using the first degree or the second degree transformation was made by assigning the day and night thermal bands to the red and green guns of a color TV monitor and analyzing the resultant display. Figures 4 and 5 show the displays corresponding to the registrations obtained with the first and second degree transformations respectively. Just by the cursor there is a lake which is clearly misplaced in Fig. 4 (the position of the lake in the night image shows as yellow), while in Fig. 5 it appears to be well registered.

Thus, it seems that for the registration of two HCMM images of the size of the ones handled here (900 lines x 1500 pixels), at least a second degree polynomial correction should be tried.

Further assessment of the registration accuracy, checking points along the coast lines, gave a good feeling about the quality of the registration, but it is to be recognized that a misregistration of one or two pixels is easily overlooked by this visual analysis, at least with these images.

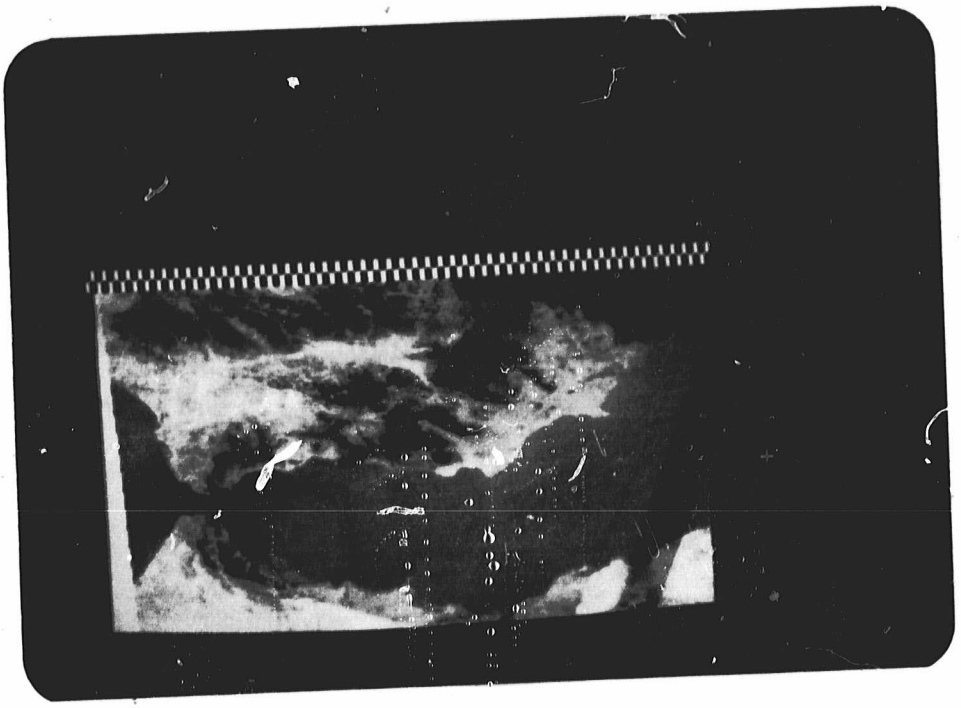

Fig. 3. False color display obtained by assigning the visible and thermal bands of the image AA0185131601,2 to the blue and green guns of a TV monitor and the registered night thermal band of the image AA067023003 to the red gun.

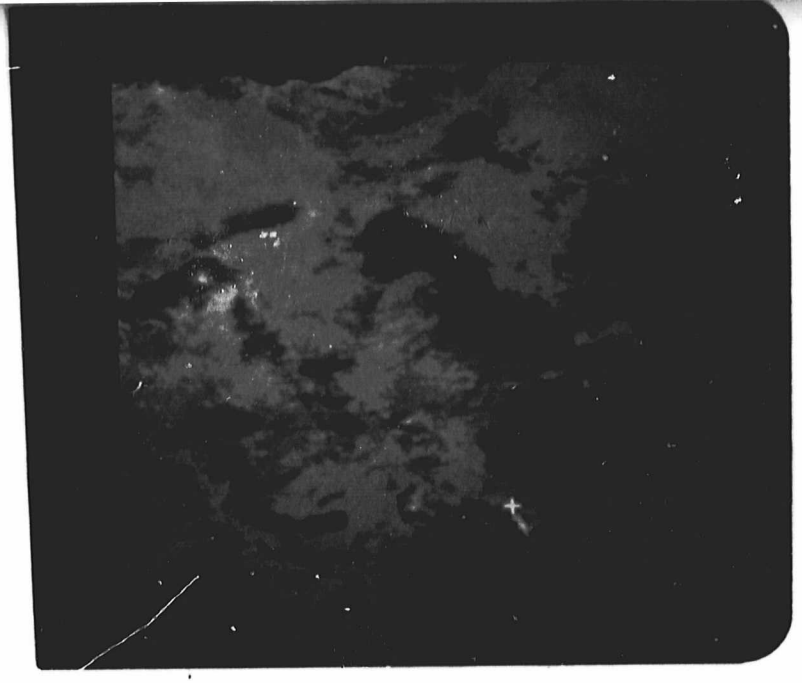

Fig. 4. False color display obtained by assigning the day thermal band of AA0185131602 to the green gun and the registered night thermal band from AA067023003 to the red gun. A pair of first degree polynomials was used for the registration. The misregistration of the lake by the cursor, showing in yellow in the night image, can be easily seen.

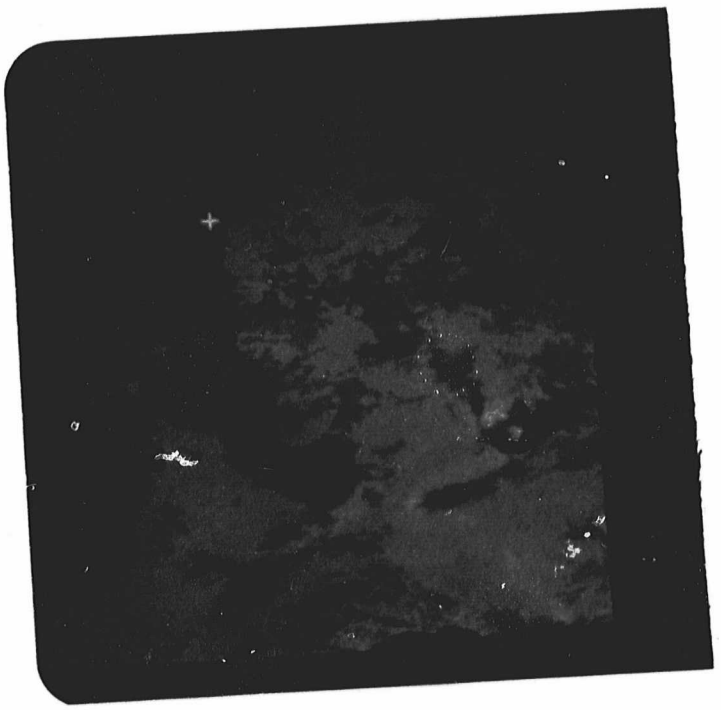

Fig. 5. Same display as in Fig. 4, except that a pair of second degree polynomials was used for the registration. The lake by the cursor appears now to register well in the images.

3.2. Registration of the HCMM images AA0072131701,2 and AA0072022303 (same date)

The same procedure described in the preceding paragraph was followed to register two HCMM images of the same date, July 7, 1978.

The night image was rotated, a few GCP's were found by an operator, and the corresponding linear transformation was used to set up the window-search pairs with sizes in this case of 20x20 and 60x60 pixels.

After the correlation matching those GCP's with correlation coefficients greater than 0.4 were used to obtain a linear transformation (the sizes of the images considered were 550x550 pixels).

The results given by the least squares fit for the estimate of the standard deviation of the location error, point towards the possibility that the matching achieved by the correlation method is completely random. This was suggested by the similarity between the obtained values and the value for the standard deviation of an uniformly distributed probability function between -20 and 20, just the permissible displacements of the window within the search areas for this case. Increasing the correlation coefficient threshold does not have a dramatic effect, as it is shown by looking at Table 2, where the estimates for the standard deviation of the location error are given for a linear transformation for different values of the threshold. The trend appears to be logical, as the threshold is increased the estimated errors decrease, but at the same time the number of points with correlation coefficients greater than the threshold is dramatically lowered, and the predicted registration errors increase as the threshold is raised.

To try to aleviate the problem, more GCP's were located manually, up to a total of 17. The first degree polynomials obtained using them served the purpose of setting up the window-search areas, this time with sizes of 20x20 and 30x30 pixels. The correlation matching gave 64 points, when a threshold of 0.5 was used for the correlation coefficient. Based on this set of points a second-degree transformation was found, the results being summarized in Table 3, where it can be seen that the values estimated for the location errors are again very close to the value corresponding to an uniformly distributed probability function between -5 and 5.

Table 2. Estimates of the standard deviations of the location error in the horizontal and vertical directions for different values of the cross-correlation coefficient threshold.
(day-night HCMM images of same date).

THRESHOLD	σ_{PIX} (pixels)	σ_{LIN} (pixels)	N° of points
0.4	11.99	12.12	121
0.5	11.49	11.95	89
0.6	10.60	11.58	45
0.7	10.10	11.71	23

Table 3. Summary of the least square fit (2nd degree polynomials) for the HCMM images AA0072131701,2 and AA0072022303

Size of the image: 550 lines x 550 pixels.

Points used in the fit and their situation on the image (points in 25 zones of the image)

0	3	0	1	3
0	0	3	3	7
3	6	3	8	4
1	1	9	1	0
1	0	2	5	0

Total: 64 GCP's

Estimated standard deviations for the location error

$$\sigma_{PIX} = 3.23 \text{ pixels}$$

$$\sigma_{LIN} = 2.95 \text{ pixels}$$

Output to input transformation (v and u are pixel and line of input image; y and x are pixel and line of output)

$$v = -0.6028 \times 10^{2} + 0.2359x - 0.1989\, x^{2} + 0.9708y - 0.4045 \times 10^{-4}xy - 0.1832 \times 10^{-4}y^{2}$$

$$u = 0.5970 \times 10^{2} + 0.9752\, x + 0.3623 \times 10^{-4}x^{2} - 0.1722y - 0.2896 \times 10^{-4}xy - 0.1829 \times 10^{-5}y^{2}$$

Estimated standard deviations of the registration errors in 25 points of the image

VERTICAL DIRECTION					HORIZONTAL DIRECTION				
4.7	2.7	2.0	2.0	2.3	5.2	3.0	2.2	2.2	2.5
2.8	1.3	0.9	0.7	1.2	3.2	1.4	1.0	0.8	1.3
1.9	0.7	0.7	0.6	1.8	2.0	0.7	0.8	0.7	2.0
1.9	1.1	0.7	1.0	2.9	2.0	1.2	0.8	1.0	3.2
3.2	2.2	1.5	1.9	4.3	3.5	2.4	1.6	2.1	4.7

The night image was resampled with the polynomials obtained from the 64 points, and the result assessed visually by displaying the thermal bands assigned to the red and green guns of a TV color monitor. The display was made having an actual pixel size in the screen of about 0.8 mm square; with this pixel size one would expect to readily find misregistrations; it was not so.

The following experiment was made: one of the images was intentionally displaced one pixel to the right. No misregistration was apparent even in the most clear features (costline, lakes, barren areas surrounded by vegetation, etc.). The experiment was repeated displacing the image leftwards, upwards and downwards, with the same result.

When the experiment was repeated by increasing the displacement to two pixels, the misregistration was detected in the most clear features.

All these difficulties seem to be caused, at least in part, by the low temperature gradients present in this particular night image from July (lack of contrast), which makes it difficult to recognize "small" features necessary for a good registration.

Figures 6, 7, 8 and 9 show the visible, day infrarred, registered night infrarred and color composite of the image. Comparison of the night band to any of the two day bands makes it look as if the night image had been smoothed (low pass-filter).

3.3. Registration of the HCMM images AA0072131701,2 and AA0072023003 to a precision corrected LANDSAT image (from the original E-1027-10144 imaged on August 19, 1972)

The idea of having the coarse resolution thermal data given by HCMM merged to LANDSAT data is attractive because the LANDSAT image provides a base in which ground features can be recognized much easily while the HCMM provides some information about the temperatures on the ground.

Besides, registration of the HCMM data to a precision corrected LANDSAT image provides a good registration of the HCMM to a cartographic reference system, in our case to UTM coordinates.

Fig. 6. Display of the visible band AA0072131701 imaged on July 7, 1978.

ORIGINAL PAGE
BLACK AND WHITE PHOTOGRAPH

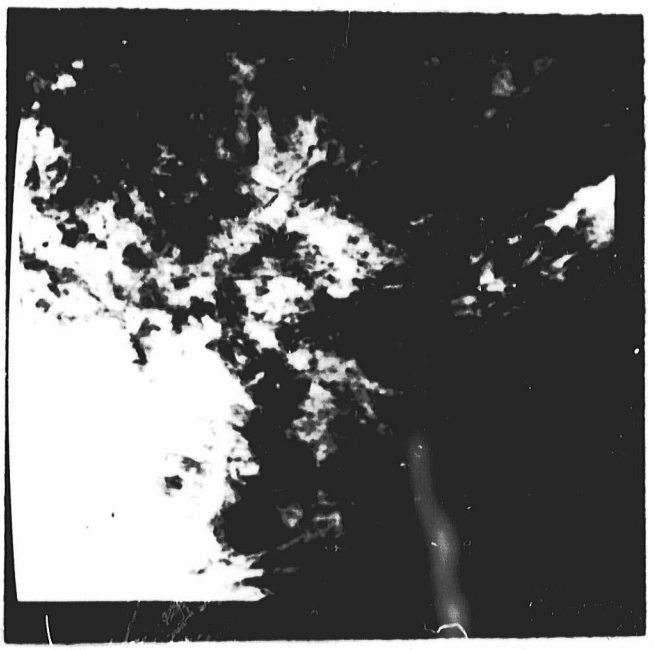

Fig. 7. Display of the day thermal band AA0072131702 imaged on July 7, 1978.

ORIGINAL PAGE
COLOR PHOTOGRAPH

Fig. 8. Display of the night thermal band AA0072022303 imaged on July 7, 1978 after registration to the day image.

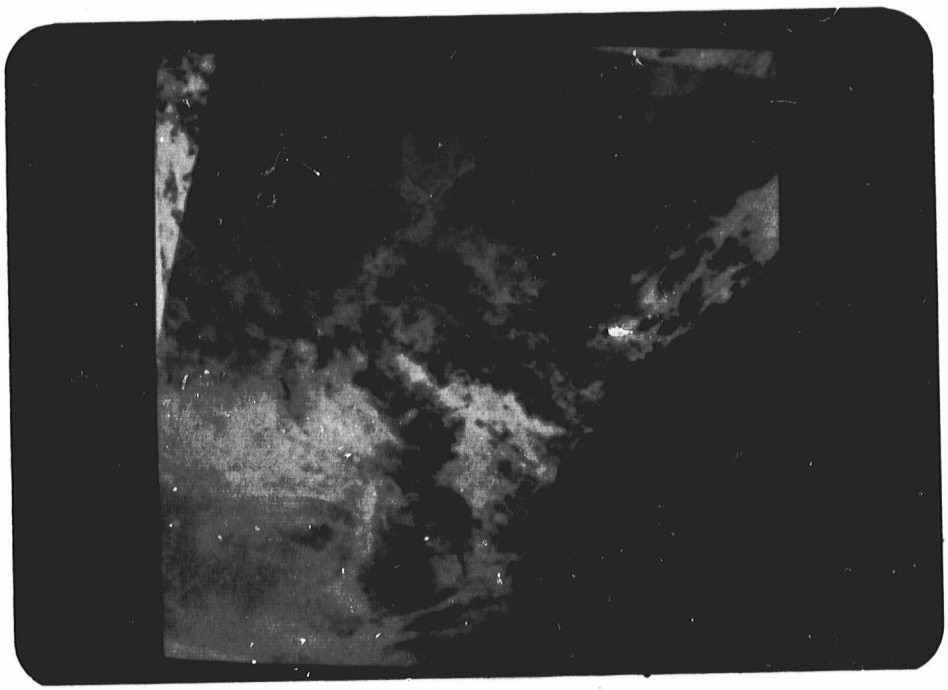

Fig. 9. False color display showing the day and night images taken on July 7, 1978. The registered night thermal band was assigned to the red gun of the TV monitor, the day thermal band to the green gun and the visible band to the blue gun.

Visual inspection showed that many of the features identifiable in the thermal day image were also seen in the MSS band 5 of LANDSAT. Thus these two bands were taken to achieve the registration.

As a first step, the thermal band was roughly registered to a degraded version of the LANDSAT band by locating six features in both bands. Our original LANDSAT image had a pixel size of 50.8 m. square, and the degraded one considered here was created by taking one pixel out of three in both directions, resulting in an effective pixel size of 152.4 m square.

The resampling of the thermal band was made using the cubic convolution algorithm, and the size of the roughly registered image was of 1240x1240 pixels.

GCP's for the final registration were obtained in the usual way by the correlation matching procedure.

The size of the window search areas were chosen to be 20x20 and 40x40 pixels, and the threshold used for the cross-correlation coefficient was 0.5.

With the GCP's given by the matching a pair of second degree polynomials was obtained. The least squares fit results are presented in table 4. The errors are expressed in pixels of 152.4 m. The increase in accuracy for this registration, compared with the superposition of day and night HCMM images is to be noted.

From the two transformations, the rough one and the second order, the second order transformation to directly register the HCMM image to be degraded (152.4 m pixel) was obtained, and the three bands of the HCMM image resampled using the cubic convolution algorithm. Fig. 10 shows part of the resampled image in the form of a color display in which the night thermal, day thermal and visible band have been put to the red, green and blue guns of the TV monitor.

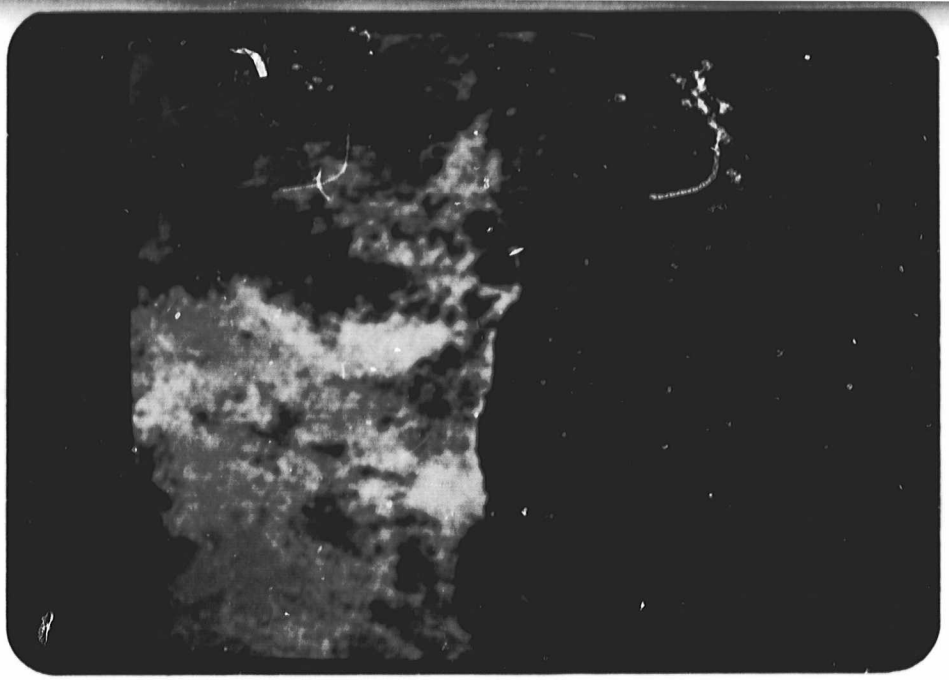

Fig. 10. False color display showing the day and night HCMM images taken on July 7, 1978 after registration to a precision corrected LANDSAT image. Pixel size is 152.4 m. square. The night thermal band, the day thermal band and the visible band were assigned to the red, green and blue guns of a TV monitor respectively.

ORIGINAL PAGE
COLOR PHOTOGRAPH

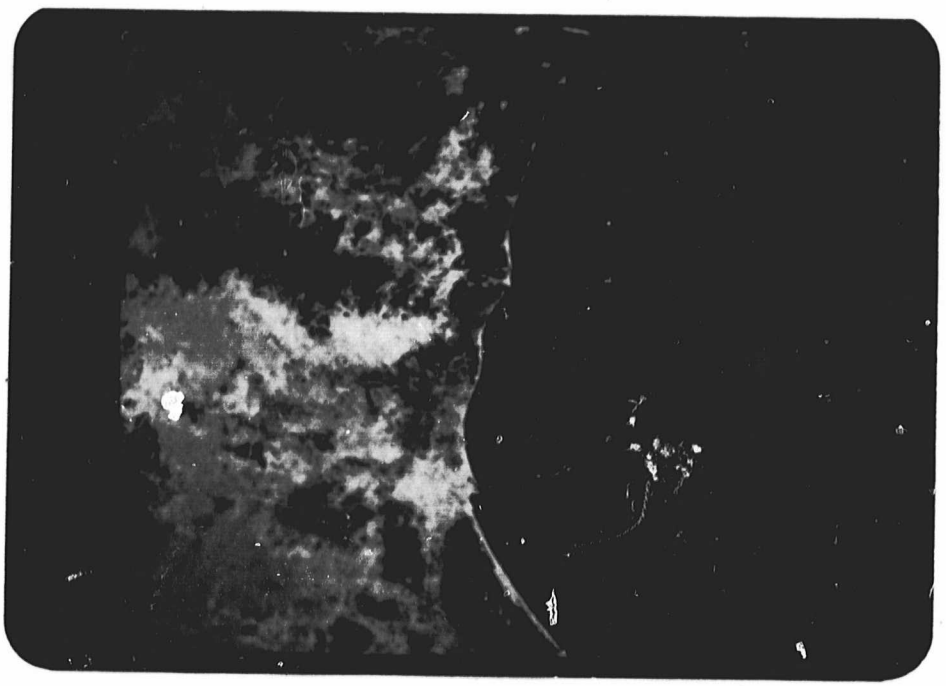

Fig. 11. False color display produced by assigning the night thermal band of the HCMM image AA0072022303 to the red gun of a TV monitor, and MSS band 5 of the LANDSAT image E-1027-10144 to the green gun.

Figure 11 shows a color composite of the night thermal band and MSS band 5 of LANDSAT. The finer structure provided by the LANDSAT image is readily appreciated.

For the purpose of further manipulating the HCMM image (temperature differences and apparent thermal inertia) it was felt that to have a registered image with a pixel nearer to the IFOV provided by the HCMM radiometer was more convenient. Thus the original HCMM image was again resampled to a pixel size of 457.2 m. square according to a pair of second degree polynomials obtained from the ones used to make the registration to the LANDSAT image by a simple shrinking of the two coordinate axis by a factor of 3.

To assess the registration accuracy a set of window-search areas were taken in the LANDSAT image and in the registered day thermal band. The correlation matching program was run and a first degree transformation function computed.

Fig. 12 is a frequency plot as a function of the cross-correlation coefficient and the sum of absolute errors in the two directions, vertical and horizontal. This plot should be compared to the one given in Fig. 1., for the night-day matching, to realize that even for an image enlarged by a factor of 3 the dispersion is much lower than for the night-day pair.

The results for the least-squares fit are presented in Table 5 and as can be seen the identity, with errors of the order of 1 pixel (152.4 m) is recovered. No explanation has been found for the high standard deviations predicted for the location error as compared with the ones in Table 4.

3.4. Day-night temperature difference and apparent thermal inertia.

Taking the registered HCMM image with pixel size 457.2 m square the difference between the day and night thermal bands was made. A display of the resultant image is shown in Fig. 13, and a histogram of the values of the difference for the whole image is given in Fig. 14.

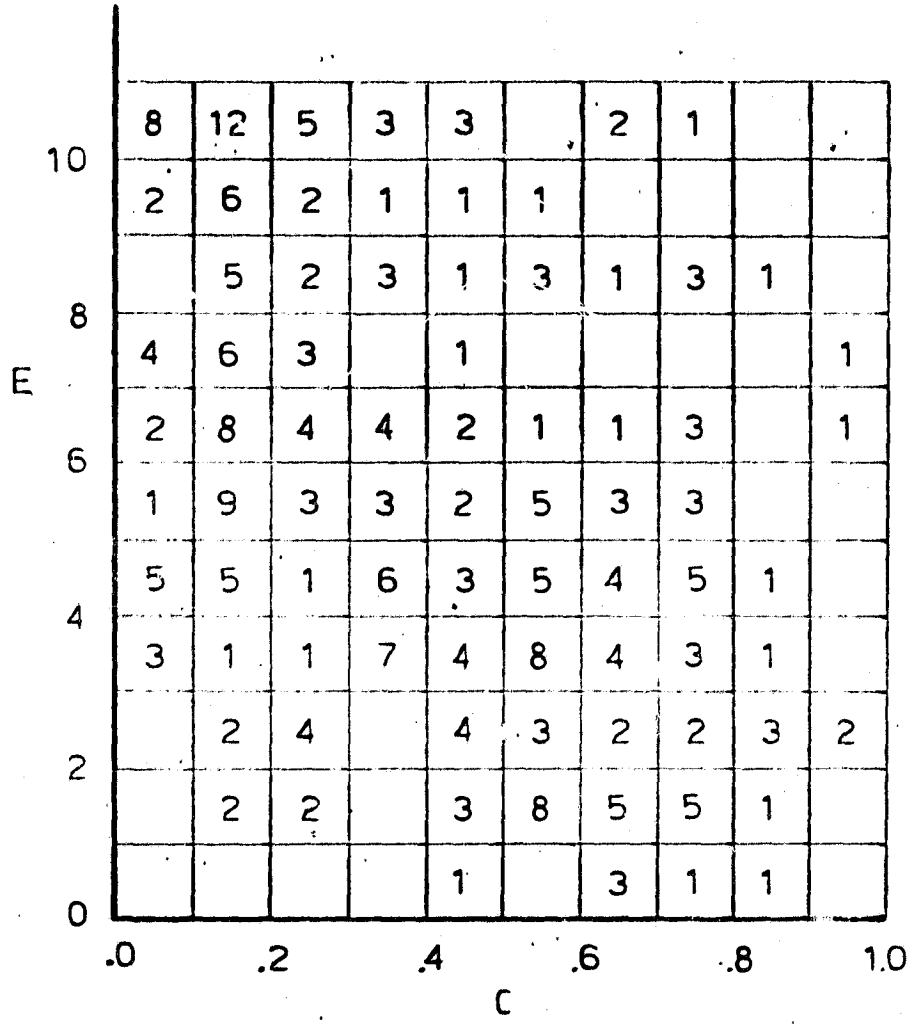

Fig. 12. Two-dimensional frequency plot for the correlation matching process between the day thermal band AA0072131702 and MSS band 5 of the LANDSAT image E-1027-10144, after registration.

Table 4. Summary of the least square fit (2nd degree polynomials) for the HCMM-LANDSAT registration.

Size of the image: 1240 lines x 1240 pixels.

Situation of the points used in the fit (in 25 zones of the image)

1	6	1	2	1
4	3	2	4	0
8	4	6	6	0
3	2	4	3	0
2	0	1	3	0

Total 66 GCP's

Estimated standard deviations for the location error

σ_{PIX} = 1.55 pixels

σ_{LIN} = 1.41 pixels

LANDSAT (152.4 m pixel size) to HCMM image transformation (v and u are pixel and line of HCMM; y and x are pixel and line of LANDSAT).

$$v = 223.8 - 1.433 \times 10^{-1}x + 3.480 \times 10^{-6}x^2 + 2.994 \times 10^{-1}y + $$
$$+ 3.615 \times 10^{-6}xy + 1.430 \times 10^{-7}y^2$$

$$u = -7.183 + 2.682 \times 10^{-1}x + 6.232 \times 10^{-7}x^2 + 1.321 \times 10^{-1}y +$$
$$+ 8.893 \times 10^{-7}xy - 8.003 \times 10^{-7}\ y^2$$

Estimated standard deviations of the registration errors in 25 points of the image.

VERTICAL DIRECTION					HORIZONTAL DIRECTION				
1.3	.6	.7	.9	1.6	1.4	.7	.8	1.0	1.7
.9	.3	.4	.5	1.3	1.0	.3	.4	.5	1.4
.7	.3	.3	.5	1.4	.7	.3	.3	.5	1.6
.7	.4	.4	.7	1.8	.7	.4	.4	.7	1.9
1.3	1.0	.9	1.2	2.3	1.3	1.0	1.0	1.3	2.5

Table 5. Summary of the least squares fit performed as an assessment of the quality of registration between the HCMM and LANDSAT images.

Situation of the points used in the fit (in 25 zones of the image)

3	3	4	1	1
13	5	1	4	0
6	4	7	7	0
6	7	3	4	0
2	1	4	6	0

Total 92 GCP's

Estimated standard deviations for the location error

$\sigma_{PIX} = 2.67$ pixels

$\sigma_{LIN} = 1.82$ pixels

First degree mapping polynomials:

$$v = 0.4098 - 0.5508 \times 10^{-3}x + 1.0006y$$

$$u = 0.4654 + 1.0009x - 0.1413 \times 10^{-2}y$$

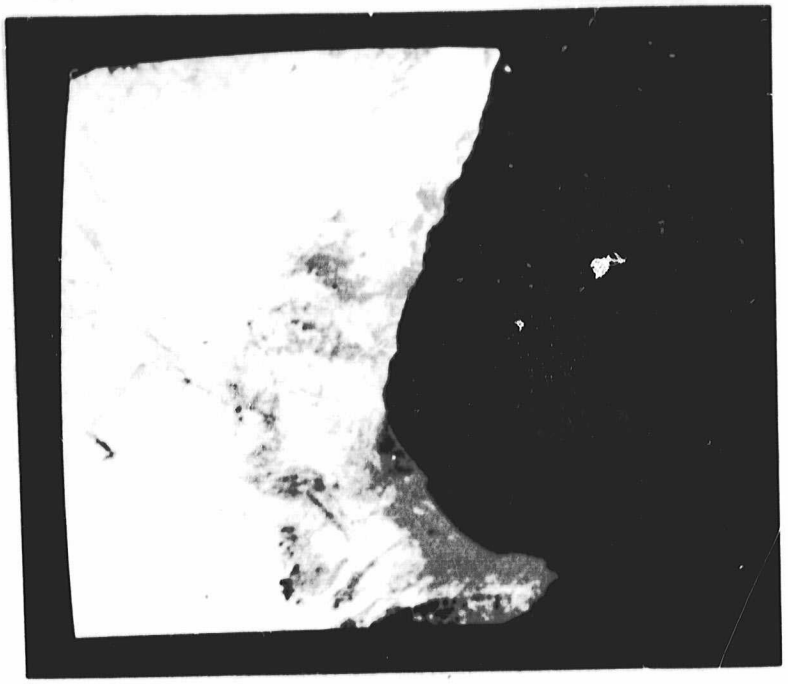

Fig. 13. Temperature difference image obtained by substracting the day and night thermal bands AA0072131702 and AA0072022303.

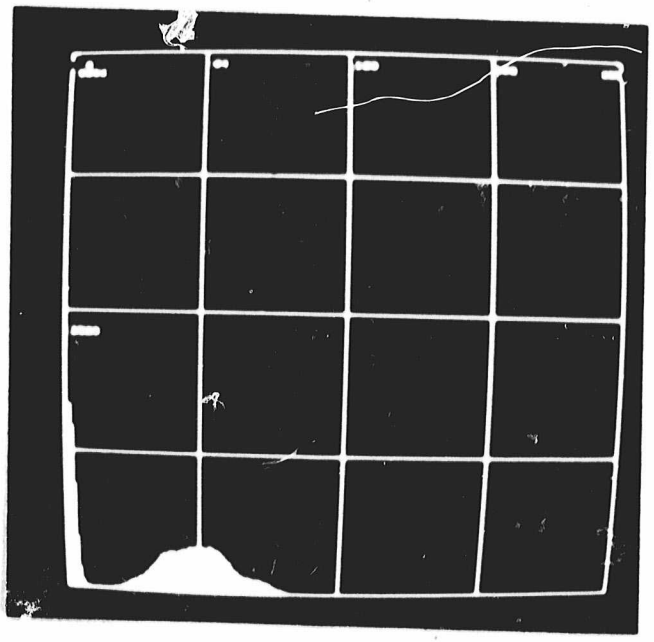

Fig. 14. Histogram of the temperature difference image shown in Fig. 13.

The implementation of this difference program is such that if negative values are found they are set to zero.

From this temperature difference image an apparent thermal inertia one was created by simply taking the inverse of the value of the temperature difference.

The actual algorithm used was the following

$$ATI = A.\frac{255}{\Delta T+1} + B \qquad \text{if} \qquad 0 \leq A.\frac{255}{\Delta T+1} + B \leq 255$$

$$ATI = 255 \qquad \text{if} \qquad A.\frac{255}{\Delta T+1} + B > 255$$

$$ATI = 0 \qquad \text{if} \qquad A.\frac{255}{\Delta T+1} + B < 0$$

where ΔT is the temperature difference, ATI is the value for the apparent thermal inertia, and A and B are two constants to be chosen in such a way as to have a meaningful histogram for the apparent thermal inertia image.

Fig. 15 shows a display of the apparent thermal inertia image and Fig. 16 the corresponding histogram the values used for A and B were 60.0 and -150 respectively.

4. CONCLUSIONS

Two pairs of day-night HCMM images have been superimposed. The registration of the first pair, corresponding to images taken on different dates, show that the use of a linear transformation is not completely adecuate for registering two HCMM images. A pair of second degree polynomials seemed to be more adecuate for this experiment.

In both registration experiments, serious difficulties were found in accurately locating homologous features in the day and night images. The matching of small subimages from the two images, based on the cross-correlation coefficient failed to give proper results, and it should be pointed out that matching of images by a human operator was

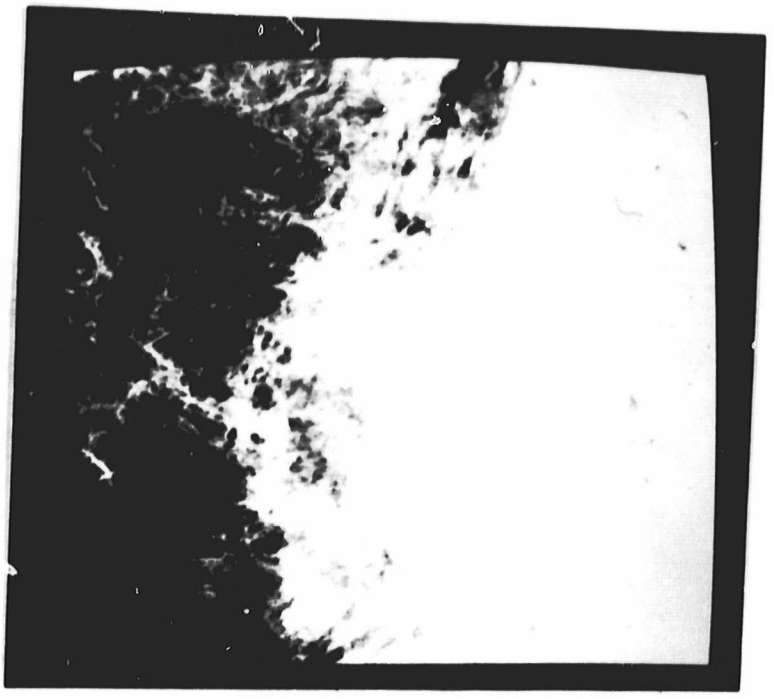

Fig. 15. Apparent thermal inertial image obtained from the temperature difference between the thermal bands AA0072131702 and AA0072022303.

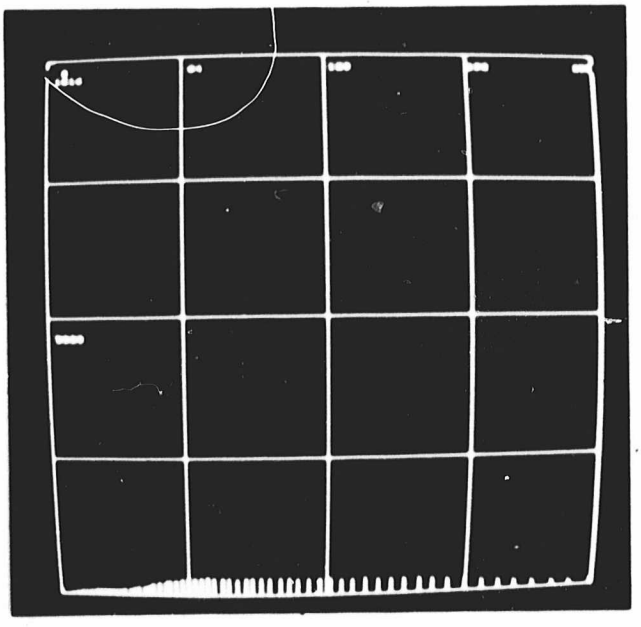

Fig. 16. Histogram of the apparent thermal inertia image shown in Fig. 15.

not without difficulties. Probably the source of the problem was the low high-frequency content in the two night images, i.e. the absence of line structure in them. This cannot be attributed to the spatial resolution of the images, because this relatively fine structure may be seen in both day images used, but rather to the time in which the night images were taken.

Due to the difficulties just stated, the registration process required quite an amount of human intervention and made the registration quality assessment quite difficult.

As for the merging of HCMM and LANDSAT data, only to say that under the image processing point of view appears without problems to do it, and whether it is useful or not it is the applications expert who has to say it, though it is a good way of achieving registration to a ground reference frame.

REFERENCES

[1] Rebollo, M. and Santisteban, A., (1978), "Digital Image Processing Applications at Centro de Investigación UAM-IBM". In Proceedings of the 11th Meeting of the International Commision for Optics. Madrid.

[2] Santisteban, A., (1976), "The Band Ratioing Technique Applied to LANDSAT MSS Images", In Thematic Mapping, Land Use, Geological Structure and Water Resources in Central Spain. Project no. 20760. Final Report to NASA del Instituto Geográfico Nacional. Madrid.

[3] Orti, F., García, A., and Martín, M.A., (1979), "Geometric Correction of MSS-LANDSAT Images using a Ground Control Point Library", In Remote Sensing and National Mapping. Edited by J.A.Allan and R.Harris. Published by the Remote Sensing Society.

[4] Bernstein, R., (1976), "Digital Image Processing of Earth Observation Sensor Data", IBM J. Res. Develop., Vol 20, pp. 40-57.

[5] Svedlow, M., Mc Gillem, C. and Anuta, P., (1978), "Image Registration: Similarity Measure and Preprocessing Method Comparisons", IEEE Trans. on Aerospace and Electronic Systems. Vol AES-14, pp. 141-259.

DIGITAL PROCESSING OF HCMM SATELLITE DATA *

Ramón López Muñiz
Sección de Teledetección
I.G.N.

INTRODUCTION

Since May 1979 we have received three HCMM digital images (Two night passes and a day pass), containing information from the East Coast of Spain (Valencia).

All the works performed up to the present are based mainly on one of these images (number A0067-02300-3), a thermal infrared night image dated July 2, 1978.

The poor quality of the negatives which have been received with the tape, forced us to generate new ones. This has been done by means of "DICOMED" image recorder, with enhaced digital data.

Four areas have been selected from this image:

Zones 1, 2	East coast of Spain
Zone 3	Gibraltar
Zone 4	Alboran Sea
Zone 5	Granada

(See Figure 1).

* REPRODUCED FROM HCM-034 FIRST PROGRESS REPORT

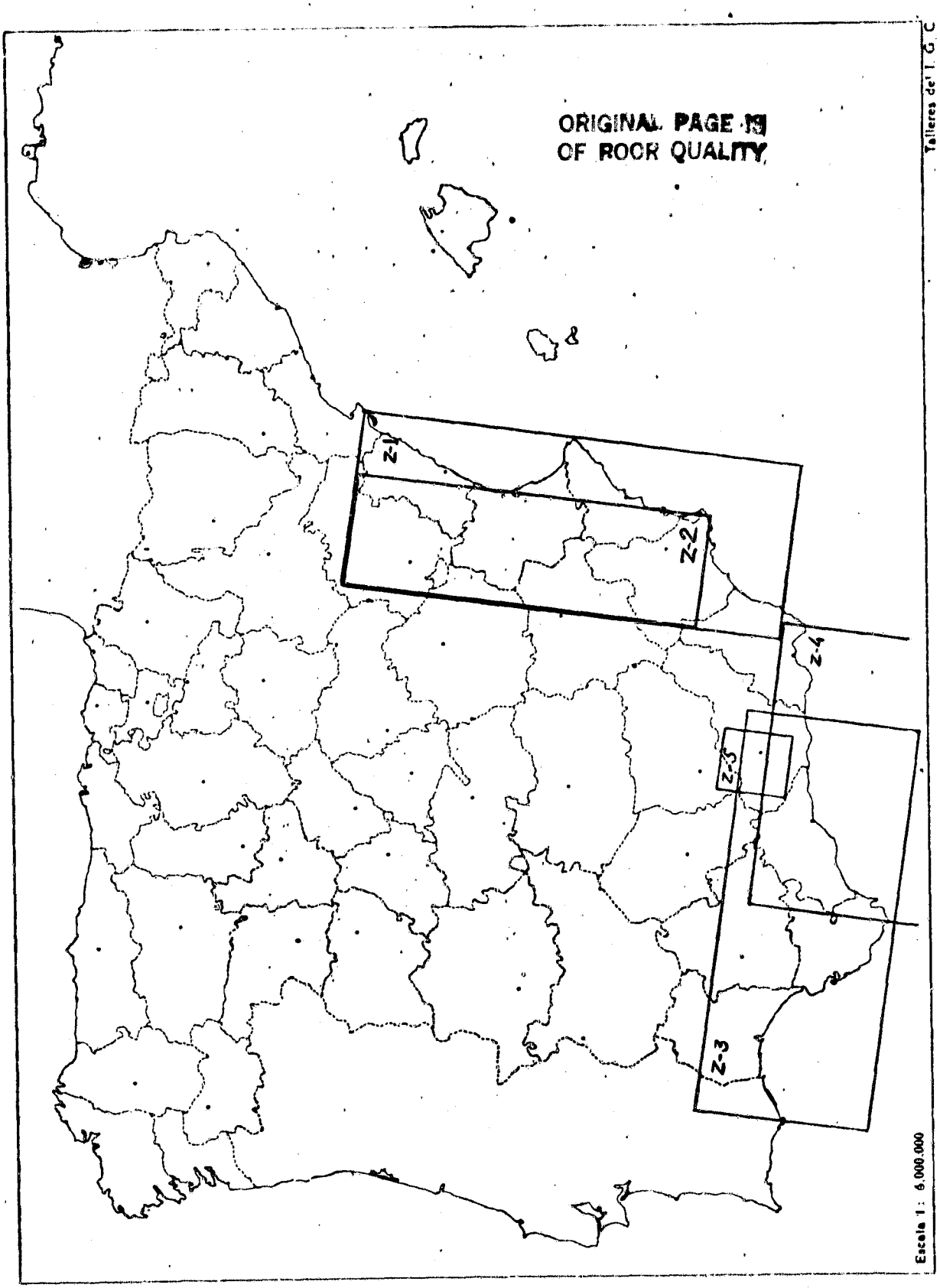

Zones selected for processing

FIGURE 1

RADIOMETRIC CHARACTERISTICS

In the present image (A0067-02300-3), 97 % of the information is contained between levels 27 and 65 (corresponding to -1.5C and 12.5°C, apparent temperatures, respectively); the largest population is to be found at level 61(11.3°C).

The selected areas of this image have the following characteristics:

- Zone 1. Ninety seven percent of the pixel values are distributed within the 26-63 dynamic range, showing a maximum of population at 61.The histogram shows two different peaks, corresponding to ground and sea responses respectively.Level 61 is Medit rranean sea water (fig. 2).

- Zone 2. As it can be observed on the map, this zone contains only the ground responses of zone 1.The dynamic range is from 21 to 53 (-4°C to 8.5°C) having a population maximum at 42 (4.5°C).

- Zone 3. It contains the southern part of the Iberian Peninsula from Huelva to Malaga including the Strait of Gibraltar.Its dinamic range is from 43 to 66 (4.7°C to 12.7°C).

- Zone 4 contains the Alboran Sea and parts of the spanish and moroccan coast.
  Its dynamic range is 41 to 65, having the largest population at 61.

- Zone 5. The last zone selected surrounds Granada.It is of great interest due to the geothermal activity.Its dynamic range is from 29 to 52 and it has a population maximum at 46.

These zones within A0067-02300-3 frame, have been radiometrically enhaced in order to obtain better quality images.

Figure number 3 matchs raw data information from CCT.This photograph has been generated using DICOMED D-47 image recorder.

ORIGINAL PAGE IS
OF POOR QUALITY

FOLDOUT FRAME

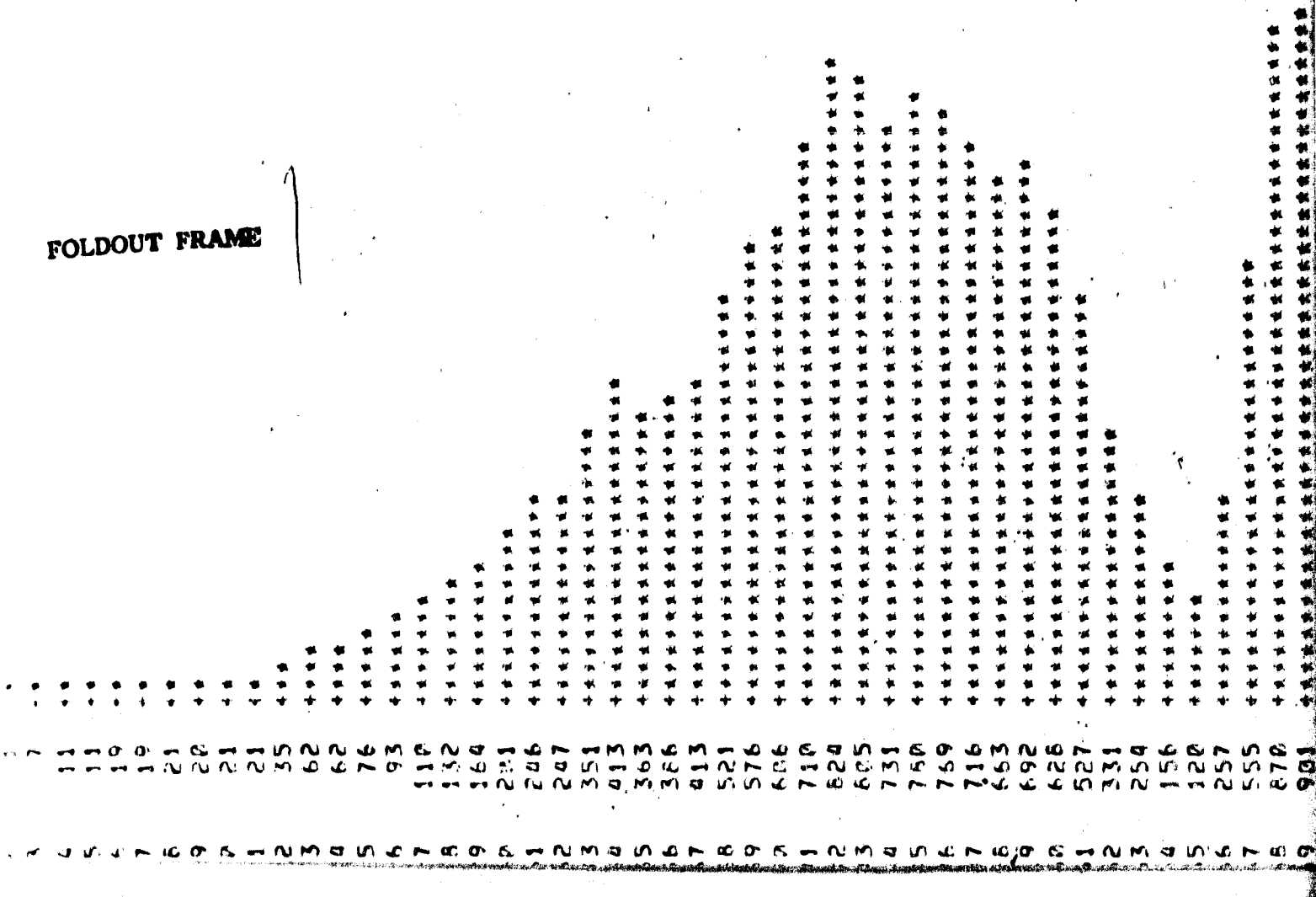

ORIGINAL PAGE IS
OF POOR QUALITY

FOLDOUT FRAME 2

Histogram of values over zone 1.

FIGURE 2

This instrument assigns a different gray level to each digital count within a range of 0 to 255.
The range of this image is narrow and therefore figure 3 shows a very poor contrast.

On the D-47 model it is possible to constrain the range to 64 levels (6 bits) from 0 - 63. Figure 4 shows the results of applying this constraint. It should be noted that on the left of the photograph (low part), several black points appear. These points correspond to pixels with values over 63.

ENHACEMENT OF HCMM IMAGERY

To obtain better quality results, two transformations have been applied to the raw data from CCT:

Linear transformation

$$l = \frac{255}{Max-Min} \quad (i - Min)$$

$j = 0$ if. $l < 0$

$j = l$ if. $0 \leqslant l \leqslant 255$

$j = 255$ if. $l > 255$

where

j = corrected level

i = original level

Max = original level assigned to 255

Min = original level assigned to 0

Uniform transformation

$$j = \frac{d\,(i)}{2} + \sum_{k=o}^{i} d\,(k), \quad \text{being} \quad d\,(i) = \frac{255}{Pt} \quad P\,(i)$$

where

$P\,(i)$ = level i population

P_t = total population

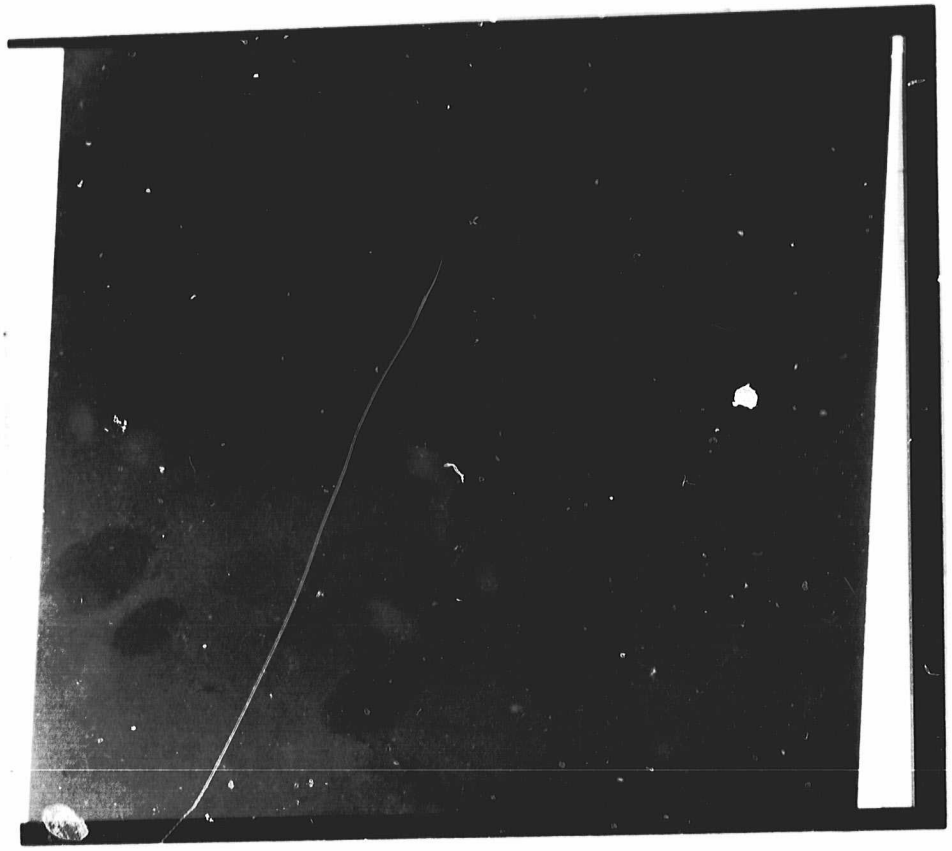

Figure 3 Raw data (8 bits) Image A-0067-02300 - 3

Figure 4 Raw data (6 bits option). Same image as Fig.3

Uniform transformation assigns the same number of points to equal intervals between 0 - 255.

Figure number 5 was obtained after applying uniform transformation to the overall image.

The next figures (number 6,7,9,11) were generated by applying this transformation to the five zones of study.

Finally, figure 10 shows the result obtained when linear transformation is applied to zone 5, as well as figure number 8 over zone 1.

In zone 5, uniform transformation reveals noise present in the image.
A future task will be the evaluation of the noise and its further supression.

Atmospheric soundings over the study zones will enable us to obtain corrected ground temperatures. To perform these corrections the NASA atmospheric correction computer program RADTRA was adapted to the IGN PDP 11/45.

By comparing corrected temperatures with apparent ones as well as with reference data, it is possible to test the goodness of the correction and, in the same way, establish the shift between both pictures.

OBJECTIVES

In this project, we established as objectives the following tasks:

1.- Image Enhacement

We shall enhace the images systematically by using radiometric corrections; therewith we pretend to obtain photographs of a better quality.

On the other hand, we shall test a process in order to supress noise and evaluate the influence of noise elimination on raw data.

2.- Output

In order to make data interpretation easier, we pretend to elaborate several outputs (color and black and white). These are the following:

- Temperature maps (day-night) with both apparent and atmospheric corrected data.

- Maps of thermal inertia

- Image classification maps (using available data).-

- Maps of thermal inertia
- Image classification maps (using available data).-

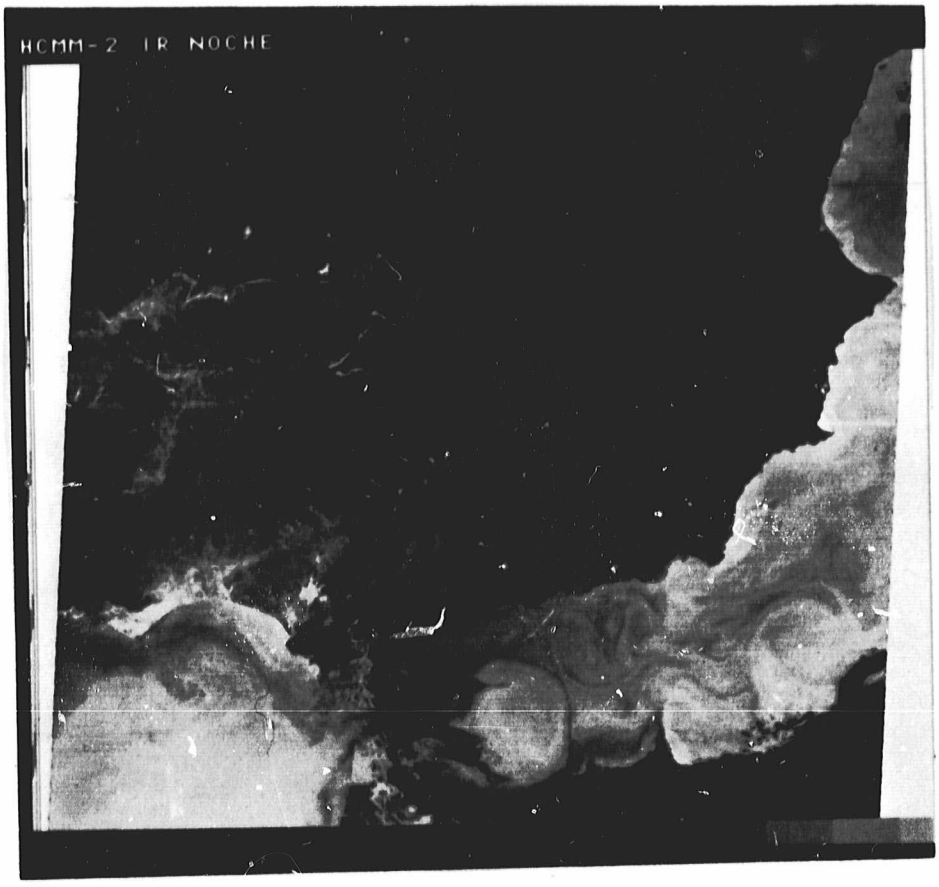

Figure 5. Enhanced data: Uniform transformation
(S.Spain, W. Mediterranean, N.Morrocco, E. Atlantic)

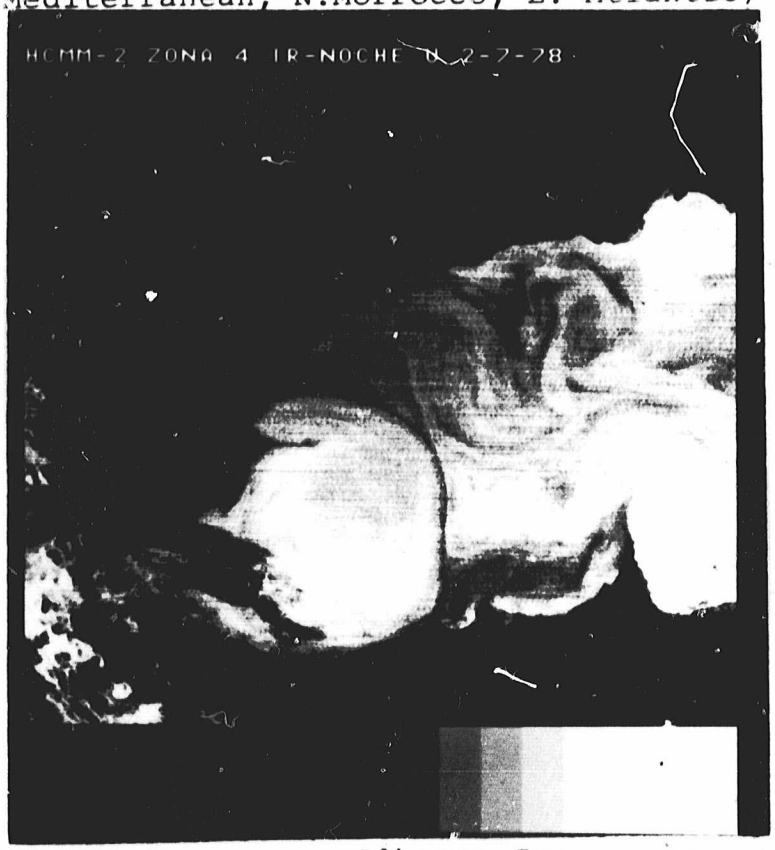

Figure 6: Uniform enhancement. Alboran Sea

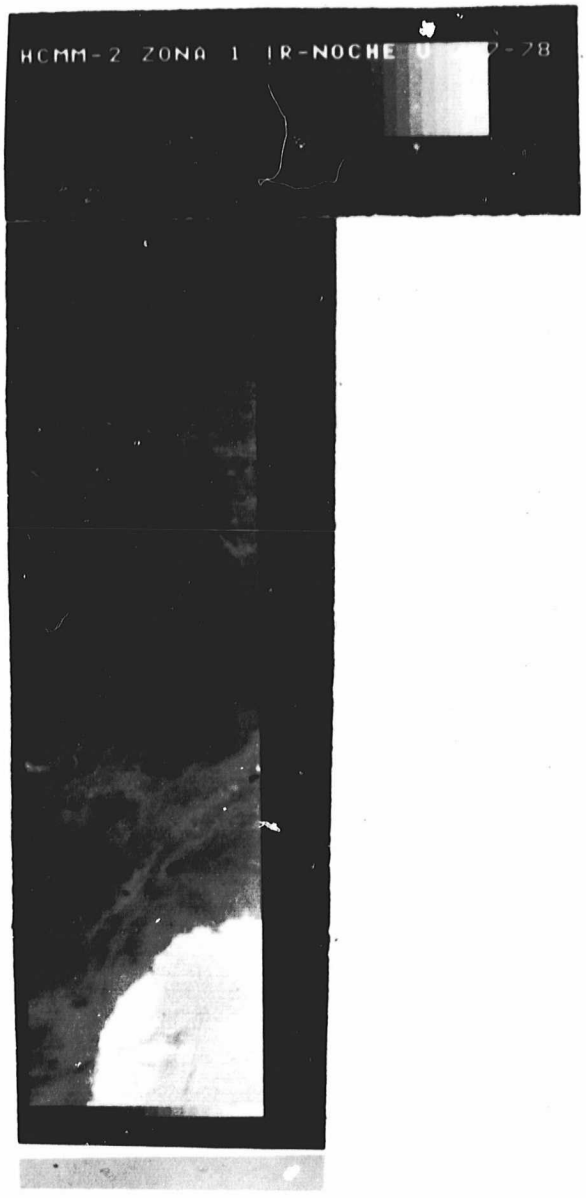

Fig.7
Uniform enhancement
(See shoreline)
Zone 2.

Fig.8
Linear enhancement (stretching) .
(compare top of both images)
Zone 2.

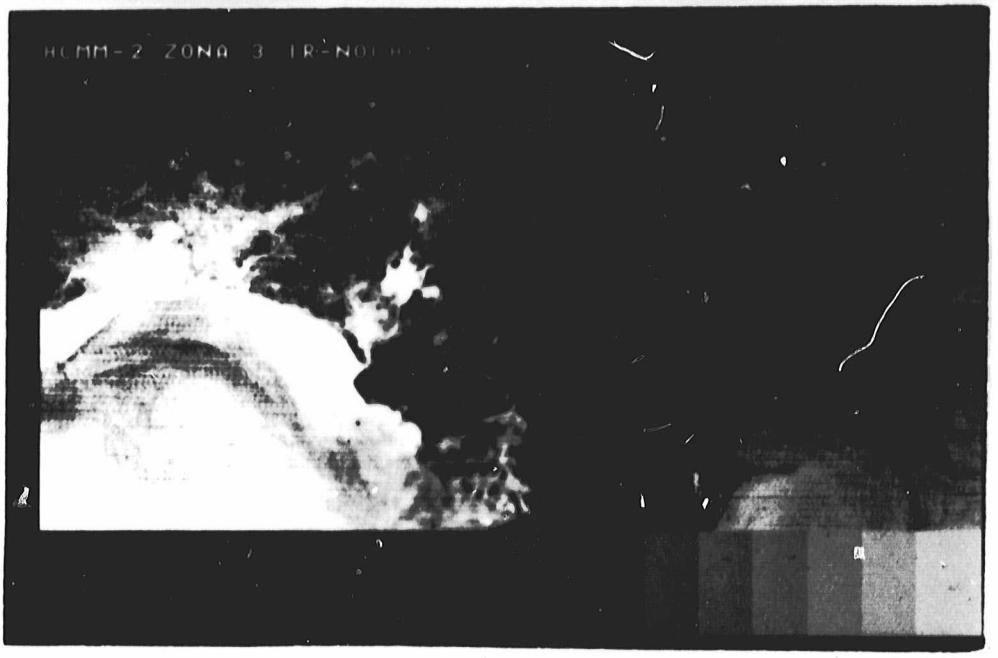

Figure 9
Uniform enhancement: S. Spain, from
Portugal to Almería, and Gibraltar Strait.

Figure 10
Lineal enhancement
Granada and Sierra Nevada

Figure 11
Uniform enhancement
of same area as Fig.10

DIGITAL PROCESSING OF HCMM IMAGES

Ramón López Muñiz
Sección de Teledetección
Instituto Geográfico Nacional

INTRODUCTION

We shall expose the performed works, referred to the processing of digital images and to the obtention of non-conventional cartographical products. The dates and scenes of major interest have been selected out of all the photographical information received from NASA, which is related to the test area of this project.

Unfortunately, in 1978 the number of clear days over the zone of the Spanish Levante were fewer than expected. We selected a series of images out of the photographical positives we had received, and we solicited the corresponding CCT's.

In order to select the images, we considered the following criteria: Absence of clouds, visual quality of the positive and the possibility of forming pairs of day-night images of the same date.- We have received thirty scenes, from which seventeen correspond to day-passes and thirteen to night passes.

OBTENTION OF ENHANCED IMAGES

Lineally enhanced photographic negatives have been obtained from twenty-four images. We used the DICOMED D-47 equipment for visualizing the negative pictures. The method followed for the enhancement is the one described in the First Report of this project, which has been reproduced previously.

The process has been applied to the twenty-four scenes of better quality and greater interest. The criterion applied for the selection was the following:

- Absence of clouds in the greater part of the image.
- Absence of clear-dark bands on the image, due to variations in the response of the IR thermal sensor, or in the gain of its associated amplifier.

Some of these twenty-four selected scenes have been admitted in spite of showing these clear-dark bands (noise); this is due to the fact that the represented scene is of particular interest.

The enhancement applied to all the scenes is the one obtained from expanding lineally the histogram of the most interesting part of the image, the part which excludes the sea and the clouds. Therewith we pretend to obtain a contrast, as vivid as possible, between the gray tones of these zones.

We must stress that a loss of quality, due to a greater presence of noise, has been observed in the IR thermal images that have been taken from the last months of 1978 onwards.

The received CCT images just enable us to form three day-night pairs, which correspond to the following dates: (See Table 1)

07.07.78; 28.7.78; 14.9.78

We must point out that the pair of the 7th of July, 1978, formed by the scenes 72 02230 - 3 and 72 - 13170- 1,2, is the only which covers the test area and has a good quality.

The pair of the 28th of July, 1978, covers an area that corresponds to the Ebro-Valley and part of the Catalunian-Levantine coast, but the night image has a poor quality.

The third pair, shot on September 14, 1978, covers a small part of the test area but the IR day image as well as the IR night image show the presence of "noise".

Consequently, the pair of September 7th, 1978, has been the only profitable for this project.

TABLE 1.

HCMM IMAGES IN CCT FORMAT PROCESSED AT IGN

	Images		
05/11/78	1513510	1,2*	Spain except Andalusia.
05/31/78	3502330	3 *	Southern half of Spain and the Strait of Gibralta
06/01/78	3613440	1,2	" " " " cloud-free, the coast only
07/02/78	6702300	3 *	Spain except Catalonia, Cantabrian area and Galic
07/07/78	7202240	3	Andalusia, Strait of Gibraltar and North Africa.
07/07/78	7202230	3 *	Spain except Andalusia and Galicia.
07/07/78	7213170	1,2*	The valley of Ebro River, east Spain and Cataloni
07/08/78	7313350	1,2	Spain, except Andalusia, Estremadura and Galicia.
07/08/78	7313330	1,2	Andalusia, Strait of Gibraltar and Africa.
07/28/78	9302130	3 *	Eastern half of Spain.
07/28/78	9313070	1,2	South of France, Pyrenees, valley of Ebro River and north-east Spain.
07/29/78	9413250	1,2*	North-east quarter of the Iberian peninsula.
07/29/78	9413230	1,2	Alicante and eastern Andalusia.
08/19/78	11513130	1,2	Valencia, Alicante, Almería, Albacete.
09/14/78	14113000	1,2	South of France, valley of Ebro River, Catalonia, the Albufera de Valencia (coastal lagoon in the Mediterrancan).
09/14/78	14102050	3 *	Spain except the north-west area, Andalusia, Estremadura.
09/15/78	14202240	3	Interior of the peninsula, the coast of eastern Andalusia.
09/26/78	15313220	1,2*	Center and south-east Spain.
10/28/78	18513160	1,2*	South-eastern quarter of the Iberian peninsula.
10/28/78	18513180	1,2	Palencia, Cantabrian area, the valley of Ebro River, Pyrenees.
11/02/78	19013090	1,2*	East Spain, Cuenca, Albacete.
11/03/78	19113270	1,2	The Iberian peninsula except Catalonia, Cantabria area and Galicia.
11/12/78	20002010	3	Center, south-eastern quarter of the peninsula (mists).
11/17/78	20501550	3 *	East Spain, eastern Andalusia, Catalonia (mists).
12/29/78	22713010	1,2*	Valencia and the valley of Ebro River.
12/29/78	22712590	1,2	Alicante, Cartagena, Almería.

* Includes part of HCM-034 test area

OBTENTION OF Δ T, APPARENT T.I. IMAGES AND OTHER NON-CONVENTIONAL PRODUCTS

In order to attain this object, the IBM-UAM Center has taken two images , which cover the area of the Levantine Coast that goes from Tarragona to Alicante, and has accomplished the registration of the night subscene with the day subscene of the same area.

By using this geometrically registered images, images of apparent difference of temperature (day-night) and apparent thermal inertia have been obtained.

Figure n°1 corresponds to the registered subscene (700 x 700 pixels) in false color. Blue has been assigned to the visible band, green to the day IR and red to the night IR.
The three bands have been enhanced independently by transforming uniformly the histogram of a subscene, which excluded most part of the sea and the clouds.

Figure 2 corresponds to the apparent Δ T day-night image.
The enhancement applied to this image makes the level 0 (black) correspond to a Δ T = - 2,75°C; sea water is characterized by a ΔT = 0,75°C and the values of the soils vary from ΔT = 13°C to ΔT = 28,5°C.

Figure 3 corresponds to the image of apparent thermal inertia, generated from the ΔT image and albedo; the algorithm used for the production is the one indicated in the "User's Manual" of this project:

TI = NC (1-a)/ Δ T. The values of this image thermal inertia are characterized by the following parameters:

Local time = 13 h 37 m

Solar declination = 22°23'

Latitude = 39°30'

These values are applicable to the center of the generated subscene.

ORIGINAL PAGE
COLOR PHOTOGRAPH

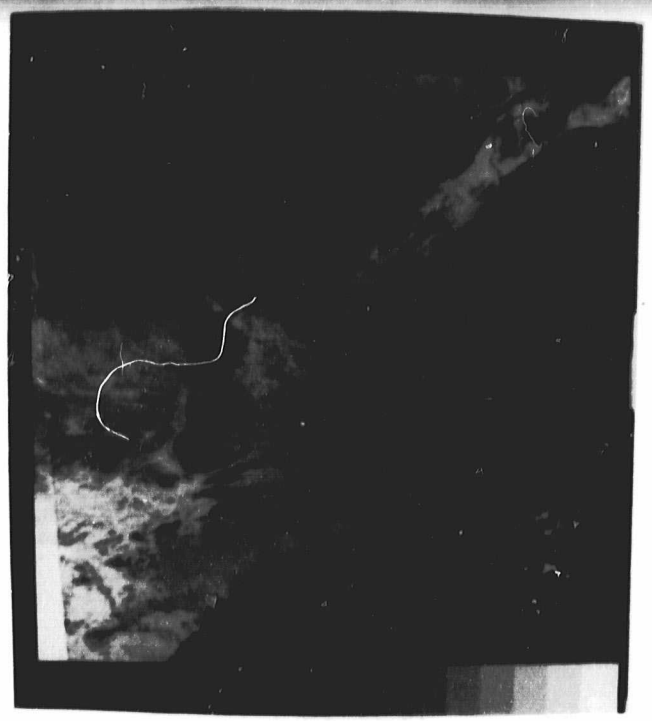

Figure 1

False color composite of night-day registered subscene in E. Spain; July 7, 1978 (night IR: red, day IR: green, visible: blue)

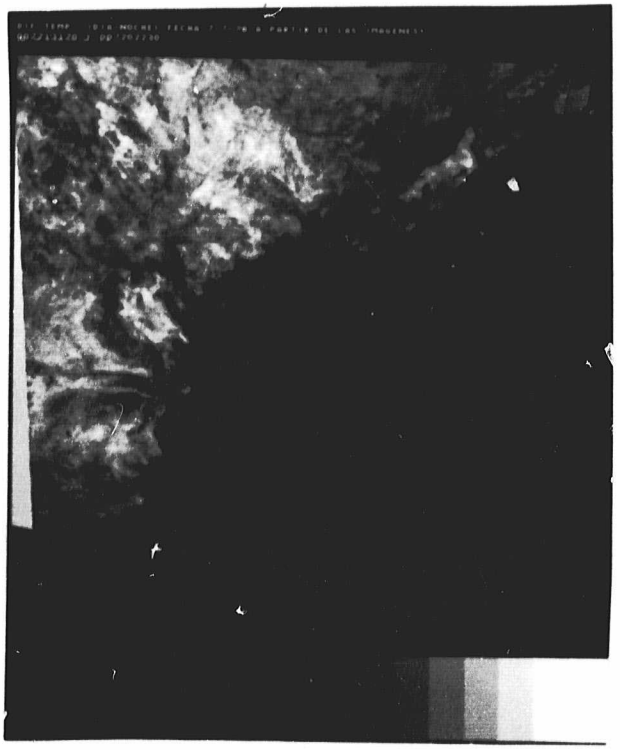

Figure 2.

Temperature difference of above subscene.

Figure 3.

Thermal inertia of above subscene.

Clouds are detected in the lower portion of the day-pass image.
Owing to the aforementioned clouds, a discontinuity appears in the ATI values.The reason is the following:

The values of the area of clouds are characterized by a ΔT (fictious) within the range -1°C to 0.5°C.- As the central zones of the clouds have a characteristic lower temperature, they generate TI values < 0, which were assigned to zero.-

The most external points of the clouds, however, generate values of $\Delta T \simeq +0°C$ which gives place to very high thermal inertia values.
By similar reasoning, we can explain the presence of dark horizontal and oblique lines over the sea, originated by noise.

NOISE REDUCTION

As previously stated, we have detected a loss of quality in the IR thermal images, which is due to the presence of darker horizontal bands (areas with a smaller response than expected).
This has forced us to reject a great number of images.The night image of September 14, 1978 for example (141- 020508), which belongs to one of the day-night pairs, was excluded for this reason.

We have tried to solve this problem by applying to the image the following procedure: As a first step we have described the "noise" that appears on the image.

Noise Description

Figure 4 represents the sum of pixels of one line S(j), versus line number j.

It can be seen that from line 350 to line 680 fluctuations appear in the S (j) values, which have a tendency to diminish its value.The same occurs from line 1130 to the end of line 1440.The fluctuations are characterized by a lack of periodicity and by a variable magnitude of fluctuation.

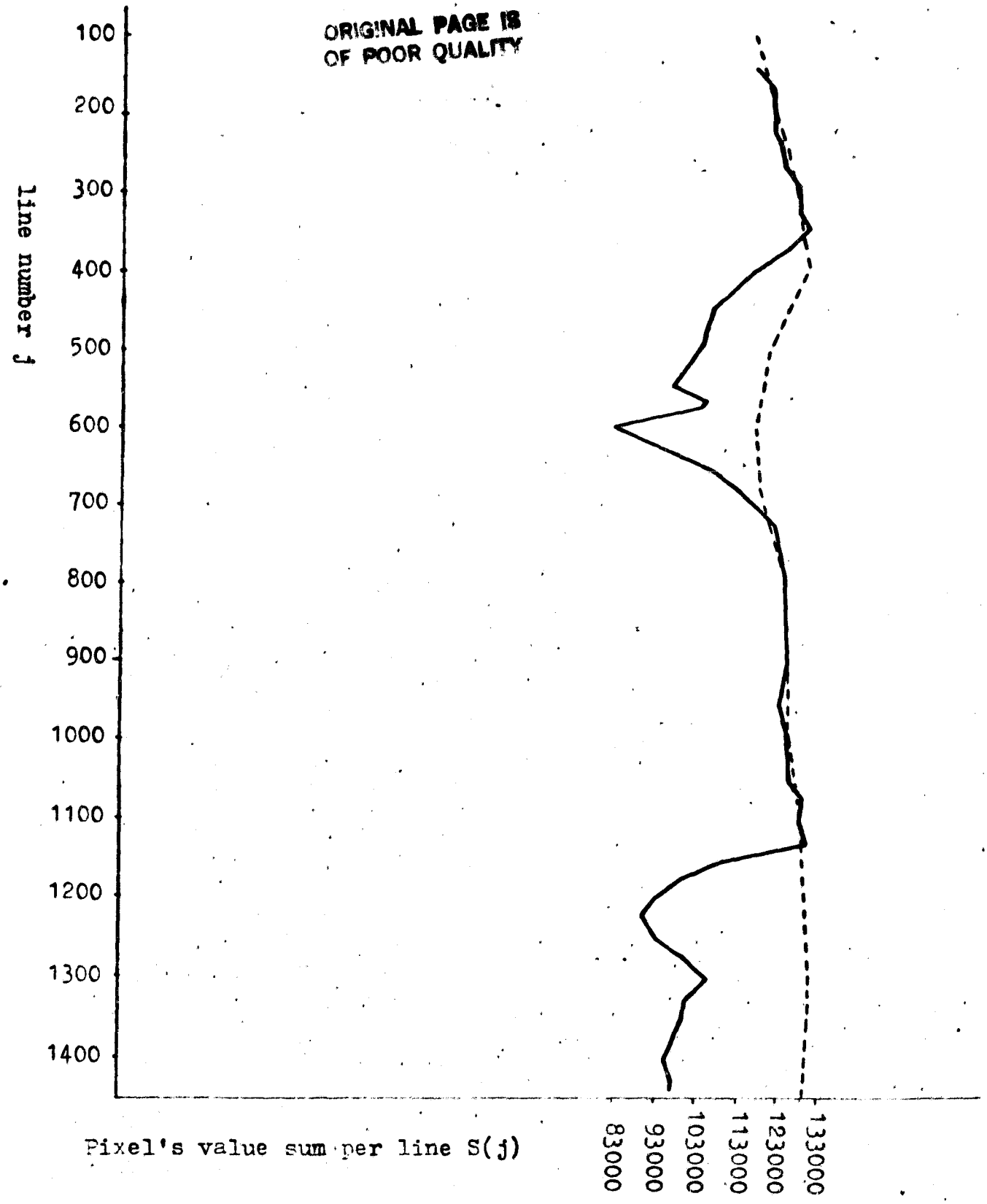

Figure 4. Pixel's value addition per line, in original (——) and corrected (- - -) image. September 14, 1978.

The correction of the noisy image was carried out as follows:

The sum S (j) of the pixel values of line j with $1 \leq j \leq 1440$, has been applied to all the lines of the image (represented by the continuous curve of figure 4).- We detected the zones which present sharp variations in these values.

We have determined, as shown below, 15 values for the sum of pixels (we shall name them SP), which are uniformly distributed throughout the image, thus smoothing the sum of the pixel values. These values coincide with S (j) in areas without noise (see figure 4).

The choice of SP values for zones where fluctuations exist is problematic. The study of noise areas has enabled the obtention of SP values by extrapolating them from the S values of areas without noise. Therefore we have considered the following:

1.- That the water-land percentage of a noisy area has to be similar to that of an area without noise.

2.- That clouds diminish the value of S (j).

The obtained SP values enable us to obtain a new series of S' (j) values by interpolation (see figure 4, dotted curve):

$$S'(j) = SP(K.100) \cdot C_1 + SP((K+1) \cdot 100)\, C_2$$

being $1 \leq j \leq 1440$ and $1 \leq K \leq 15$;

K has to comply that $K \cdot 100 \leq j \leq (K+1) \cdot 100$.

The constants are:

$$C_2 = \frac{j - K \cdot 100}{100} \quad , \quad C_1 = 1 - C_2$$

S' and S values enable us to obtain new values p' for each pixel by means of:

$$p'(j,i) = p(j,i) \cdot \frac{S'(j)}{S(j)} \qquad \begin{matrix} 1 \leq j \leq 1440 & \text{line number} \\ 1 \leq i \leq 1680 & \text{pixel number} \end{matrix}$$

Figure 5 corresponds to the unprocessed image.
Figure 6 shows the result of the correction. Descompensation between zones has been eliminated, though "minor variations" between lines of a smaller periodicity still remain.

This correction has improved considerably the quality of the image, so that it is valid for a qualitative analysis (fotointerpretation).
Its application to quantitative studies however (obtention of temperature measurement) is questionable because of the modification which has been carried out in the pixel values.

In order to check the quality of the above mentioned correction, we have performed the following test:

The apparent temperature of three cities has been determined: Barcelona, Zaragoza and Valencia.- Barcelona and Zaragoza belong to the area of the image which has not been affected by noise, while Valencia belongs to the corrected area.

	Image Coordinates (line,pixel)	Apparent temperature (°K) Original Image	Apparent temperature (°K) Corrected Image
Barcelona	789, 1199	294.5	294.5
Zaragoza	688, 825	293.8	294
Valencia	1287, 836	289	296

Table 2. Apparent temperatures from the original image, and the corrected image.

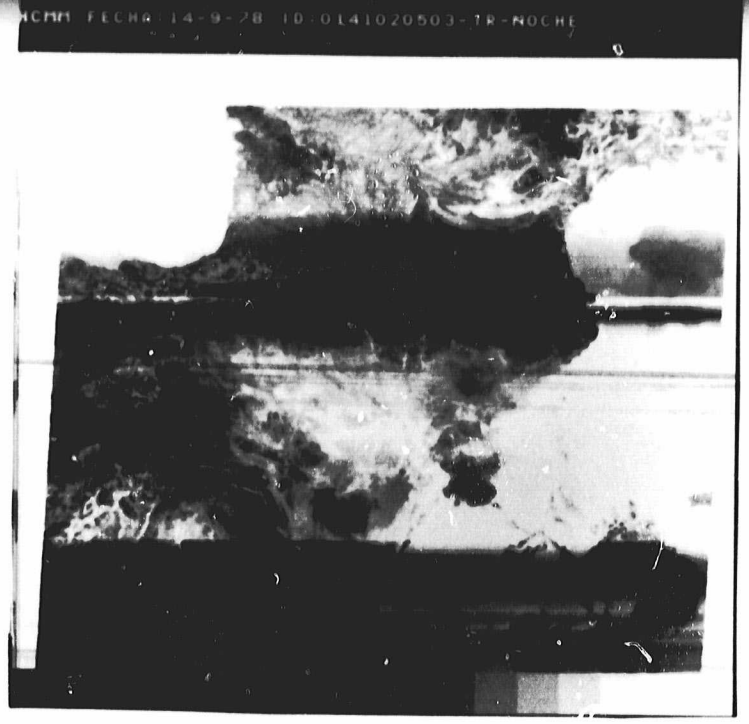

Figure 5.
Noisy night image (N.E. Spain) September 14, 1978

ORIGINAL PAGE IS
OF POOR QUALITY

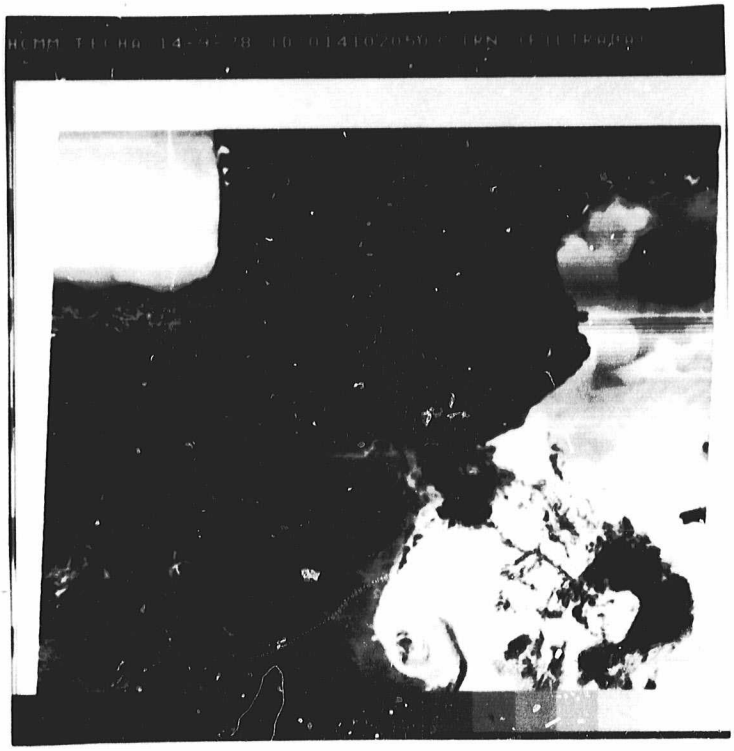

Figure 6.
Noise filtered night image; compare with above figure

ORIGINAL PAGE
BLACK AND WHITE PHOTOGRAPH

The National Meteorological Institute performs daily atmospheric soundings at Midnight and Noon in La Coruña, Madrid and Palma de Mallorca.

The test area of this project lies approximately between these two last cities. As the data of Palma de Mallorca's midnight sounding showed the presence of clouds, we used the data of Madrid's (Barajas) midnight sounding of September 14th, 1978 for determining the atmospheric correction.

Making use of John Price's program RADTRA, we obtained the following results for the three cities:

Barcelona

$T = 1.240\ T_s - 70.05$ Angle of view = 15.8°

Zaragoza

$T = 1.233\ T_s - 67.93$ Angle of view = 7.7°

Valencia

$T = 1.230\ T_s - 67.06$ Angle of view = 0.30°

The following table shows the results of the correction, as well as temperature field data, which have been obtained by thermographs of the meteorological boxes in each city at the time of the satellite's overpass.

TABLE 3

	Apparent temperature (°K)	Corrected temperature (°K)	Ground-Truth Temperature (°K)
Barcelona	294.5	295.1	292.8
Zaragoza	294	294.5	291.2
Valencia	296	297	296

In this image in particular, temperatures ranging from 20 to 24°C, show that the atmospherically corrected satellite temperatures are above the temperatures measured on the field.
The correction made on this image has raised the response of noisy areas to the point of obtaining area temperatures coherent with the rest of the values.

CONCLUSIONS

All the received data, the photographical positives on one hand and the CCT's on the other, show a loss of quality due to the presence of noise on the IR thermic images; this loss of quality is evident both on the day-images and on the night images.This presence of noise is responsible for errors, which can reach 10°C in some areas.

Some visible images show a similar phenomenon (noise of a larger frequency); this perturbation however is of small importance compared to that of the thermal IR.

We have to emphasize that there is another factor which can lead into error when measuring temperatures from satellite data: The presence of mists, which has been detected mainly on the images of autumn 1978.

On the other hand, we must point out that the IR thermal sensor seems to be out of calibration: the apparent temperatures and those measured on the field are different, and this difference can't be compensated applying the atmospheric correction, which is of about 1°C on the processed images.

In these conclusions we have to underline as a significant result the following:

The combination of two passes of the same area, a day-pass and a night-pass, reflect the orographic and climatic characteristics of the zone. This result appears on false color images as well as on images of thermal inertia.We consider it a significant result, though we must say that the present satellite resolution is certainly not the most adequate for the study of the test area of this project, nor for the study of the rest of the Iberic Peninsula.-

THERMOLOGY

C.- THERMOLOGY

-"Thermal Mapping in the Agricultural Area of Valencia"

Joaquín Meliá & Vicente Caselles

Universidad de Valencia

-Note on "Analisis del campo de Temperaturas proporcionado por el Satélite HCMM en la Zona Agrícola de Valencia"

M.Sc. Dissertation.

Vicente Caselles Miralles

Universidad de Valencia

THERMAL MAPPING IN THE AGRICULTURAL AREA OF VALENCIA

J. Meliá
V. Caselles

Departamento de Termología
Universidad de Valencia

INTRODUCTION

Our first objective in the use of radiometric measurements, as supplied by the HCMM satellite is directed towards agricultural meteorology. We are particulary interested in the study of surface temperature.

It is well known that this temperature shows important local fluctuations, and this makes its determination by "in situ" measurements very difficult. For this reason, it is very useful to have a global map of the earth's surface temperatures, similar to that given by the satellite. Checking the "in situ" measurements with those of the satellite, we can get a better estimate of the surface temperature.

This report shows our first results.We have to point out that, due to the small number of pictures received and to the delay, the inicial project had to be modified.

STUDIED AREA

We centered our study in an area of 20 km, that runs along the coast of Valencia, from the Cape of Cullera to Puzol.This area is showed in figure 1. This map also shows the positions where the truth stations were placed. These stations belong to the Instituto Nacional de Meteorología.

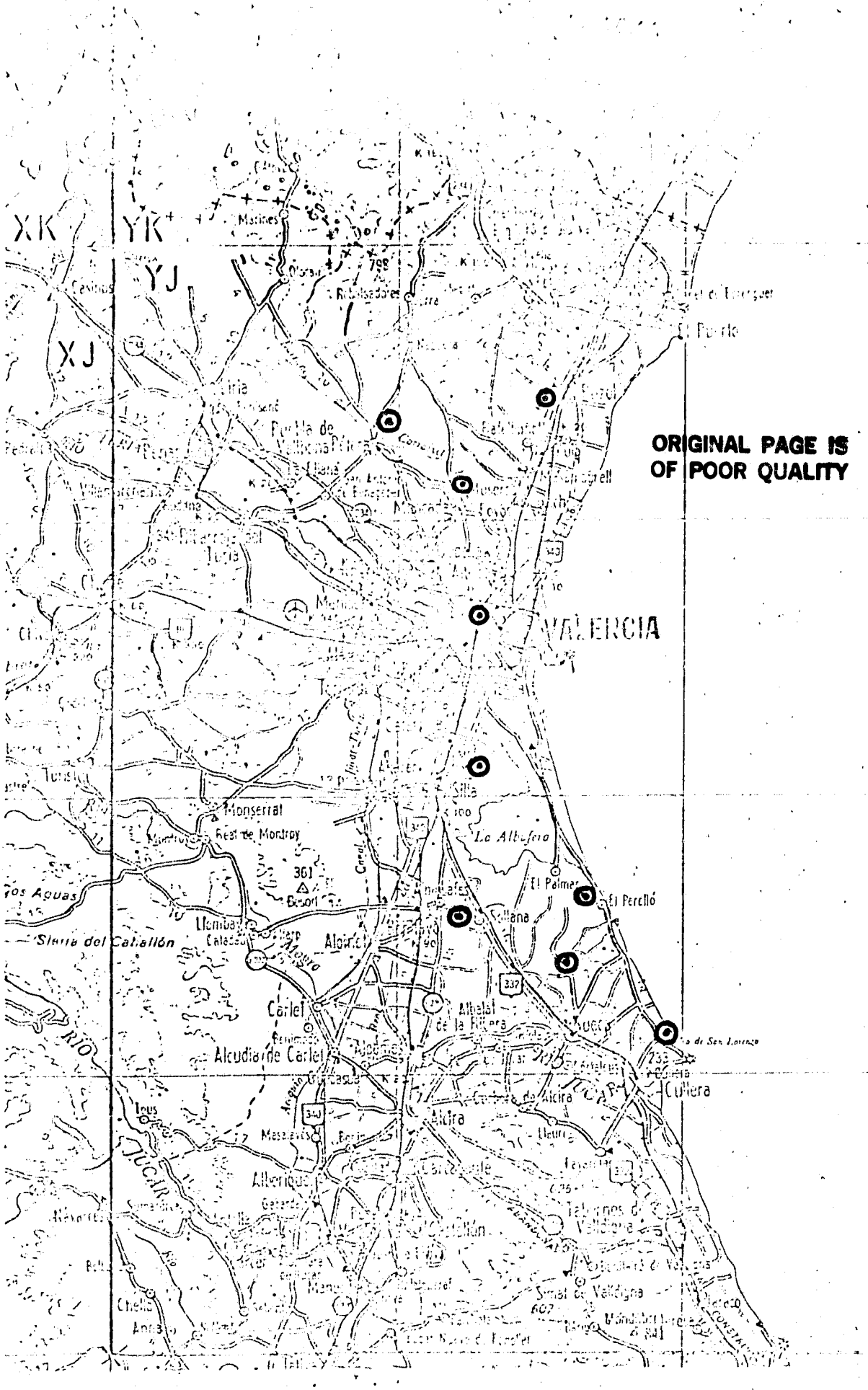

Figure 1

Map showing location of area studied in this report
⊙:location of ground-truth station (I.N.M.)

ANALYZED MEASUREMENTS

We shall present the results derived from the digital images of the thermal infrared channel that correspond to the 7th of July, 1978 (day and night data), and the 2nd of November 1978.

As measurements by our own network were not available, we used air temperature data at an altitude of 1.5 m, in those places shown on the map, as gathered by the Instituto Nacional de Meteorología.

PREVIOUS ANALYSIS

The satellite-obtained measurements over an homogeneous surface of water, whose temperature and albedo were supposed to be uniform, proved that accidental errors affect the albedo 0'4 % and the temperature 0'3 to 0'4°K, as a result of quantification of the digital signal (0-255).

In this zone, the computed standard deviation of temperature coincided with the accidental error (0'4°K); the albedo, however, is 0'7 %, thus higher than the accidental error.

LOCATION IN THE DIGITAL PICTURE OF THE GROUND STATIONS

Due to the lack of facilities, we were obliged to locate the truth stations on the digital image by hand. We based our work on the discontinuity of the coast: With a topographic map of the area and an auxiliar grading, we obtained a correlation between geographic coordinates and pixel, with an error of about half a pixel.

ATMOSPHERIC CORRECTION

Using the RADTRA program, with few modifications, we found that for the range of studied temperatures, the atmospheric correction is about 1-2°C.

For this correction we were forced to use the soundings performed in Madrid Barajas and in Palma de Mallorca, as soundings are not available in Valencia. The computed error with this correction is about $\pm$ 0'2°C.

After doing the necessary atmospheric correction of the measurements taken "in situ", T_{IM}, we compared them with those registered by the satellite, T_{SAT}, thus obtaining the equation:

$$T_{IM} = 13'17 \exp (0'02\ T_{SAT}),$$

for the range of temperatures $7 < T_{SAT} < 25$ °C ,

with a correlation coefficient, r $r = 0'95$.

Figure 2 represents the adjustement of the experimental points which have been obtained.An error appears systematically in the calibration of the thermal infrared channel, so that the apparent temperatures (T_{SAT}) are always inferior to those registered "in situ", even after the atmospheric correction.

This difference in quantity ΔT corresponds, in the interval studied, to the following equation:

$$\Delta T = 27'8 - 9'1 \text{ Ln } (T_{SAT})$$

IDENTIFICATION OF HOMOGENEOUS ZONES

These temperature measurements provided by the satellite enabled us to determine different zones with a doubtless thermal homogeneity.

We were able to identify six areas, as indicated on the map (fig.3). We believe that the detrmination of areas of equal temperature is of great interest for agrometereological purposes.

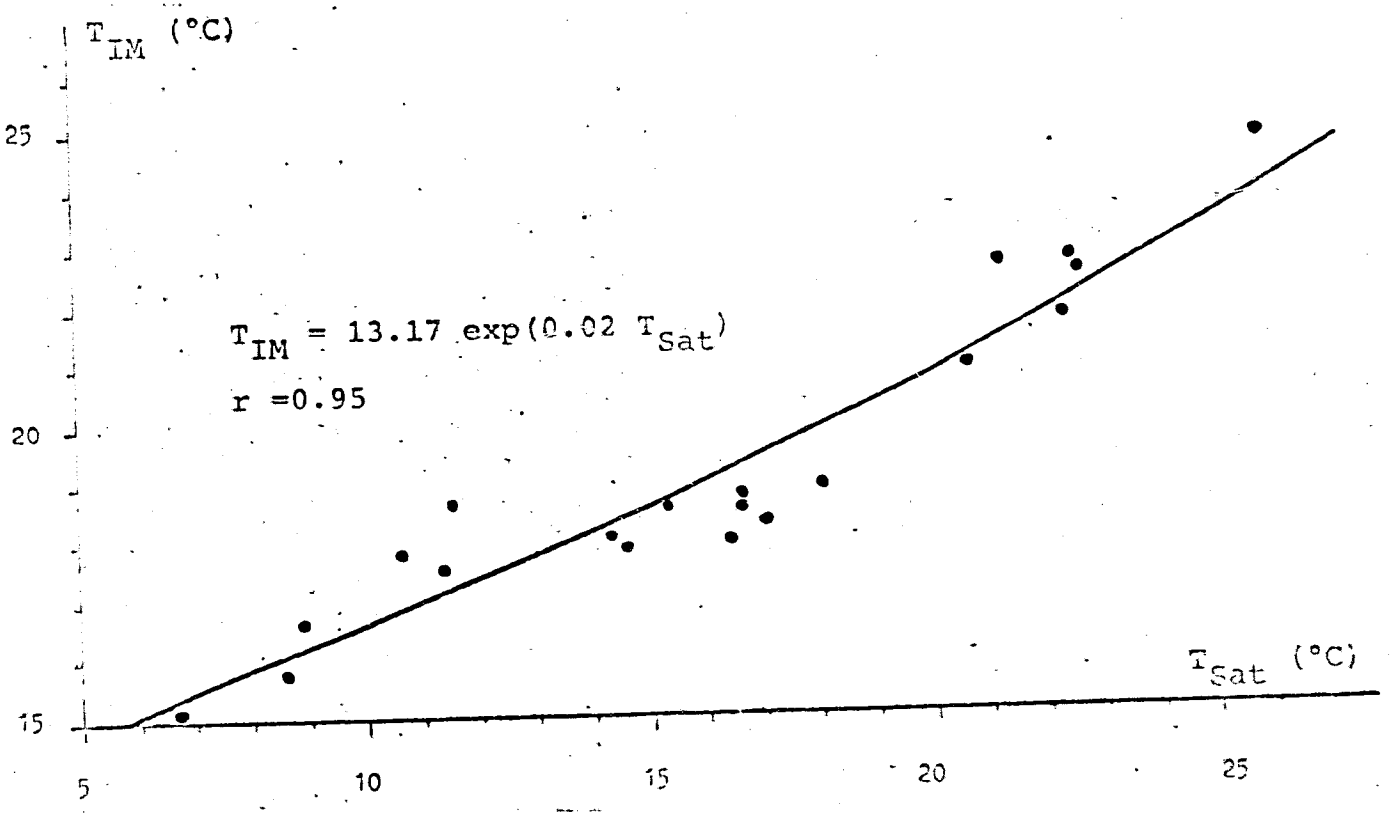

Figure 2

"In situ" temperature measurement (T_{IM}) versus satellite derived temperature (T_{Sat})

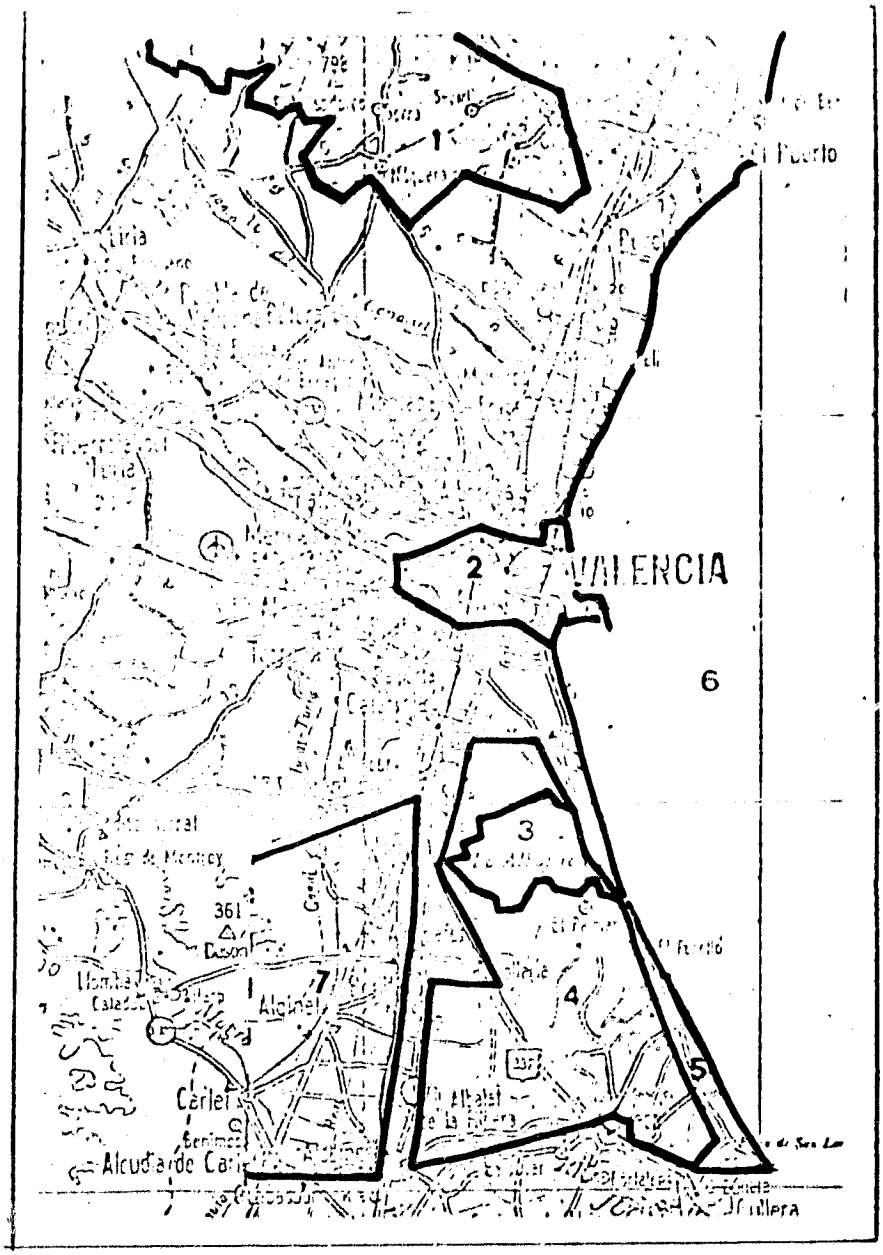

Figure 3

Different thermal areas correlated to land cover areas, identified in HCMM images (July 7 and November 2, 1978):

1 Conifers
2 Urban (Valencia)
3 Lagoon (Albufera)
4 Rice fields
5 Sand
6 Mediterranean Sea
7 Orchards

M. Sc. Dissertation

A M. Sc. dissertation in spanish, entitled "Análisis del campo de temperaturas proporcionado por el satélite HCMM en la zona agrícola Valenciana", has been presented by - Vicente Caselles Miralles, under the direction of Dr. Joaquín Meliá Miralles.

The main results have been exposed in the preceding paper.

Copies of the above dissertation can be requested from - the author.

OCEANOGRAPHY

D.- OCEANOGRAPHY

- "Note on the Use of the HCMM Data in The Alboran Sea"
  Gregorio Parrilla
  Instituto Español de Oceanografía

NOTE ON THE USE OF HCMM DATA IN THE ALBORAN SEA

G.Parrilla
Instituto Español de Oceanografía
Madrid.

SUMMARY

A mainly qualitative comparison between the distribution of surface isotherms on the Alboran anticyclonic gyre and a HCMM satellite summer image, has been performed.
Although the data correspond to different years and the absolute values differ, the situation and the temperature differences between isotherms are very similar for both pictures.We believe that the satellite data could be useful for helping to solve partial questions in the variations of the gyre.

GENERAL DESCRIPTION OF THE ALBORAN SEA

The Meditarranean Sea is a concentration basin.The loss of water by evaporation is higher than the gains by rain and river run offs, because of the dry and arid climate of the zone; however the contribution of water from the Atlantic that flows through the Strait of Gibraltar helps to keep the water balance.At the same time, some Mediterranean water flows to the Atlantic Ocean, so that the salt budget is being mantained.- The inflow from the Atlantic has an average of about 10^6 m^3 sg^{-1}, which means that the Mediterranean waters are renewed in a period of about 100 years.

The Alboran Sea is the westernmost basin of the Mediterranean, limited by the Strait of Gibraltar and the 0°30'W meridian.Its mean depth is around 1000m and its maximum depth about 2000 m.
In this sea, very different water masses are superimposed: relatively fresh water flows to the East on the surface,and to the West flows,deeper, Mediterranean water of a higher salinity .

C-2

For the purpose of this report, we shall describe the Atlantic water. Its path is peculiar, mainly between Gibraltar and the 3°W meridian. Here the water forms an anticiclonic gyre, after entering the Strait (fig.1); this gyre has about 40 nautical miles in diameter and has a relatively strong thermal front in its northern part. This gyre has been detected in most of the oceanographical works made in the Alboran Sea, in satellite imagery, and it has also been reproduced in experimental laboratory models (Whitehead and Miller, 1979).

Giving a general description, the gyre has a negative horizontal temperature gradient from its center outward, which is stronger in the North (order of 0.1°C km^{-1}); this gradient is to be found in all seasons (Fig.2, 3 and 4).- Its salinity is lower than that of the surrounding waters, according to its atlantic origin (fig.5).
Almost all scientists who have studied this gyre have demonstrated its permanence; on the other hand, it has been verified that its location shifts frecuently, and relatively fast. How? This is a question whose answer satellite data may help to find.

DATA

The data used in this work belong to different sources.The oceanographical information has been given by the Spanish Data Center and NODC files, while satellite data are taken from HCMM images.Both data are from the same season (summer), but unfortunately, from different years.We hope to avoid this in the future and work with whole sets of data from different seasons.

METHOD AND RESULTS

The comparison between oceanographical and satellite data has been mainly qualitative, due to the fact that the absolute values of temperature given by satellite are quite different from the oceanographical ones, though there is a great resemblance between them.

From the data of a NATO cruise the Summer of 1962, in which the Spanish boats "Xauen" and "Segura" participated, we have plotted the horizontal distribution of the temperature in the first ten meters of the water column (fig.6).

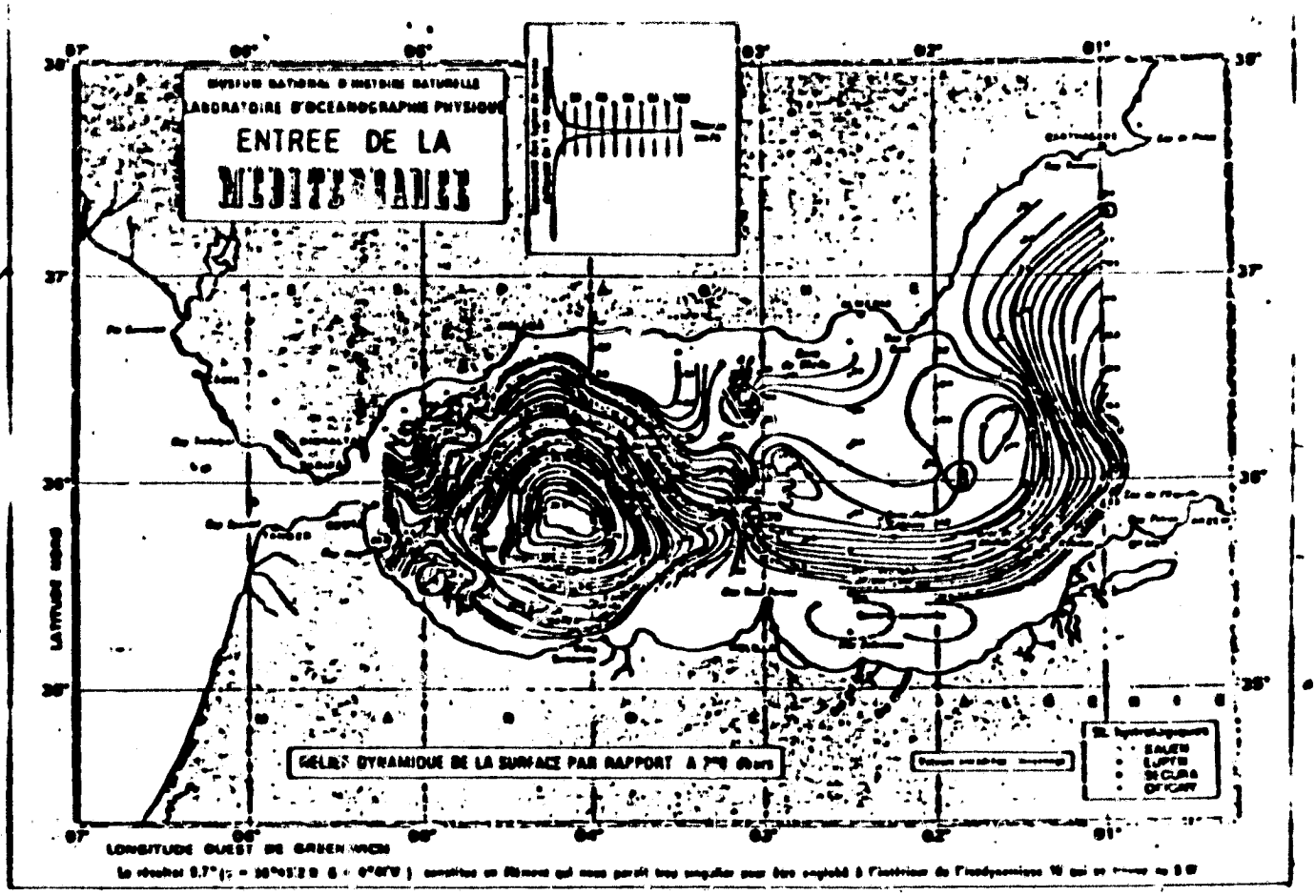

Fig. 1 Surface dynamic topography relative to the 200 db. surface. July-August 1952. Contour in dynamic centimeters (LANOIX, 1974).

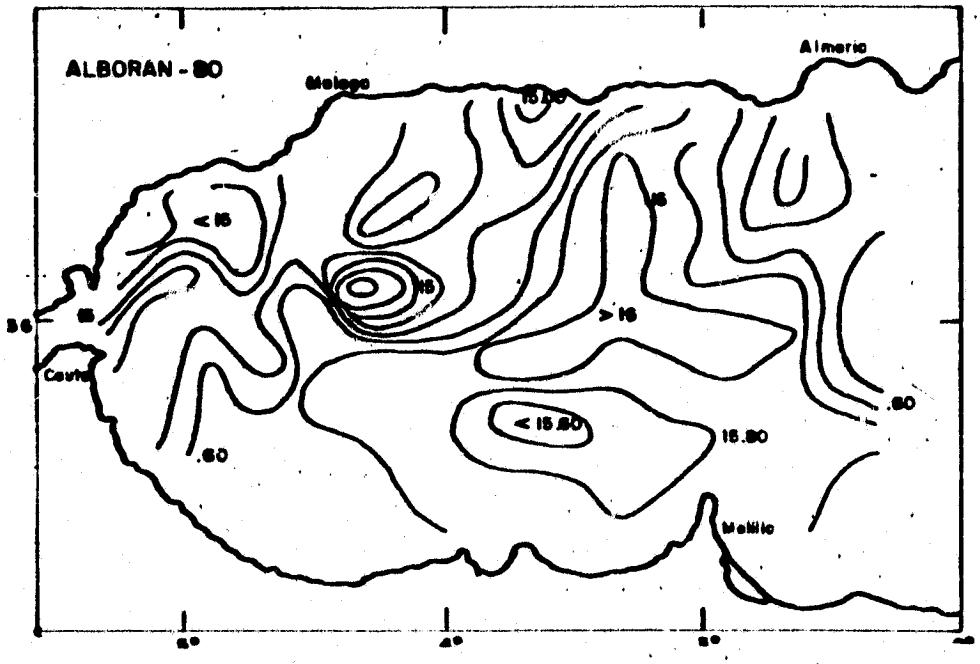

Fig. 2 30 m. isotherms. Alboran 80 cruise. April 1980.

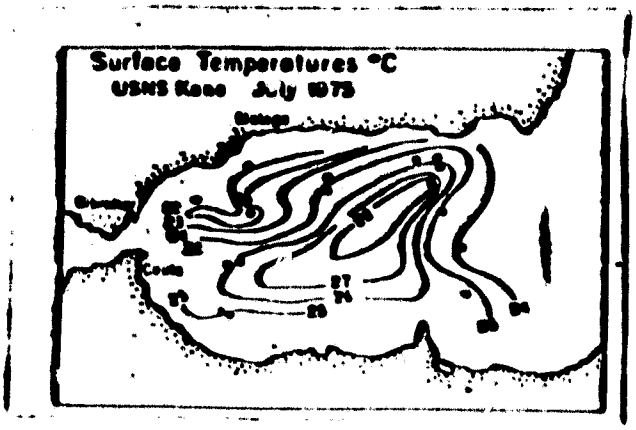

Fig. 3 Surface temperature (Stevenson, R.E. 1977).

ORIGINAL PAGE
BLACK AND WHITE PHOTOGRAPH

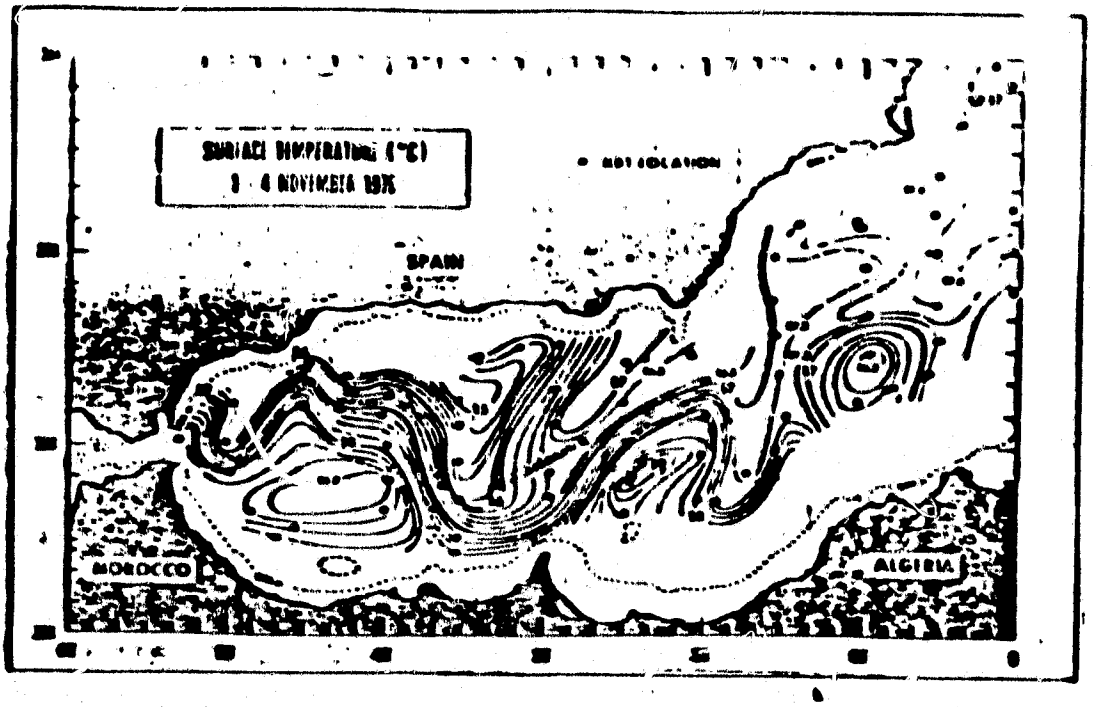

Fig. 4 Surface temperature (Cheney, R. 1978)

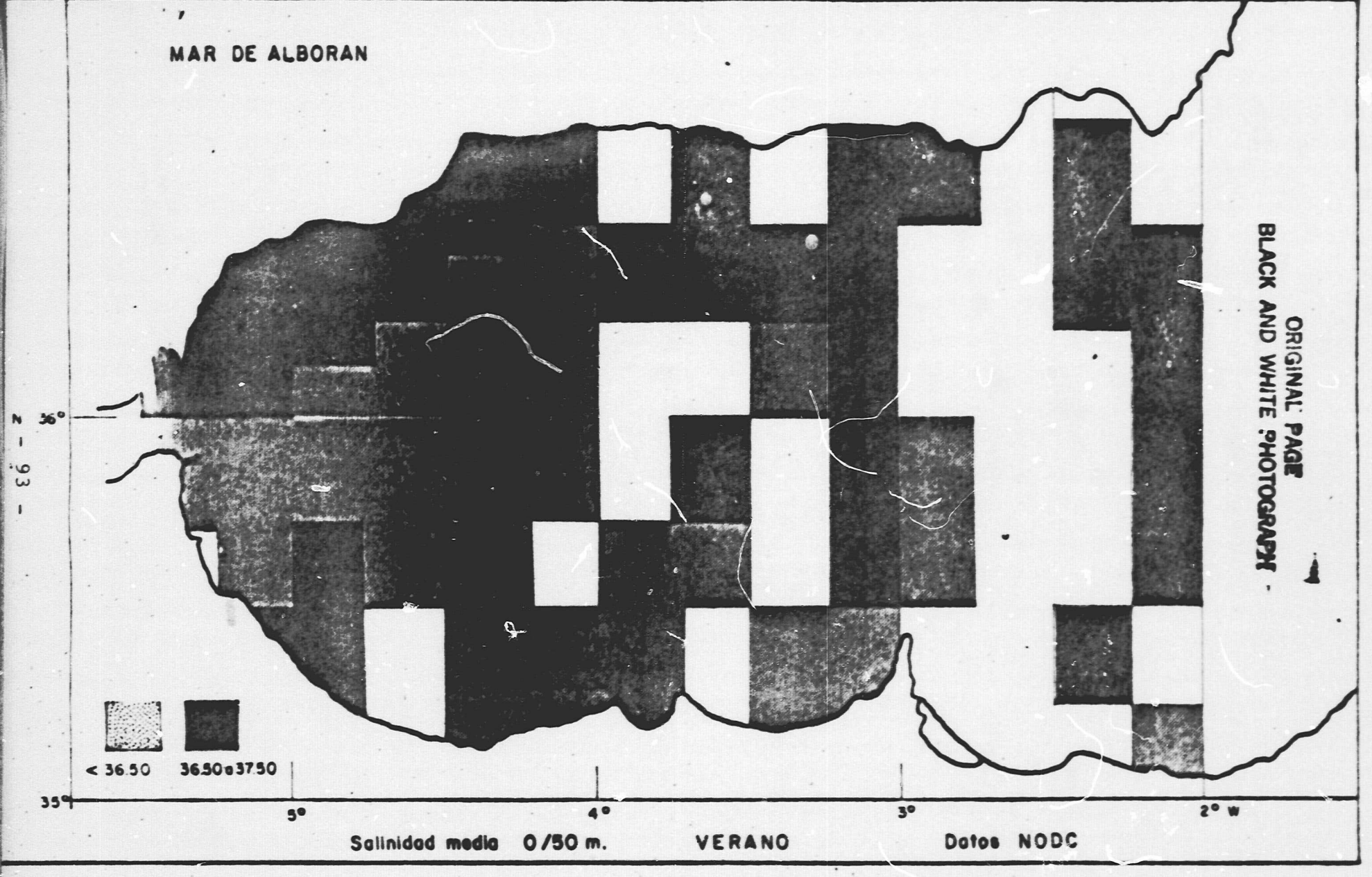

Fig. 5 Summar average salinity for the 0-50 m. layer.
NODC files.

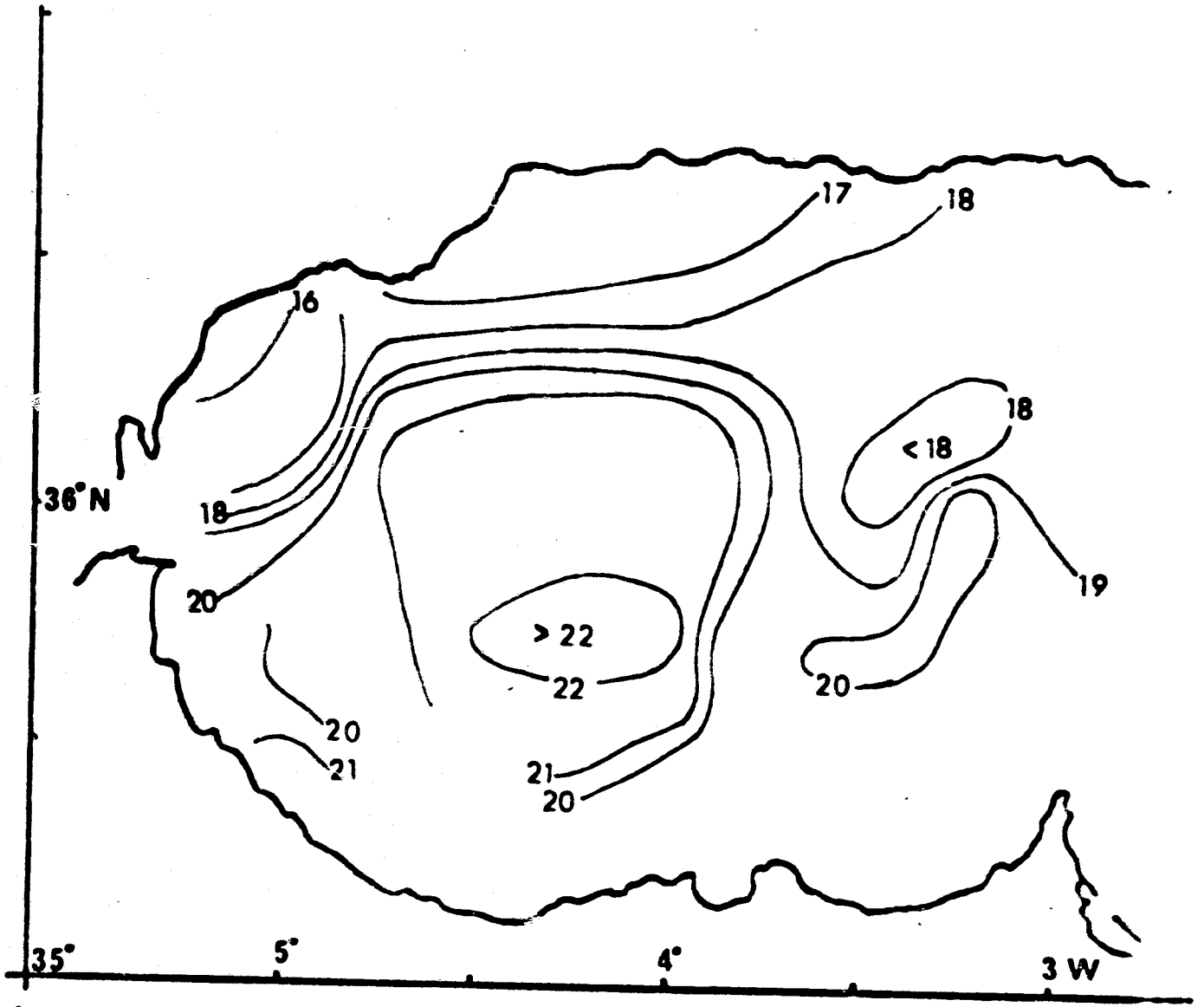

Fig. 6 0-10m. isotherms. Summer 1962 (PELUCHON Cr. 1965).

The isotherms follow the curved path of the gyre.The temperature maximum (22°C) is located to the south of 36°N and more or less on the 4°15' W meridian, and a thermal front is to be found in the North with a gradient of the order of 0.2°C km^{-1}.-

The above mentioned picture belongs certainly to a determined year; however, when matched with others, it reflects quite exactly the general situation in summer.

As far as the satellite data are concerned, we have carried out a density slicing and graphic translation from an enlargement of the gyre region. This enlargement belongs to the satellite image (A-0067-02300-3), taken on the night of July, 2nd, 1978 (fig.7&8).
If we examine the situation and the distribution of isotherms we can observe a great similiarity between this image and Fig.6.
The temperature difference between the warmer water of the center and that of the Northern border is of about 4°C, almost the same given by the oceanographical data.We believe that this striking similarity enables us to place great hope in the capabilities of the satellite data.

CONCLUSIONS

As said before, there is no doubt about the resemblance between the oceanographical and satellite data descriptions of the Alboran Sea.
Nevertheless, the phenomena in the Alboran Sea are very complex, and the knowledge of surface temperatures will just provide a partial understanding of these phenomena.

However, we believe that a good synchronization between oceanographic surveys and satellite overpasses, would enable a more relieable interpretation of the satellite data, mainly of those referring to temperature.

The measurement of the real value of temperature is an important factor to monitor the variati of the gyre, one of the main problems we have to deal with today.

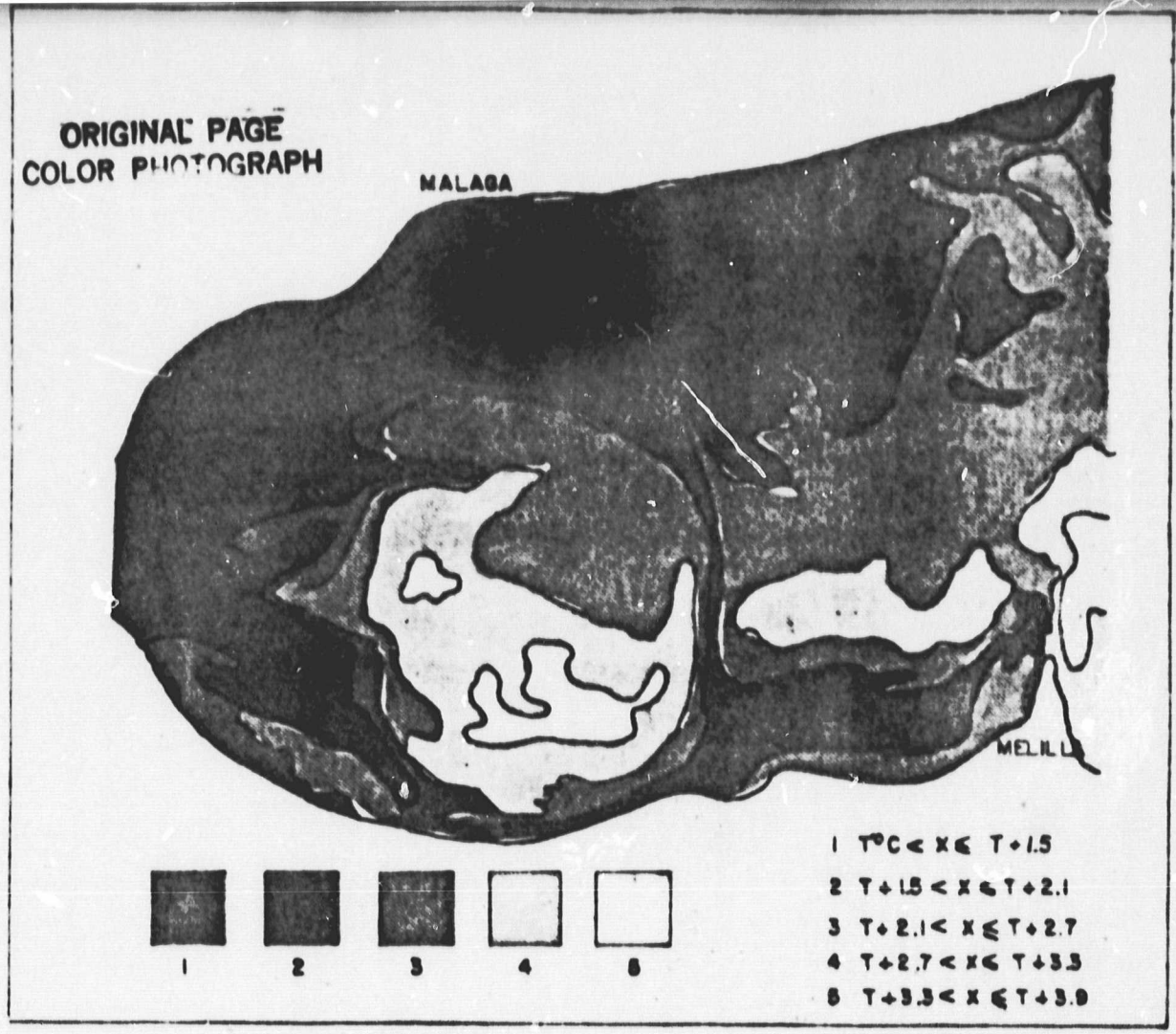

Fig.7 Graphic Reproduction of HCMM Satellite Image July 2, 1978.

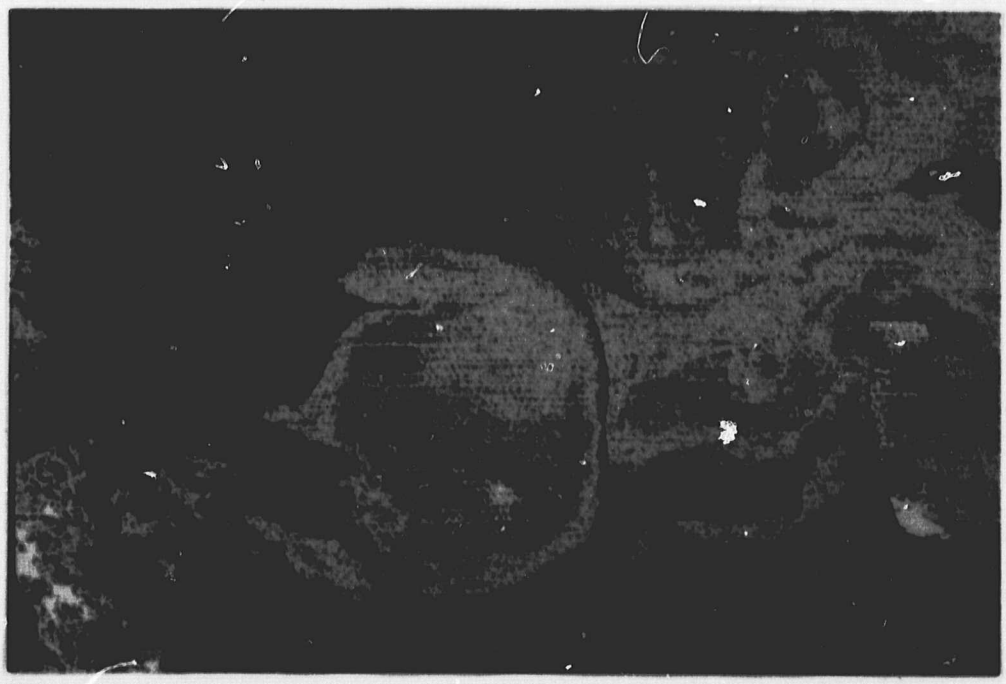

Fig.8 Density slicing of HCMM. July 2, 1978. Night Infrared Image (code A-0067-02300-3).

ACKNOWLEDGEMENTS

Support was recieved under the Program of collaboration between Instituto Geográfico Nacional and NASA,Research HCMM 034; and under the USA-Spain Treaty of Friendship and Cooperation (Cooperative Program 3044).

I also have to thank Guillermo Díaz del Río and Fortunato Ortí (Scientific Assesor, UAM-IBM Scientific Center) for their help in satellite image analysis.

G E O L O G Y

E.- GEOLOGY

- "Geological Analysis of HCMM Images"
  (Reproduced from the First Progress Report)
  Pedro Herranz
  Universidad Complutense

- "Applications of HCMM Images in Geology"
  Pedro Herranz
  Universidad Complutense

GEOLOGICAL ANALYSIS OF HCMM IMAGES(*)

Pedro Herranz
Departamento de Estratigrafía y Geología Histórica
Universidad Complutense

INTRODUCTION

An analysis based on geological criteria and following a methodology very similar to that used in conventional photointerpretation, has been carried out over the following images:

* A - A	0127 - 13360 - 1	DAY - VIS.	31 AUG 78
* A - A	0127 - 13360 - 2	DAY - IR.	31 AUG 78
* A - A	0157 - 02050 - 3	NIGHT-IR.	30 SEP 78
A - A	0087 02020 - 3	NIGHT - IR.	22 JUL 78
* A - A	0120 - 13060 - 1	DAY - VIS.	24 AUG 78
* A - A	0184 - 12590 - 3	NIGHT - IR.	27 OCT 78
* A - A	0115 - 02200 - 3	NIGHT - IR.	19 AUG 78
A - A	0185 - 13180 - 1	DAY - VIS.	28 OCT 78
A - A	0185 - 13180 - 2	DAY - IR.	28 OCT 78
* A - A	0185 - 13160 - 1	DAY - VIS.	28 OCT 78
* A - A	0185 - 13160 - 2	DAY.- IR.	28 OCT 78
* A - A	0190 - 13090 - 1	DAY.- VIS.(NEGATIVE)	2 NOV 78
* A - A	0190 0 13090 - 2	DAY- IR. (NEGATIVE)	2 NOV 78
A - A	0191 - 13270 - 1	DAY - VIS. (NEGATIVE)	3 NOV 78
A - A	1091 - 13270 - 2	DAY - IR. (NEGATIVE)	3 NOV 78

* These images include more than 20 % of the test area.

(*) REPRODUCED FROM THE FIRST PROGRESS REPORT

From a geological point of view the following foregoing conclussions have been achieved:

- The most important geological results were obtained just outside the test area, due to the following reasons:

A great part of the test area is located on alpine mountain ranges, characterized both by difficult tectonics, at a mesostructural level, and by stratigraphic series, which differ considerably in little thickness.This explains the fact that the area of a pixel contains several folds, fractures and lithographic units similar to "members".
This appears clearly in the area containing parts of the provinces of Alicante, Murcia and Albacete.

However, the best results have been obtained in great macrostructural or stratigraphic "units" (continental teriary basins, hercynian mountain ranges, great granitic batholits).

On the other hand, as the test area includes one of the most densely populated areas of Spain, whose agricultural, industrial, transport and city planning activities are among the most important ones of the country, the human action is decisive; at times, this action is independent from the geological substratum and it can even act against it (i.e. artificial cultivation terraces, irrigation by means of channels, which lie far away from the surgency or from the natural aquiferous).

Therefore, the geology is masked.The contrary occurs in non-populated areas of the Peninsulas' s midlands.Here, the only common human activity is gramineous cultivation in natural areas which are suited for it, horticultural cultivations in natural fertile river plains and spontaneous forest; this makes the identification of lithologies over which they are settled, easier.

The achieved geological results allow us to complete fold traces at a regional scale (e.i..Montes de Toledo-Sierra Morena), large fractures (Cordillera Cantábrica, Pyrenees, Cordillera Ibérica, Cordillera Costera Catalana, etc.), fractures with a little replay which affects the continental subhorizontal Tertiary (Tajo, Duero and Ebro basins), to distinguish compact lithologies and rocks of a high crystallinity (Hercynian mountain ranges, plutonic rocks and part of the Alpine Mountain ranges), which have a very different thermal behaviour when compared to little consolidated rocks of a terrigenous origin (Continental Tertiary, Quaternary covers).

Both, the criteria applied in order to perform this work, and the results achieved by using it, will be stressed below:

VISIBLE BAND IMAGES

Visible band images have a coarser resolution than Landsat ones but as the area within a frame is greater, a great extension can be observed simultaneously under similar climatic conditions, solar illumination and with a similar seasonal vegetation.

Visual analysis and interpretation of these images in lithology can be deduced from changes in vegetation.Three types of vegetation can be distinguished:

a) Forests (coniferous, mediterranean, heaths, some prairies, etc).Tones are dark gray.

b)Horticultural terrain, irrigated land.Tones are medium gray with broad granular texture.

c) Cereals (excluding rice and corn) on unirrigated lands, harvested between middle July and late August (depending on the species and the altitude of its location).

Generally speaking, these three types of vegetation correspond to the following morphological and geological elements:

Forests:

Mountain ranges and hercynian or alpine massifs, with very variable lithology and prevailing highly crystallized rocks; abrupt reliefs between sea level and 2500 meters of altitude; in this altitude arborescent vegetation decreases suddendly in the main mountain ranges.

Irrigated Lands:

They are to be found over various quaternary deposits in the lower river terraces and in the coastal areas of Levante.There are exceptions seated on high river terraces or tertiary plains; in this case, they are irrigated either by

means of channels or by deep water extraction systems.

Unirrigated Lands

It is mainly developed over the terrigenous parts of the continental tertiary basins (Duero, Ebro, and Tajo-Mancha include the biggest areas, Almazán and Arcos de Jalón, on the contrary, are among the smallest) which contain all kinds of intermediate rocks between calys, marls, sands and conglomerates. Some spots of cereals appear also over quaternary slope deposits over ancient alluvial fans, etc. This happens for example with the "rañas" of Extremadura and Montes de Toledo. These "rañas" or "Piedmonts" were formed in the flancks of the quartzite paleozoic mountains at the end of the Pliocene Period-beginning of the Quaternary; they are constituted of residual tongues (transversal to these mountains), which are leaned along the mountains. They can reach 8-10 km of longitude and they contain all possible grainsizes between clay and blocks.

It should be noted that the continental tertiary basin of Badajoz ("Tierra de Barros") appears with a surprising dark tone; this is due to the dark brown-reddish soils and to the broad (intensive) cultivation of vineyards (instead of cereals).

Something similar is to be found in the marine tertiary depression of land of the Guadalquivir, filled by marls, clays, diatomites, etc.: It shows large areas cultivated with vineyards and olive trees (these are very intensively cultivated), sunflower, cotton, etc.

Morphology is mainly observed when looking at the illumination contrast between slopes which is mainly observed when looking at the illumination contrast between slopes, which is intensified by a much more dense vegetation in the umbrias.

In the image of October, 28 the morphology is even more intense because of a small snow pack over the axial pyreneean zone.
Each system of regional fractures with morphologic meaning, can be observed in images, in which horizontal projection of solar rays form an angle between 20° and 60° with the direction of the system of fractures.
As it is known, morphological analysis is strengthened enormously by looking at these images from the North.

Some socle fractures which appear out of the postectonic Tertiary (as it is affected by a slight replan), can be detected, as they condition and vary the river courses (f.ex. basins of the Duero and Tajo').

Summaring up, the image from the visible band we employed, performs an indirect lithological and structural control through vegetation. The clearest line is precisely the one that separates "vegetation" from "no vegetation".

Remember that dry cereals harvests have been carried out in later August; therefore, areas with this kind of cultivation can't be distinguished from non productive areas.

Comparisón of illuminated and non illuminated areas shows the morphology and therefore the principal fractures which stand out strikingly if they have in addition a "grinded band" (greater permeability and better soils), for example Valle del Jerte, NE of Cáceres).

DAY INFRARED IMAGES

This is the image which presents the greatest difficulty when trying to perform a conscious analysis, due to the various factors (which we are now trying to quantize) that condition the quantity of energy registered by a sensor in one certain area.

In ground level and known lithologies, there are cases in which only assumptions about the ratio of reflected energy and emitted energy are feasible. On the other hand, we could detect in summer images low atmospheric masses of high temperature.

Nevertheless, we have to say that performing an empirical analysis, the best geological results were achieved by using this kind of image (exactly the image of October, 28).

In this image, it is possible to distinguish lithologies showing enough continuity on the surface, even when they don't imply change of vegetation. The best results were achieved in the Hercynian structures (mountains of quartzites) of the Eastern Montes de Toledo and Eastern "Sierra Morena", increasing in a net way the quality of Landsat images.

It is not the goal of this "Pre-Report" to give a description of the numerous results obtained.

Taking into account the morphology and fractures showed by it, strong contrast between sun illuminated slopes and shadowed ones enables an acceptable control, although in the high mountain areas it is impossible to discriminate between snow zones and rocky areas with the same temperature (within an image).

Finally, it must be noted that a comparison between visible and IR bands has been carried out with simultaneous images.
Since thermal IR almost ignore grass, that on the other hand is so well distinguishable using visible band, this grass can be eliminated during the analysis process by comparing both images.
We have even performed (for a short period of time) a stereoscope observation of both images, visible and IR, which anables an enlargement and control of this contrast.

Summarizing, it must be pointed out tha IR images, gathered in autumn, and without important storms either at the satellite's overpass nor within the three days before it, gives the best results from a geological point of view, although it must be emphasized that the test area shows poor results.

In summer images, with sun rays in a very vertical position (56°), high ground temperatures, temperature inversions, reflections, etc., the results are very poor, mainly in the warmest areas, though fertile areas and surrounding mountains stand out clearly.

NIGHT INFRARED IMAGE

Images gathered in very different meteorological conditions, have been analyzed.
The results have been very different.However we have to say that they are of little value when trying to determine geologic substrates (unless we are interested in a very general description).

We believe that is here where a higher resolution power is missed and where the largest number of images, in different temperature ranges, would be necessary in order to perform the visual analysis.

Notice, for example, that the images have a general tendency to stratify gray tones; this stratification coincides with that of the altitudes. Generally speaking, the resolution for lithologies within those "thermal data" is optimum, though it is very coarse and even null in the rest of the cases.

In other words, "forms effect" overcomes strongly "lithologic effect"; the importance of heat capacity and conductivity is not very great. Therefore, it is in the plane zones of the air's temperature where a connection between changes in radiation and changes in lithology have been clearly observed.

The most interesting morphologic, geologic, biologic, climatic and human elements, are the following:

- In morphology, the strong emissive contrast between western and southern slopes gives sharper reliefs than northern and eastern ones.
This effect, which is attenuated throughout the night (as more time has passed since the "differential day insolation"),
cant be analyzed more than once every night due to the orbital characteristics of the sensor-carrying satellite.

In night thermal images it has been impossible to detect incised valleys of high reliefs, and also intramontan depressions of land, whose cooling is very slow when compared to the surrounding reliefs.
This has been impossible in other type of bands.
In the southern valleys of the Pyrennes this effect is very impressing;
in this case it would be also very interesting to obtain consecutive images in one night

We hope to analize soon these images as well as other analogous ones, but employing the temperature maps performed by the Instituto Nacional de Meteorología, corresponding to the same dates the images were gathered, and also astronomic data about the time of the sunset each day, in order to know exactly the time passed in each point from tha end of the insollation.

In geology it seems indubitable that only areas of sedimentary, metamorphic and igneous rocks, compact and highly crystallized with disperse materials,

terrigeneous, porous or little compact materials, are distinguishable with HCMM resolution.

It would be interesting to analize the cooling curves of different lithological areas throughout the night in order to compare them.

The effect of water-loving or arborescent vegetation masks lithological effects reducing, especially during summer, the emission level. The recent occurence of storms can be detected by soil moisture and lower temperatures; the same happens with air masses as well as irregular diurnal insolation caused by clouds.Generally, after the storm, the contrast diminishes.

Among the human factors, the clarity of rice areas as black spots (S.SE of the Albufera) and the unexpected scarce e ect of great cities may be emphasized.

CONCLUSIONS

The morphological interpretation of images, may be an important aid for analyzing them methodically, since geological ground-truth is known with a superior detail than images resolution.

Therefore, we can explain possible local anomalies, which aren't justified by agrobiological, meteorological and hydrological analysis, by means of lithological maps.

The low quality of negative or photographic paper employed, together with the broad range of reflectance or emission level, advised us to delay a deeper analysis of the images until maps of radiation levels from a broad number of images (even without correcting the effects of relief) are available, or at least, until a dense enough periferic net is available or in the worst condition, until standarized profiles in scan lines are available.

In order to obtain a better benefit from the thermal images, it is necessary to use the meteorological bulletin with local data (air temperatures, rainfall, cloudiness and meteorological maps) at the date of the image and two days before.Besides, it is necessary to know the hour of the sunset in the four angles of the image, or at least in the center of it, referring to the same horary than for obtaining thermal dates.

APPLICATIONS OF HCMM IMAGES IN GEOLOGY

P. Herranz Araujo
Departamento de Estratigrafía y Geología Económica
Universidad Complutense
Madrid.

1. GENERAL PROCEDURES

1.1. MATERIALS USED

The images listed in section 8 (Appendix) of this chapter were used for the study, printed on 23 x 23 cm. paper in black-and-white.

These prints exhibit the data from IR-day, IR-night and visble band (0.5 - 1.1um) exposures. The images displaying day/night temperature differences or apparent thermal inertia could not be used.

For purposes of comparison, LANDSAT images (mainly band 7) and "flight B" aerial photographs (in black-and-white and on scales varying between 1/30.000 and 1/35.000, and also more than twenty years old) were also consulted.

From time to time, bulletins from the National Meteorological Institute were also consulted.

1.2. EQUIPMENT USED.

The instruments employed were very limited, as a direct interpretation was performed, similar to that common in panchromatic photography or in interpreting a single band.

Thus, in the course of the work, the following were used:

- Normal drafting instruments.
- Measuring instruments and a manual calculating machine
- Transparent and semi-transparent plastic sheets
- A light table
- A Minolta EP-1 photocopier, with a manual brightness control, suitable for copying on both transparent paper and on transparencies.
- Zeiss M-2 and Condor stereoscopes (with dual viewers), etc.
- Dark room equipped for black-and-white photography.

For field work, prior to analysis of the images, the typical instruments for geological and stratigraphical surveying were used. Laboratory work followed that done in the field: petrology sedimentology, biostratigraphy, cartography, etc., all of which imply a wide range of instruments used indirectly and prior to the main study, and which need not be listed here.

1.3. METHODS FOR GATHERING FIELD DATA.

In view of the low resolving power and the scale of the images, it was considered unadvisable to proceed with a study of a small sub-area within the proposed pilot area. It was thought more advantageous to compare, in a global fashion, the new images to already existing geological maps on different scales.

These geological maps (with complementary data: stratigraphic, tectonic, and petrological details, etc.), are the work of innumerable authors and span a period of more than one hundred years.

A mere bibliographical listing of the more important works containing geological cartography pertaining to the pilot area

and its surroundings would well exceed the space for it here. Listed below, then, are the most essential of these works:

- Geological Map of Spain, on a scale of 1:1.000.000 by the I.G.M.E. (various editions).
- Tectonic Map of Spain, on a scale of 1:1.000.000, by the I.G.M.E. (1972).
- Geological Map of Spain, on a scale of 1:200.000, by the I.G.M.E. Synthesis of Existing Cartography (1970-71).
- Lithological Map of Spain, on a scale of 1:500.000 by the I.G.M.E./I.N.E./S.G.O.P. (1970).

As works which were elaborated by our own Center and which cover a wide range of cartographic data, the following should also be pointed out:

- Hydrogeological Map of the Province of Albacete, on a scale of 1:25.000, elaborated by the Department of Stratigraphy at the Complutense University/Institute of Economic Geology (1965-68, unpublished), divers authors.
- Doctoral theses of: C. VIRGILI (1948), Tarragona (Triassic period); A. GARCIA QUINTANA (1977), Valencia (Cretaceous period); C. ARIAS (1978), Albacete (Cretaceous period); J. J. GOMEZ (1978), Valencia (Jurassic period).
- Various hydrogeological studies in Murcia (1965-70, unpublished) different authors (including the present author).

As other areas of Spain outside the pilot area were also taken into consideration, many in-house and independent studies apart from those listed were consulted. The research temas at our Center are organized along stratigraphic lines:

a) Precambrian - early Paleozoic

b) Permian - Triassic

TECTONIC OUTLINE

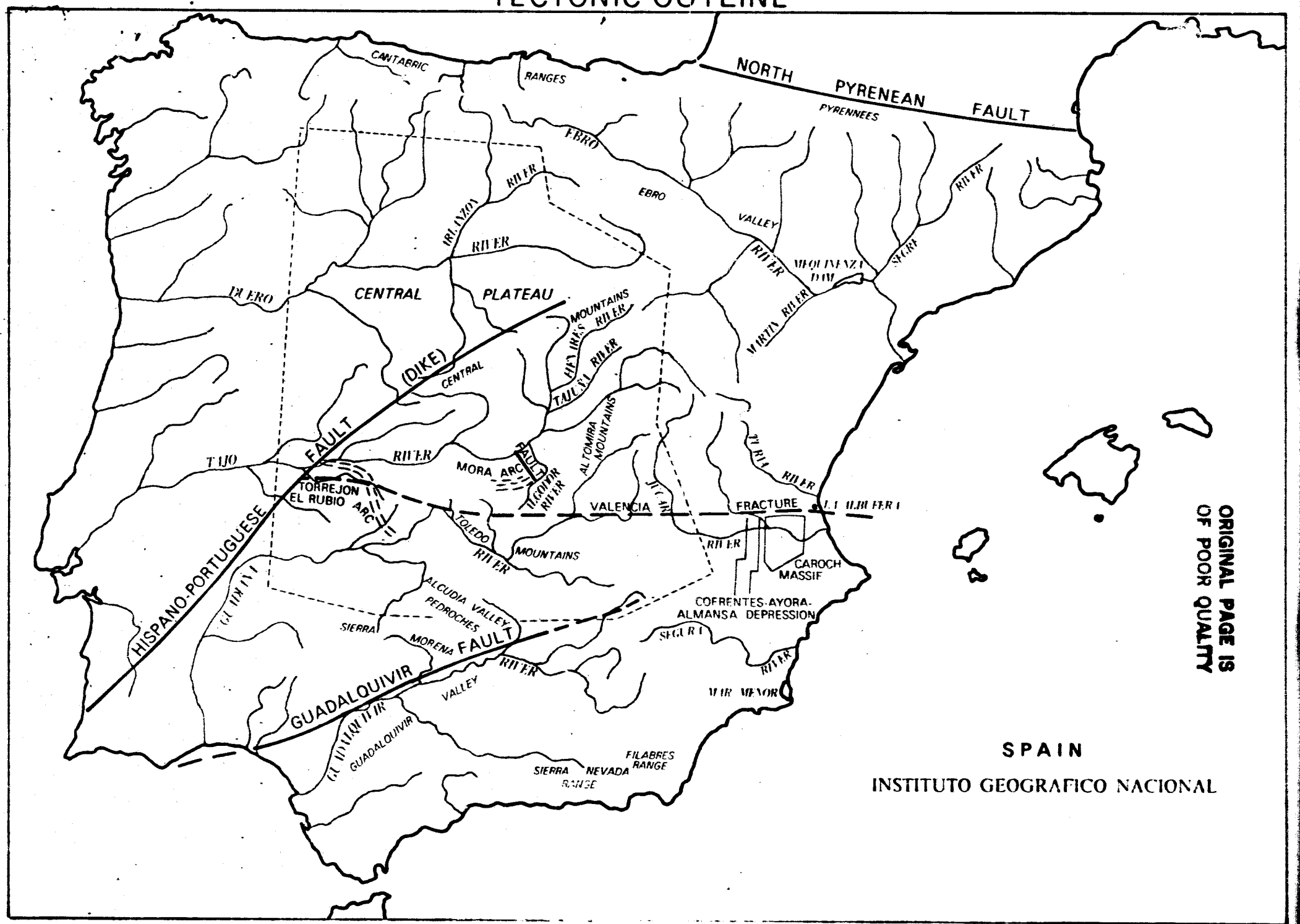

SPAIN

INSTITUTO GEOGRAFICO NACIONAL

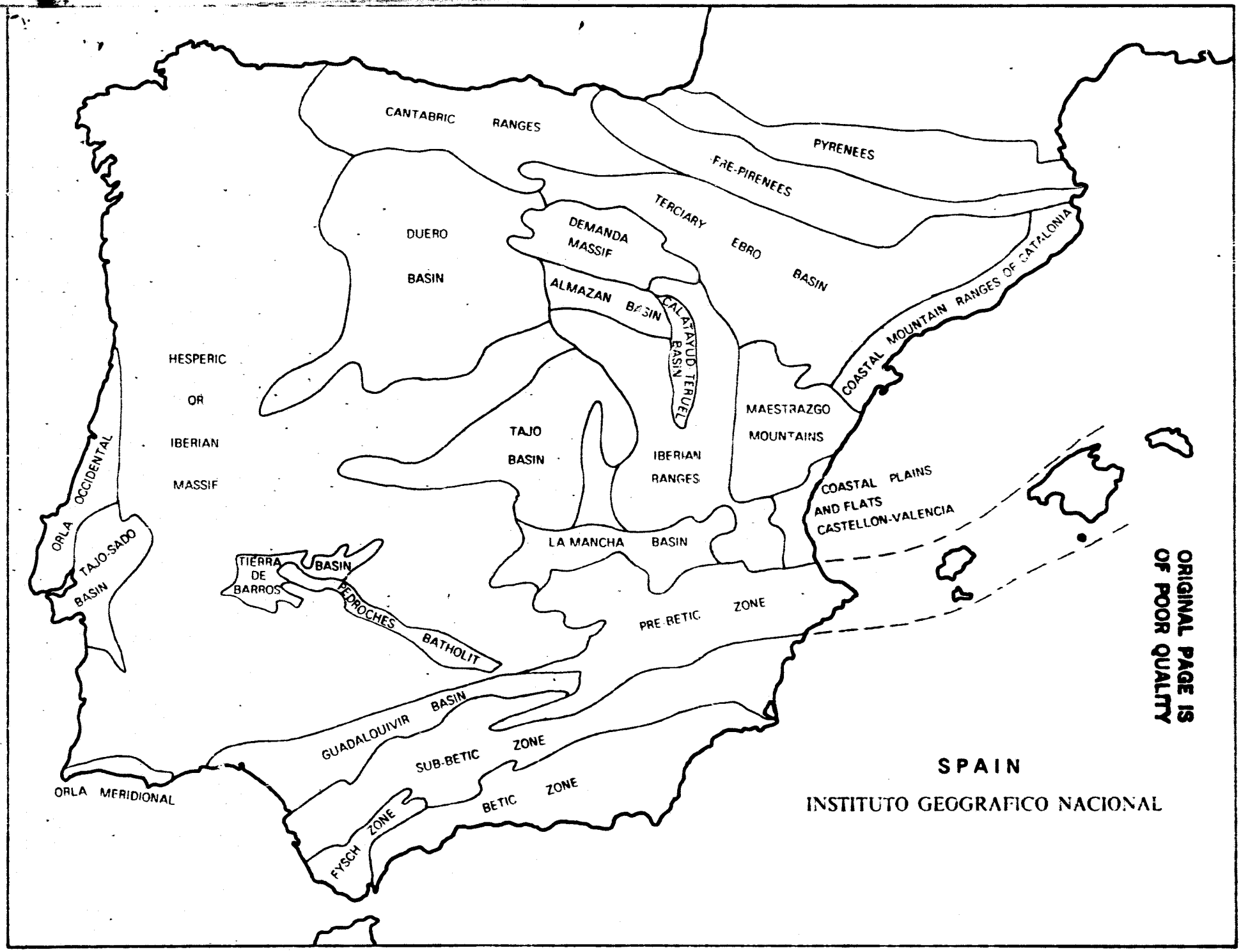

c) Jurassic

d) Cretaceous

e) Neogene (continental)

and the study area of these teams consists mainly of the NE, E, SE, and SW borders of the central plateau of Spain.

Thus, an abundance of reference work was available, published and unpublished, both within the pilot area as well as outside it.

The procurement of data with respect to the "ground-truth" did not prove to be difficult, as as an ample stratigraphic and cartographic bibliography was available. Nor did the gathering of complementary information concerning vegetation, soils, crops, etc. present difficulties, these being obtained through personal interviews with various members of our Department and the Institute, who possess an in-depth knowledge of a good number of geographical areas.

It bears mentioning that, given that geology is a stable element within thw overall environmental framework, data which had been gathered quite some time ago proved useful, thus requiring no new surveys at this time.

1.4. MTEHODOLOGY: INTERPRETATION PROCEDURES

As mentioned above, the interpretation procedures were similar to those used in black-and-white photography. Briefly, the steps which were followed are:

- A careful analysis of the basic parameters and nominal features of the images received, special care having been taken witn respect to:

. the size of the pixel and the resolving power
. the spectral bands used in this project
. shape and geometry of the image

- A general analysis of the atmospheric conditions prevailing at the time of data recording and during the previous 72 hours (air temperatures next to the soil, wind directions, precipitation, weather maps, etc.).

- A general analysis of the conditions of cultivated and natural vegetation at the time of recording, with special emphasis on the farming customs in each region, particularly in the case of extensively cultivated cereals (planting, germination, and harvest times, etc.).

- A careful analysis of chance elements which could lead to confusion: forest fires, floods, local storms, dust clouds, thermal inversion in the atmosphere, jet exhaust trails, dew and frost occuring under high pressure systems, etc.

- A general analysis of the incidences of human activity in non-farming areas: population centers and their surroundings, major transportation arteries and their respective aureolas in the images, etc.

- A detailed and careful comparison of the most highly contrasted and descriptive areas in each image with ground-truth data begining with the better-known areas, of which LANDSAT images, aerial photography and detailed geological maps are available. In these areas, a test or contrast of the images was performed; that is, a correlation between a complex of the true land conditions and their graphic representation. These areas were chosen in such a way as to assure that the pure geological component of ground-truth

area be very important and not obscured by other factors, and that in addition it cover an area large enough to affect a good number of adjoining pixels, whether in the case of fractures or in that of outcrops.

The control area indicated, then, was chosen for having the following characteristics:

. Clean outcrop as free as possible of serious alterations, overlying materials, vegetation, etc.

. Outcrop with a known altitude and having a topographically horizontal surface or, in accordance to the data relating to the incidence of solar rays and the position of the satellite, a surface which does not refect light during daylight exposures.

. Outcrop covering a sufficient area so as to extend through many pixels.

. Outcrop free from local micro-climates known for their anomalies (e.g., sheltered depressions, mountain passes, areas surrounding dams in arid areas, etc.).

. Outcrop far from areas having an atmosphere with a high pollution content (metal works, cement factories, heavy industrial or urban areas, etc.).

- A tracing of the outcrops or fractures from an ideal observation point to the more difficult areas. Thus the relative influence of the above mentioned factors was observable, viz., those factors tending to interfere with interpretation (such as vegetation, artificial surfaces, soils, absolute differences in altitude, changes in topographic morphology, atomospheric pollution, etc.).

In many cases, an outcrop or a fault, visible in the field and compatible with the resolving power of the system, is lost due to these intervening factors.

- Finally, on a hypothetical or experimental basis, the attempt was made to identify geological factors by means of their direct or indirect influence on elements within the sphere of the physical surface, which are more easily accounted for by the system than are the underlying geological facts themselves.

As far as the exact procedures of interpretation are concerned, it is obvious that the human element involved plays an irreplaceable role in the overall analysis of the information, and not in standardized or uniform fashion. The experience, intuition, imagination and personal "tricks" available to each interpreter conditioned the results.

In terms of these "tricks", the following were available to our team:

- Photocopies of differing contrasts and brightness levels derived from the same photographic image. Blending of the same by means of a stereoscope.
- Stereoscopic blending of the visible light and infrared images from the same exposure. The blending of daytime and nighttime infrared images, due to their different shape and arrangement, was found to be nearly impossible.
- Superimposition of transparencies of the visible and day-infrared images on a light table.
- Superimposition of transparencies of the images a light table with a slight misalignment to highlight linear elements and sharp changes in tone. Superimposing the negative and the developed print of the same image, again with a slight disalignment, produces a similar result.

2. FINDINGS

2.1. GEOLOGICAL UTILITY OF THE IBERIAN PENINSULA PROJECT

Some of the conclusions put forth in the first report, dated 30th September, 1979, are reaffirmed herein, and new ones have also been added.

- The best data and results obtained outside the pilot area, as the latter, though quite interesting from the point of view of agricultural, oceanographic and human factors, presents serious drawbacks in a geological analysis on a scale such as the one used in the images, particularly due to the following:

  . The pilot area is not made up of a natural geological unit, rather it forms part of the units below:
    . Terciary Ebro Basin
    . Coastal mountain range of Catalonia
    . "Maestrazgo" mountains
    . Iberian Ranges
    . Coastal plains and flats
    . Pre-Betic Zone
    . Sub-Betic Zone
    . Betic Zone

  . The pilot area constitutes of the most complex zones of the Iberian Peninsula in terms of cartography and tectonic factors, with an abundance of outcrops and faults of a size less than one pixel.

  . Abundant Mesozoic shelf's stratigraphic series, very complex and varied that, in general, lack homogeneous formations, thick and without lateral continuity of facies. Rhytmic series are also frecuent.

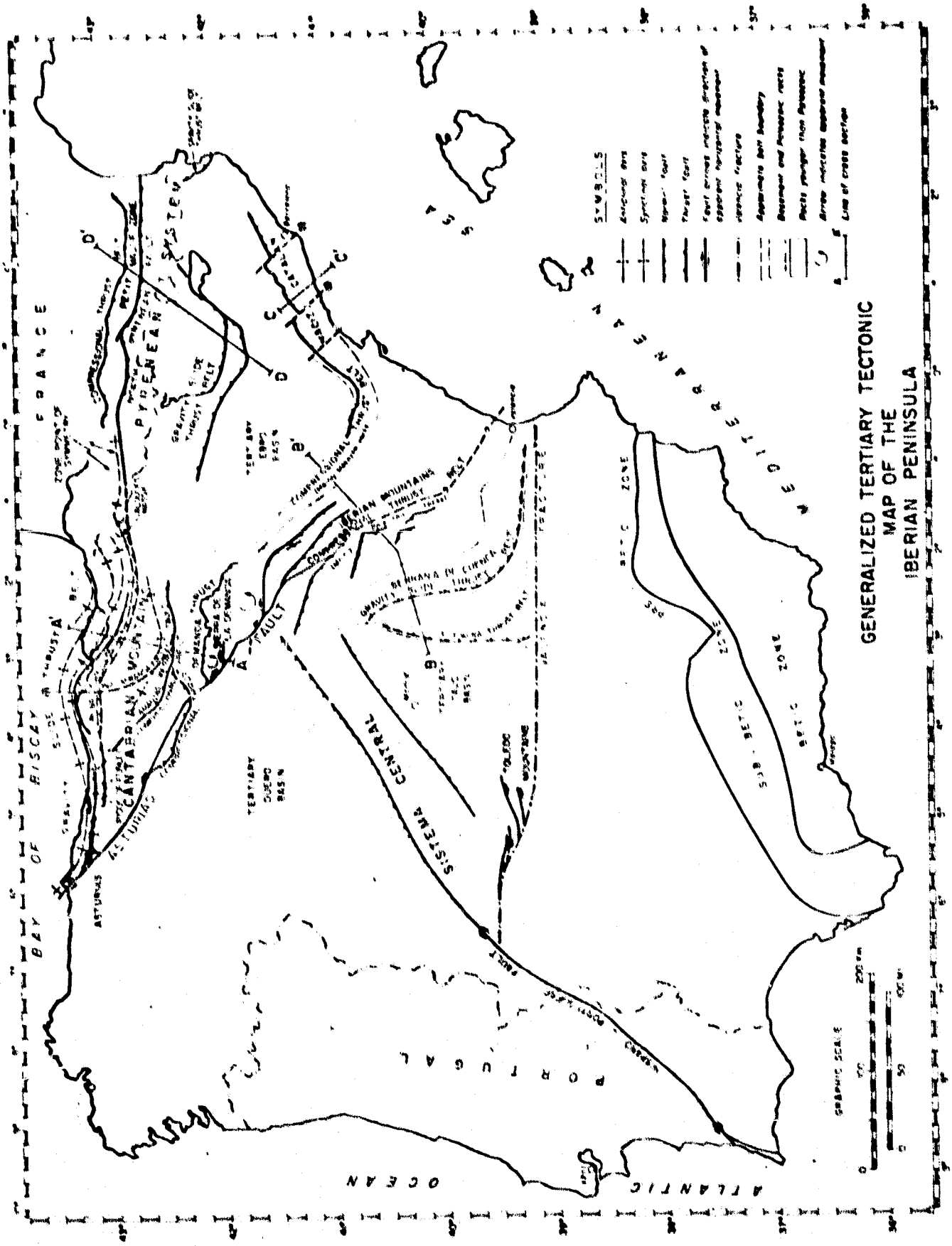

Figure 3 (see text 2.1)

As in addition there are few materials which remain in a horizontal position, and the total thicknesses do not measure very much, it is common for the total width of the outcrop of a System to be less than one pixel, including various formations of different lithologies.

- As for cenozoic materials, these frequently accompany tectonic movements. There are both continental and marine variations, with numerous instances of stratigraphical discontinuities and unconformities. In general, loosely compacted detritic materials are present.
- There are quaternary and pre-quaternary volcanic materials in a large number of small outcrops, particularly in the southern portion of the pilot area.
- Quaternary materials abound and are of many different types, the majority being typical of a "mediterranean climate". There are, then, both currently existing and fossilized beaches, coastal plains in evolution fluvial deposits filling valleys and river deltas, hillside deposits rich in "terra rossa", etc.
- The morphology of the area is quite complex. The terrain ranges from sea level to more than 2.500 m. above sea level in the southern part of the zone (Filabres Range, Sierra Nevada Range). There is, then, a sharp primary relief effect, particularly in the infrared night-time exposures. But it is the great variety and intricacy of the relief features that complicate all aspects of observation, as the effects of lighted hillsides as opposed to those that are shaded have a definite impact on visible light, infrared daytime and infrared nighttime

exposures, producing an intricate mosaic which masks the geological substratum.

. The high population density the intense human activity on the coastal strip (with the exception of the southern part of Almería) produce highly transformed surface characteristics. These act to hide geological facts, while producing other situations which may be confused with them. The widespread presence of small farming tracts is an additional source of confusion.

On the basis of the above factors, and so as not to present a paucity of geological findings, it was felt necessary to take into account additional areas of the Iberian Peninsula. The study was even expanded to images which comprise the south of France, the north of Africa, and the Mediterranean.

- The best results were achieved, as may be expected, in the areas which possess the following characteristics:
  . Homogeneous and very thick net stratigraphic units, having lateral continuity, infrequent alteration and sparse vegetative covering.
  . Major faults, recent or old, but which precipitated the deposit of thick materials in one of its flanks. Also those fractures having an impact on morphology or which condition the drainage system.
  . Extreme aridity and its accompanying factors: high visibility in the atmosphere, a clean torrential drainage system, and sparse vegetation in connection with geological points of interest.

  These regions provide the poorest results in IR daytime shots and during the summer, due to the existence of

thermal inversions and extermely high ground-level temperatures, which seem to exceed the upper-range sensibility of the recording mechanism.

It should be mentioned that the best images, of course, are those which include the northern border of the Sahara, the Atlas Mountains, and the Antiatlas (which were not studied). Within the confines of the Peninsula, the granite bathylith of Los Pedroches, the Alcudia valley and the meridional mountain systems of the southern subplateau all stand out. This is true also of the three continental terciary river basins, currently washed by the Duero, Tajo, and Ebro Rivers.

In addition, as in aerial photography, the "transparency effect", of large faults is demonstrated through the supervening accumulations. Subtle changes in vegetation, morphology, the direction of the drainage system, etc., show the existence of major faults detected at other points where the accumulations are absent. Examples of this have been found in the three terciary basins.

- As for the three types of images analyzed (IR-D, IR-N, and visible light), there has been no change of opinion regarding the criticism which were made of each in the first report, dated September, 1979. As a summary of and complementary to those comments, the following observations are listed below:

  . The geological interpretations to which the images supplied were subjected were bases on the following factors in the order listed:

  1) Conditioning of spontaneous vegetation by geological causes.

2) Conditioning of morphology by faults and lithology (formation of topographical characteristics and drainage systems).

3) Distribution of cultivation as conditioned by geological and hydrogeological causes.

- The visible light images which produce the best results are those taken during the fall, perhaps due to the appropriate angle of solar rays. In exception to this are the shots taken following a rainstorm, which tends to darken and level the soil, diminishing contrasts (leaving a trail of moisture). The images coinciding with the more direct rays of the sun during the summer atenuate relief shadings, produce regions with a high degree of reflection and are affected by acute atmospheric disturbances (haze, thermal updrafts, dust clouds, etc.). Winter images are also not very contrasted, perhaps due to the sparse weed vegetation, the presence of bare forests covered with a floor of dark, decomposing leaves, and the presence of recurring dew or frost, all under very oblique and dim lighting conditions.

- Daytime infrared images also produce the best results in the fall. We believe that this is due to the fact that the surface temperatures at that time of year are more suited to the thermal scale. During the summer, one can observe that the zones which are typically hotter appear in white in the developed prints; there exist areas in the Guadalquivir River valley, the southern submeseta, and the Ebro River valley which, constituting as they do topographical depressions, reach air temperatures

of 35º to 40º C (at 1.5 meters above ground) at the time of the exposure. The exact ground temperature reached is at present unknown, but one may postulate that it is atenuated by the coincidental fact that light-colored materials predominate in the afore mentioned areas. During the winter daylight infrared images show extensive dark areas, which are covered with snow or which experience temperatures below 0º C.If the image in question is free from cloud formations and coincides with a high pressure system, the nighttime radiation can be seen to have been so continuous and prolonged that recurrent frost on shaded hillsides, large amounts of ground moisture, fog and mist can be detected in the image. Geological considerations become secondary under such circumstances; the range and contrast of the shades of grey in these images are quite restricted.

Both summertime and autumnal images in IR-D are softened and darkened following the occurence of a rainstorm for at least a period of 48 to 72 hours.

- Due to the inadequacy of the scale of the thermal recorder with regards to the low surface temperatures which ensue 7 to 8 hours of irradiation and which obtain in the absence of solar energy, evidently the nighttime infrared images produce poor results in the fall and winter.

On the other hand, the IR-N exposures taken during July, August, and September provide the most promising results, at least in the case of areas at mid-range altitudes (approx, between 200 and 1.200 meters). Below 200 meters there exist highly sheltered hot areas of undetermined

dimensions. Above 1.200 meters the irradiation is acute at the time the shots are taken. Moreover, once these altitudes have been reached one is dealing with mountain systems, hercynian or alpine, whose composition is more compact and crystaline and, though their calorific potential may at times be high, their heat conductibility allows for rapid cooling.

During the summer or at the beginning of the fall, with these IR-N images the best global results vis-a-vis the broad folding structures of the southern meridional submeseta are achieved (Alcudia valley and Toledo Mountains) the mountain systems composed of paleozoic quartz at the edges of the folds are distinguishable from the precambrian schist nuclei.

Summing up, the visible light images are consistently inferior in quality and content to LANDSAT images. The most useful IR-D are those taken in the fall, particularly if there has been no precipitation during the 2 or 3 days prior to the recording of the image. Together with the visible light shots the IR-D provide more information than the LANDSAT image alone, especially when it comes to distinguishing some types of vegetation (forests/weeds and low shrubs/cereals). The IR-N taken in the summer achieve very good results with regards to mid-range altitudes, and those taken in the fall (in the absence of immediately preceeding rainfall) provide good results at low altitudes. Nocturnal images taken in the spring have very poor results, although they do highlight population centers.

- The fundamental contribution of the HCMM images derives from their instanteneous and synoptic nature. Earlier images, albeit on a more advantageous scale, were taken

at different angles, with different shapes and arrangements, lighting, vegetation, and atmospheric conditions, and using different types of instrumentation. Thus, the composition of an overall picture depicting the entire peninsula using the LANDSAT images was quite a painstaking process. With regards to the HCMM images, no image covers the entire peninsula, but large-scale geological units do appear. The perturbations originating from the movement of the satellite in its orbit are generally moderate in visible band images, perhaps due to the appropriateness of the time chosen for the shots with respect to the angle of the sun's rays.

- The negative aspects and limitations of the optical images, which stand out the most are as follows:

  . Low resolving power vis-a-vis the size of the typical geological units and structures of the Iberian Peninsula: inside one theoretical pixel many important geological facts may at times lie. Moreover, the current understanding of surface geology and geological cartography far surpasses the details brought out by the images. The geological questions currently under study in Spain are mainly concerned with biostratigraphy, paleogeography, dating, etc., which can only be poorly resolved by means of a satellite. As previously noted, it is in the realm of tectonic megastructures and large fractures having morphological repercussions where the best applications of satellite technology are foreseen. As commonly known, the western boundary of the Mediterranean, which includes the small Iberian plate as well as the Alborán micro-plate, presents problems in megatectonics which are as of yet unresolved.

. Barring possible maladjustments in the instrumentation, it seems that the thermal scales used are frequently exceeded (at both extremes). For the Iberian Peninsula, then, a system having a lower resolving power but a wider-ranging scale would be preferable. For example on a given summer day, ground temperatures may vary from 0º C in a shaded glacial region in the Pyrenees to 65ºC in dark rocks located in an Andalusian lowland.

Once the range of the most informative temperatures, from a geological point of view, has been determined, data from high resolving power as well as meteorological information may be brought to bear on this research. According to meteorological data, and in relation to the IR-N images, it appears that the maximum lithological contrast foreseen for the surface temperature of rock lies between 10 and 20º C, this being for extensive areas characterized by little relief (between 500 and 1.500 meters in altitude).

. For reasons believed to be instrumental in origin, it is apparent that in many optical images the scale of grey tones lacks distinct differentiation, and in this way the 16 tonal gradations are not always acheived in the contrast band nor in the images.

Undoubtedly, if new images highlighting discrete intervals (including the use of artificial color) were to be planned, the criteria to be followed for geological purposes would differ from those required by other disciplines and objectives.

2.2. SPECIFIC GEOLOGICAL FINDINGS IN THE EASTERN HALF OF THE IBERIAN PENINSULA.

Geological elements heretofore unknown were not discovered. On the other hand, new complementary data on major geological structres and unresolved problems were forth coming. A synopsis of the many localized phenomena dealt with in the commentary on each image, selected according to their importance and frequency of occurrence, is provided below:

- A superior demarcation of the continental terciary basins (Duero, Ebro and Tajo). Also small minor basins of the same time scale, either joined to the above or occuring in isolation: Almazán (Soria), Tierra de Barros (Badajoz), Calatayud-Teruel, etc.

  Through combined study of the images, border facies could be distinguished (more recent, of a thicker grain size, having an angle of deposit associated with the peripheral paleo-reliefs), which are characterized by differences in vegetation, cultivation and morphology vis-a-vis the center of the basin.

  A long-disputed controversy was resolved as well: the demarcation of said basins by fractures, at least in part. As pre- and syn- sedimentary and not post-terciary faults are in question, they are not visible on the surface. These faults created an escarpment which was later buried by materials along the border of the basin, and which even today scarcely outcrops. This is also true in the case of the important Guadalquivir fault, which describes the NW limit of the marine terciary fault which is found there.

These fractures (and at times monoclinal flexures) have always been both problematic and contraversial as to their characteristic and even as to their existence. Their presence having been postulated on different grounds and by means of various criteria, their effects were definitively manifested in the LANDSAT images, although it is only now that they can be observed for the first time at one viewing, due to the more extensive coverage of each image.

- A heretofore unobtained perspective of the mega-fractures which affect the Peninsula and neighboring areas. Perhaps from this time forward the true import of certain fractures should be reconsidered, fractures whose importance was doubted or which were held to be of little transcendence. For example:

  1. The fault occurring at a 145º angle along the Algodos River, cutting across what is known as the "arco de Mora", to the east of Toledo.

  2. The fractures co-occurring with the "Plasencia" or Hispano-Portuguese Fault, which goes from the center to the SW portion of the Peninsula.

  3. The fracture systems occurring at a 25-30º angle in the Central Mountain System, the Eastern Sierra Morena, the NW portion of the Peninsula, Catalonia, eastern interior coastal region, and the coast of Almería (these last three lying within the pilot area).

  4. The faults occurring at approximately a 100-110º angle, located in the central-western Pyrenees, probably associated with the North Pyrenean Fault, which runs approximately E-W.

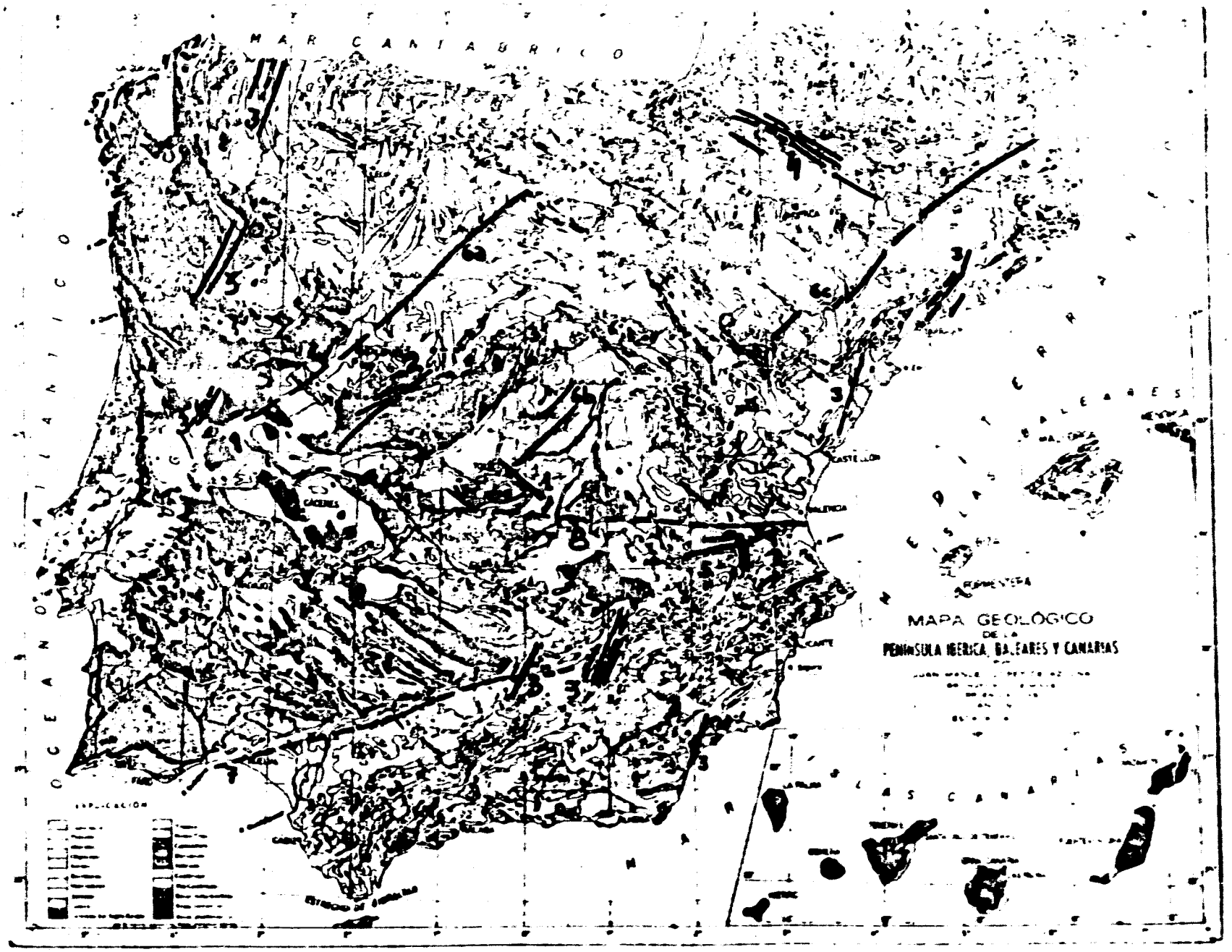

ORIGINAL PAGE
BLACK AND WHITE PHOTOGRAPH

Fig. 4. Geologic Map of the Iberian Peninsula, showing faults (see text 2.2)

5. The parallel faults (at approx. 80º and 170º angles) which demarcate the El Caroch Massif and the mid and lower course of the Jucar River and the Cofrentes-Ayora-Almansa basin, all of which lie to the SW of the province of Valencia. The results here surpass the definition of the LANDSAT images.

6. The hypothesized basement fractures, running at approximately a 40º angle along the borders of and underneath the three terciary basins, having experienced possible later adjusting movements whose main consequence would be the straight sections of the following rivers:

   6a. Arlazón River, in the Duero Basin
   6b. Henares and TAjuña Rivers, in the Tajo Basin.
   6c. Segre and Martin Rivers, in the Ebro Basin.

7. The much-disputed Guadalquivir Fault, running at a 60º angle, can be observed in its entirety in a great number of images, although it mainly lies below the Terciary, more to the SW than where previously supposed, along the Huelva-Sevilla-Cordoba axis. It is chronologically antecedent to system # 3.

8. The Valencia fracture, still quite problematic, which runs E-W and covers a long distance (partially sketched by ALIA (1976 and later works) and SAENZ de SANTAMARIA (1976)) seems to show up to the south of the Altomira Mountains and more to the east than before through the use of the HCMM images. At this point in time, however, insufficient field and geophysic data are available to characterize this hypothetical fracture.

- Greater continuity was achieved in tracing the the edges of the hercynian mega-folds of the Toledo Mountains and the Eastern Sierra Morena than with the LANDSAT images, but only in IR-D and IR-N. These fold edges are composed of quartzite, as opposed to the schist found in anticlinal nuclei and the slate in synclinal nuclei. The thickness of the quartzite (generally inclined at 30 to 80º angles) does not normally exceed 300 meters. The width of the outcrop falls below the resolving power of the system; however, the relief, almost Appalachian in character, produces rings of rubble on both sides of the quartzite (thickly forested). These always have a width of more than 1 km., which in this case is compatible with the size of the pixel. In the synclinal and anticlinal areas, which are wide, have little relief, and contain the soft materials mentioned above, grazing and the cultivation of dry cereals predominate. The contrast in the thermal images is quite sharp from one area to another.

- As far as pure geomorphology is concerned, a localized phenomenon already noted in the LANDSAT images was confirmed: the existence of a strange relief parallel to the present course of the lower Ebro River, more to the north as well as at the height of the Mesquinenza Dam. There seem to be morphological remains possibly left over from an earlier course of this major river, quite a few meters above its present level.

- Promising perspectives for current marine geology have opened up due to the IR-N images. These images provide an astounding look at bodies and currents of water of different temperatures in the western Mediterranean.

An enterprising project would require joint efforts in the following areas:

. Complete hydrographic study at the mouths of major rivers (flow capacity, seasonal regime, etc.).
. Sedimentological study of solid materials carried by these rivers, in terms of both quantity and composition as well as grain size, seasonal variations, etc.
. Study of the mechanisms of deposition at the motuhs of the rivers.
. Construccion of a sedimentological model which would amply and systematically reflect marine and beach phenomena.
. Comparison of the model so designed with a hydrodynamic model. Oceanographic research for this second model could rely on significant aid from the satellite images.

Especially in view of the high amount of pollution in this area of the Mediterranean, the results would be extremely insightful. As far as the evolution of the coasts is concerned, should mention that the materials which make up the beaches, in the Castellón area are correlated eith the contributions of the Ebro River and, that following the operational start-up of major dams in the basin of this river, its delta and some of the aforementioned beaches are regressing.

- As for the more negative results related to geology, almost all of them have to do with the reduced size and the dispersion of the phenomena which were intended to be found:

. Thermal springs and acqueous emanations frequently are to be found in the pilot area. CRUZ-SANJULIAN and

GARCIA-ROSELL (1975) list more than 50 emanations in this part of the Peninsula. The highest temperature exceeds 52º C, and the highest flow volume is close to 50 l/sec. Some of these emanations are due to acute positive anomalies in the geothermal gradient.

Positive results were not obtained in the correlation of the true ground readings with the IR-N images. It seems that this is due to the relative smallness of the phenomena with respect to the pixel and to the wide variation in relief, which acts to hide or mask localized thermal anomalies.

. Underwater emanations of karstic, subterranean, on thermal waters proceeding from the continent were not discovered. It has not been determined whether or not this is due to their nonexistence (improbable), to their diffusion and mixture with sea water, to the similarity in temperature with sea water, or to their relative smallness vis-a-vis the system's resolving power.

3. PROBLEMS AND DIFFICULTIES

The problems which have hampered progress in the study are so familiar to those who have been directing the Project that it would be redundant to bring them up herein. From the point of view of the utilization of the images for geological purposes, the major difficulties were as follows:

- The irregular receipt and distribution of photographic images. It would have been better to wait until all of them had been acquired and then to have selected the most useful. On some occassions effort was wasted on trying

to interpret low-quality images which at the last second were substituted by other similar ones of a better quality. With the entire catalogue at our disposal, it would have been possible to do the same work with less effort, in a shorter amount of time, and in a more intensive manner.

- The recording time of all the data was not known with enough advance notice, with the consequent impossibility of gathering pertinent meteorological data after the fact (the only recourse was to dated weather bulletins, which were not always accesible).

As for general negative aspects of the Project, the collaborators in the research who the project after it had begun lacked the following:

- Sufficient advance information as to the technological and bureaucratic aspects of the Project. Part of this kind of information did not reach our level until 1978 and even after. This includes the news received in January of 1979, wherein the continuity of the Project was put in doubt.

- Sufficient information regarding the monetary budgets available for field work, laboratory equipment, administrative materials, drafting, typing, English translations, etc., as well as the ways and means of justifying and accrediting the various expenditures.

4. SUPPLY AND QUALITY OF THE DATA

Comments and criticisms regarding the subject matter dealt with herein have already been put forth in sections 1.0,

2.0, and 3.0. At this point in time we wish to add the following:

- Regarding the resolving power, it bears mentioning that this turned out to be even lower than that foreseen for the pixel size employed. We are, however, unaware of the technical reasons behind this.

- As a counterbalance to the above there is the global view of large areas of the peninsula heretofore unavailable in earlier images.

- There exist at times numerous atmospheric perturbations above the pilot zone: stagnation cloud formations, hot air masses, etc. In this area there is a need to carefully select the times of year in which these phenomena are less frequent.

- The supply of the photographic materials has been quite irregular, unpredictable, and limited. For the geological puposes at hand , it would have been advisable to have laboratory services capable of making copies on request on different types of paper (hard or soft), on transparent backing, etc., and in different sizes, degrees of exposure (to highlight grey tones), etc. It is common knowledge that in photointerpretation different copies derived from the same negative can provide varying or complementary details.

  In our case these "special order" images must be requested from the same laboratory where the digital-optical conversion is done, and only as long as a previously standardized catalogue is available.

- We wish to repeat the need to have this catalogue at our disposal so as to choose among the images, rather than

analyzing in progress the good and bad images that come up without knowing if better-quality images will later appear. Had the satellite functioned as planned, the amount of material to be analyzed would have been overwhelming.

5. RECOMMENDATIONS

This section directly follows the discussion in sections 3.0 and 4.0 as the suggestions herein are put forth with a view toward avoiding repetition of those problems already mentioned, and in order to improve or broaden the results of any future projects of a similar nature. Specifically, for future research we would like to suggest:

A) Technical and Scientific Aspects

- Pixel size and resolving power such as would represent an improvement over and not a retrogression from those of the LANDSAT images, even if this supposes a loss in the global view of large areas. For the geology of mobile areas and for countries possessing advanced cartography, a high resolving power is required.
- Careful scheduling of the times of year, days and hours in which the data should be recorded, in collaboration with the local meteorological services.
- In view of the results to date, it would be extremely beneficial to have access to the IR-D and two IR-N images corresponding to 24 hour periods, one of the IR-N having been taken 2 to 4 hours after sunset, the other 8 hours after the first --in any case before sunrise.

This suggestion is bases on the following:

. Winter nighttime images are too dark and lacking in contrast at the time at which they are taken.

. Summer nighttime images at the tiem they are taken are already dark but are still useable, with the exception of low-lying, hot, sheltered areas, which still have warm or hot air that produces diffuse contours.

. Two successive images taken on the same night would provide a wealth of data concerning apparent thermal inercia, even in the case of visual interpretation.

. Two successive nighttime images (seperated by a few hours) of the western Mediterranean, given the thermal inertia of the water, would be similar in the informatio they provide, but would in addition evidence the movement and changes in form of currents and bodies of water. Simultaneously viewed through a stereoscope they would produce a false paralellism and a consequent false relief, which in turn could be used to quantify the magnitude of the displacement and its velocity vis-a-vis horizontal parameters.

- There is a definite need to have prior access to a catalogue of the different images so as to enable the user to request new copies, specifying the particular charateristics desired; i.e., highlights, contrasts, etc.

- As for auxiliary profiles done according to scan lines in accordance with the size and attitude of the peninsular geological structures and the attitude of the sweep lines themselves, more than 25 of these profiles per image

would be necessary in order to adequately contrast and control tonal and lithological variants.

- Together with the HCMM images, wather satellite images of the same day and the two previous days would be needed. Images taken under wider-ranging weather conditions than those used in this project would also be necessary.

B) Organizational Aspects

- Systematic notification of the research team as to the times set for the gathering of data, sufficiently in advance (in spite of the possibility that these data may not be recorded due to some undetermined reason).

- Easier access to other previously existing materials having to do with the area under study and which are not restricted in their distribution.

- A detailed account, on the level of each individual participant in the research, of the availability of equipment and materials, and the nature, means of justifying, coverage, and availability of monetary budgets, in order to facilitate the planning of the scope of and means available for each research task to be undertaken.

6. CONCLUSIONS

From the visual analysis and interpretation of the images received the following conclusions regarding the Project are forthcoming (according to geological criteria and with reference to the Iberian Peninsula and the surrounding areas):

- In terms of visible band images nothing new has been added with respect to previous images from other projects.

- The results from infrared images are encouraging, under certain meteorological conditions and with respect to: fold mega-structures, large basement fractures having morphological repercussions, recent paleogeography and marine geology (present detrital sedimentation in coastal regions and flatlands, undersea erosion, etc.)

  The thermal resolution in the infrared images is perhaps too great as compared to the graphic representation of the images. On the other hand, the temperature scale does not range high enough for summer daytime images, and not low enough for nighttime images of the high altitude zones of the Peninsula, especially during the fall and winter.

- The resolving power is disproportionately limited for highly mobile geological zones, characterized by rhythmic formations, abundant irregularities, small folds, and a varied topography. It is also limited for zones whose surface geology has been scrutinized to the point where the corresponding cartography is available on a scale of 1:50.000 or even 1:25.000.

- In the area studied positive results were not as to attained the locating of positive geothermal anomalies and hot springs for both of which there exists partial control in the field. Unfortunately, the phenomena being dealt with here predominantly occur in the SE portion of the peninsula, which is one of the zones having the highest ambient temperatures (annual average exceeds that of the central plateau by more than 10º C). Moreover, this zone, which is alpine in

type and is prone to seismic activity, is characterized by a quite varied and young relief. This means that, due to differences in altitude and in the lie of the hillsides, the thermal effect hinders any observations to be made. Perhaps and exhaustive analysis of numerous systematic and geographically pinpointed profiles might contribute something new to this.

7. BIBLIOGRAPHY

It would be impossible to include here a list of the geological studies of a regional nature employed either directly or indirectly in the analysis of the images and their comparison with ground-truth information. Moreover, it would be quite difficult to distinguish between the observations made by others and which have been public knowledge for some years now from those of the present author. To the studies and abstracts cited informally in section 1.3 the following are now added, by reason of their direct bearing on the problem at hand:

ALIA MEDINA, M. "Una Megaestructura de la Meseta Ibérica: La Bóveda Castellano-Extremeña". Estudios Geológicos, 32, pp. 229-238, Madrid (1976).

CRUZ-SANJULIAN, J. & GARCIA-ROSELL, L. "Termalismo en España Meridional". Boletín Geológico y Minero, 87 (2), pp. 179-186, Madrid (1975).

SAENZ DE SANTAMARIA, F. "Generalized Terciary Tectonics of the Iberian Peninsula". Boletín Geológico y Minero, 87(5), pp. 456-461, Madrid (1976).

The following images were subjected to the process of interpretation:

AA	0141-13000	DAY-VIS	14	SEP.	78	see	fig.	6a
AA	0141-13000	DAY-IR	14	SEP.	78	"	"	6b
AA	0184-12590	DAY-IR	27	OCT.	78	"	"	7
AA	0185-13160	DAY-VIS	28	OCT.	78	"	"	8
AA	0185-13160	DAY-IR	28	OCT.	78	"	"	9

Registered and enhanced subscene of the images:

AA	0072-13170	DAY-VIS	7	JULY	78	see	page	165
AA	0072-13170	DAY-IR	7	JULY	78	"	fig.	5
AA	0072-02230	NIGHT-IR	7	JULY	78	"	page	170

And also the following set of images that present less interest:

AA	0087-02020	NIGHT-IR	22	JULY	78	
AA	0115-02200	NIGHT-IR	19	AUG.	78	
AA	0120-13060	DAY-VIS	24	AUG.	78	
AA	0127-13360	DAY-VIS	31	AUG.	78	
AA	0127-13360	DAY-IR	31	AUG.	78	
AA	0157-02050	NIGHT-IR	30	SEP.	78	
AA	0185-13180	DAY-VIS	28	OCT.	78	
AA	0185-13180	DAY-IR	28	OCT.	78	
AA	0190-13090	DAY-VIS	2	NOV.	78	(Negat.)
AA	0190-13090	DAY-IR	2	NOV.	78	(Negat.)
AA	0191-13270	DAY-VIS	3	NOV.	78	(Negat.)
AA	0191-13270	DAY-IR	3	NOV.	78	(Negat.)

OPERATIVE METHOD

We followed a known method, which has given good results when trying to control sudden superficial changes (vegetation, fires, devastating storms, etc.): It consists on the observation in one area of two simultaneous images of different bands or two images of one band but corresponding to a different date.

The observation by means of a stereoscope of both simultaneous images VIS/IR, has given the following results:

- A quick elimination of the semitransparent cloud covering, which could lead into errors by means of a sharp contrast (the typical subjective scintillation).

- The enhancement of important fracture lines, most of which are already known (though some of them are still debated at the present).
  All fractures, certain or doubtful, have a common denominator: an outstanding morphologic response even if they appear with senile forms.

R E A D I N G

Confirmed Fractures

Covered, deduced or doubtful fractures

Structural ranges with morphologic response

First Order Geologic contacts: borders of sedimental basins, discordances, etc.

Little consolidated Continental Tertiary Materials (clays, sandy clays, limestones, etc)

Little consolidated Marine Tertiary Materials (marls, clays, sandy clays, limestone)

Recent fluviatile sediments

Precambrian Nuclei (schist,...)

Directions of transportation in sediments

Possible River-Paleocourses

(5) Geographic reference of areas or elements described in the text.

Both images have a bad quality for a visual interpretation with geologic criteria, when seen separately.
Apart from the cloud covering which is partly transparent for IR, the first image also shows the presence of "noises" which diminish the resolution power;The second image seems to be affected in all the area of the Meseta by the typical summer thermal inversion, with high temperatures on ground level.

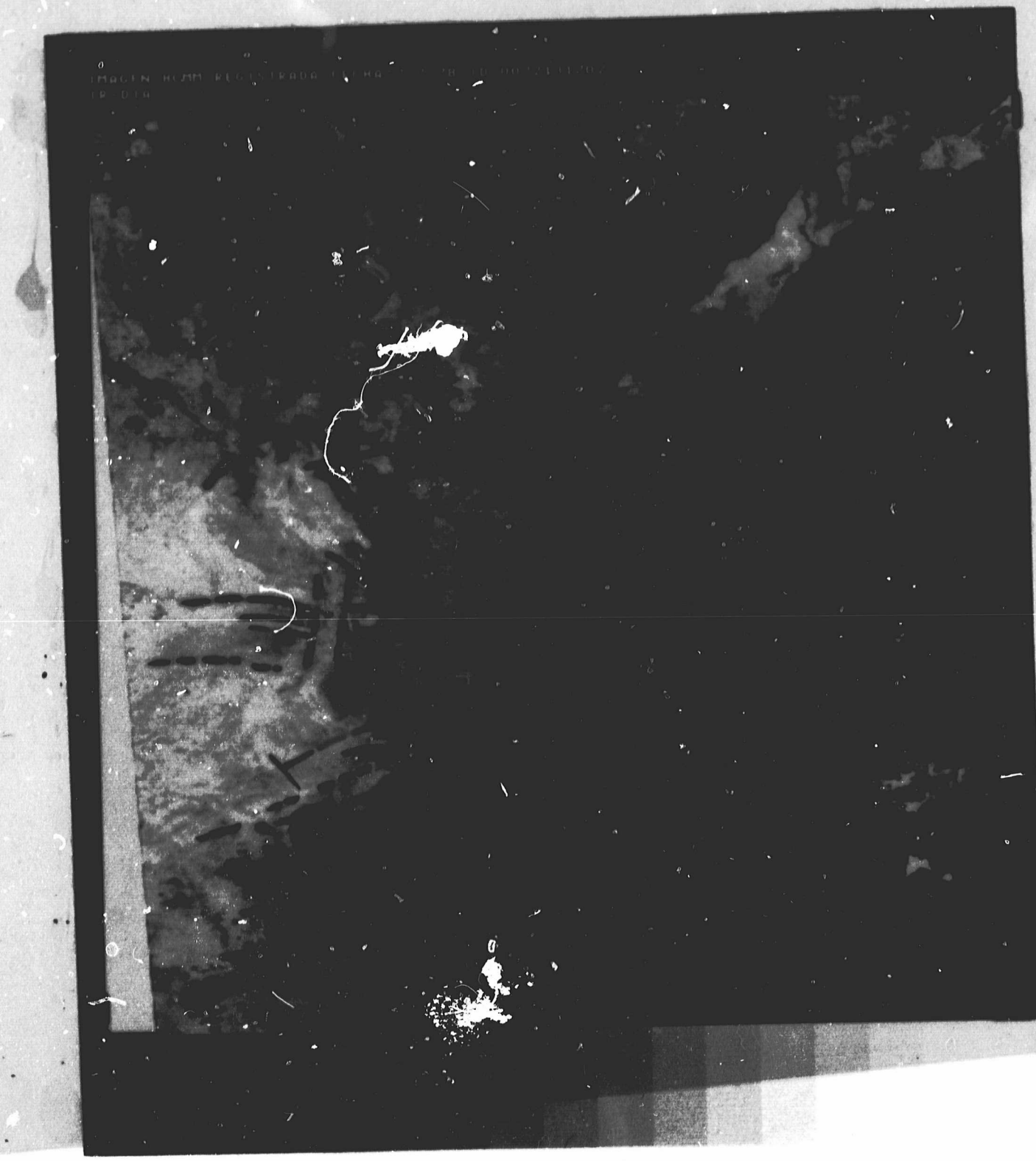

ORIGINAL PAGE
BLACK AND WHITE PHOTOGRAPH

Fig.5 Image 0072-13170-2 and overlay
(see also image 0072-13170-1, page 165)

These images don't provide anything new, when compared to similar ones which have been already analyzed.

As can be seen, the test-area is covered by clouds for the most part; therefore we shall consider other areas, even outside the Iberic Peninsula.

A simultaneous observation of both images with a stereoscope has been performed and we obtained some striking results.
The limit between different types of vegetation is different in both images; sometimes this produces a pseudostereoscopic effect.Something similar occurs with the shades of the clouds: the visible shade is instantaneous but the "thermal shadow" is left behind as the cloud moves forward.
Besides this, in the thermal image the sunny part can't be distinguished from the shaded part.

From a geological point of view, really new elements are not distinguishable.Great fractures with a morphologic effect stand out.
This occurs on the North-Pyrenaen fault (1) and on those that enter the Peninsula through the Rhone Valley, between the Montagne Noire and the Prealps (2), cutting the East Pyrenees and the East part of the tertiary basin of the Ebro River.No important data can be obtained neither in the nucleus nor in the axial zone of the Pyrenees (3).

Oblique fractures can be observed between the Pyrenees (3) and the Prepyrenees (4); these are important for trying to deduce the Northpyrenean fault's real nature as well as the direction of the shift of its horizontal component (1).- These kind of fractures border the longitudinal morphologic depressions of land which are characteristic of this area; they contain interesting natural gas traps.

In the Pre-Pyrenees (4) morphologic ranges of stratigraphic and lithologic origin, can be observated better than faults.
The contact with the Ebro River's tertiary depression of land is rectilinear; it probably corresponds to a line of paleofracture, which is not visible in the surface at present, though it can be demonstrated by fotogrammetry due to the fact that it detects sudden changes of lithofacies, morphology, etc.

As far as the East part of the tertiary basin of the Ebro River is concerned (5), it is obvious that the thermic image shows a general situation of high temperatures on ground level in an area which has scarce vegetation.

Therefore, fertile river valleys stand out very clearly.

Once again, the meandering stain between Pina del Ebro and Fraga formed by the umbria vegetation of a series of reliefs stand out. This stain should be analyzed with geomorphologic criteria and detailed topographical maps in order to check if it corresponds to a Paleobasin of the Ebro River itself.

ORIGINAL PAGE
BLACK AND WHITE PHOTOGRAPH

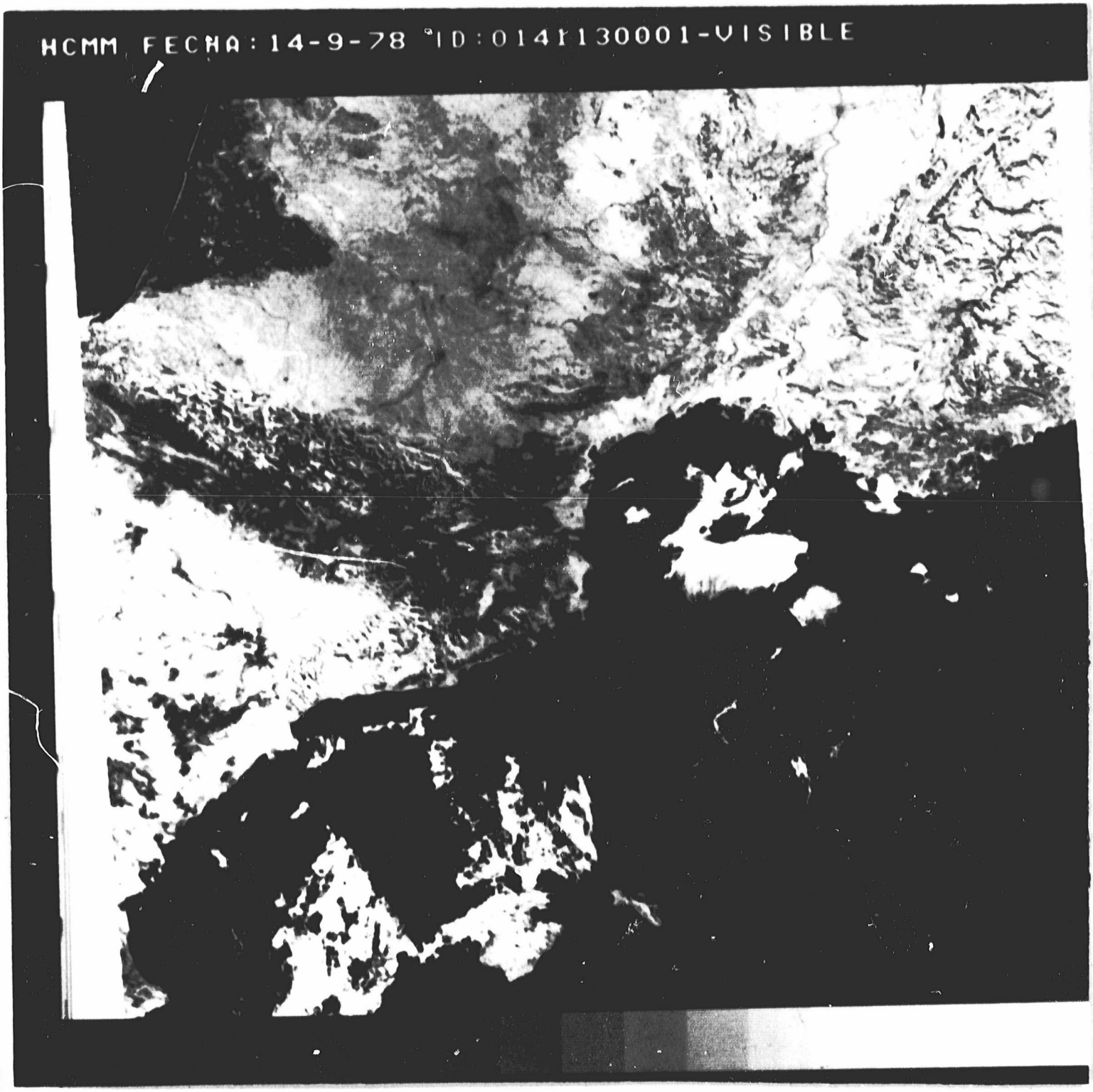

Fig. 6a Image 0141 - 13000 - 1

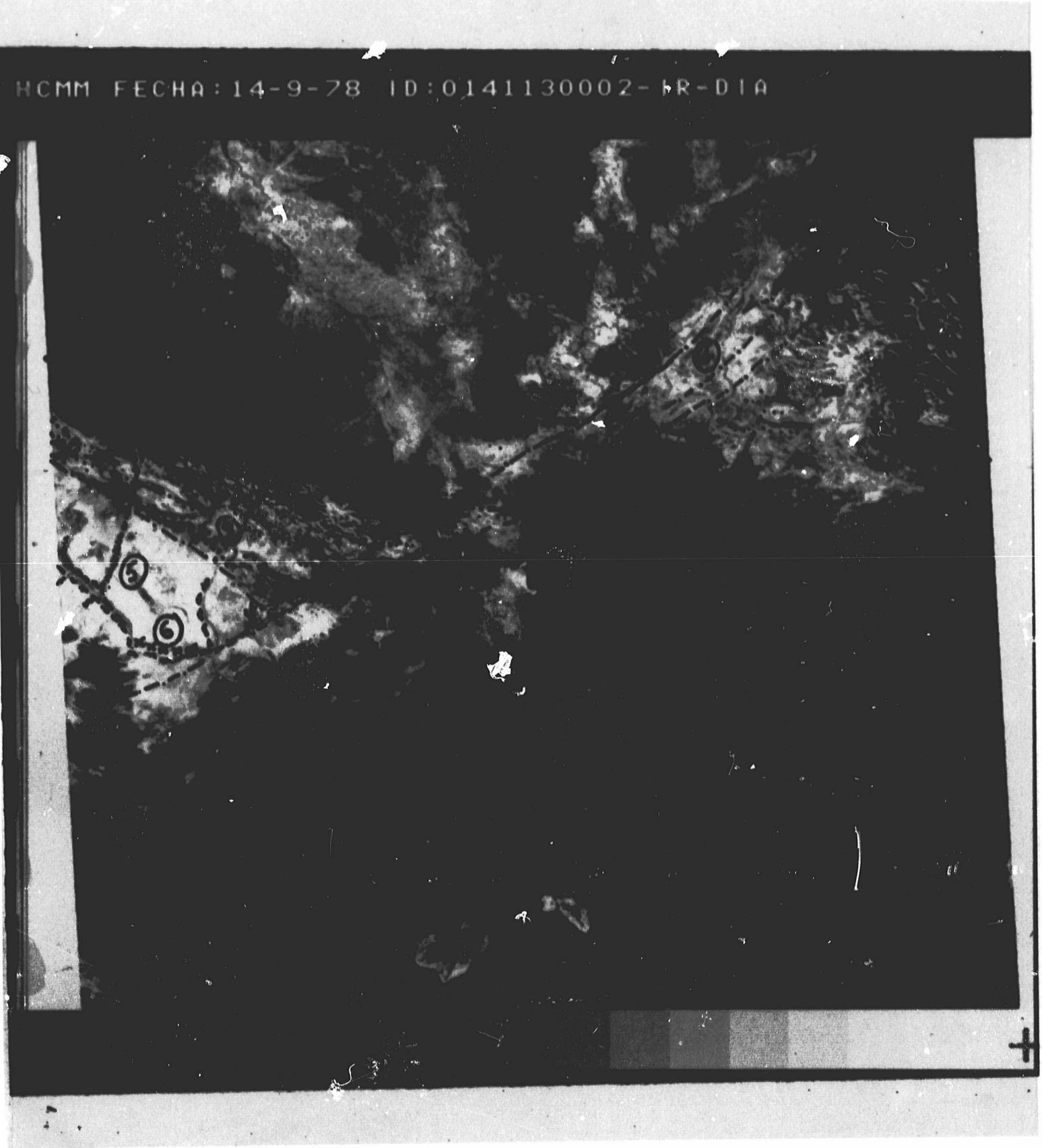

Fig. 6b Image 0141 - 13000 - 2 & overlay

This image includes a great part of the test area.It only shows a cloud covering in the North-Eastern part of the Península and the Balearics.

From a geologic point of view, three units can be differentiated:

1.- Areas of contrasting tones, which correspond to outcrops of Plutonic, Precambric, Paleozoic and Mesozoic rocks.

2.- Areas with medium tones, whether uniform or not, which correspond to cultures in fertile valleys (5) or to great forest masses (6); the first are located on low river terraces, the forest masses on different lithologies. The Ebro Delta (7) lies between these zones of intensive culture.

3.- Areas of light tones, formed in the greatest part by terrigenous tertiary or quaternary materials (generally continental basins) were not much affected by tectonic movements and were not compacted too much.
These materials are generally scarcely lithificated and their cementation, degree of crystallisation (and in some cases high porosity) when compared to igneous, precambrian, paleozoic, mesozoic and even paleogenes lithologies, makes the thermal conductivity decrease strongly.

Therefore, supposing an uniform insolation of the whole area, it is logical that these rocks stand out clearly, especially in depressions of land, which are much more protected from the wind and have reached higher temperatures during the day (depressions of land of the Ebro (6), Valles-Penedés (9), Reus-Valls (10), Júcar (11), Gallocanta (12), Calatayud-Teruel, etc.

Other tertiary and quaternary areas, with strong insolation and different degrees of protection by nearby reliefs are i.e. Almazán-Arcos de Jalón (13) and the coastal plains of Tortosa-Vinaroz (14), Castellón (15), Liria and Chiva Torrente (16), Monteälegre del Castillo (17), Campo de Cartagena (18) and central depression of land of Mallorca.

But we have to point out a most important factor:

Generally speaking, materials of the Pre-Miocene Period are those which show structural reliefs which are much more abrupt and massive and which have the greatest differences of altitude.- Therefore, the thermic effect of the relief and the insolation contrast between slopes is also much stronger.To say it in other words: compact and crystalline lithologies with a higher thermal conductivity, correspond to those areas which have the most abrupt relief and the greatest differences of air temperature and of the insolation conditions.

It should be noted, finally, that areas of the meridional and western slopes of high reliefs (20), radiate much more energy than low zones in which doubtlessly, air temperature is higher.

At the time of the register, the mean emission of the continent is still superior to that of adjoining marine waters and much greater than the emission of continental waters (21).

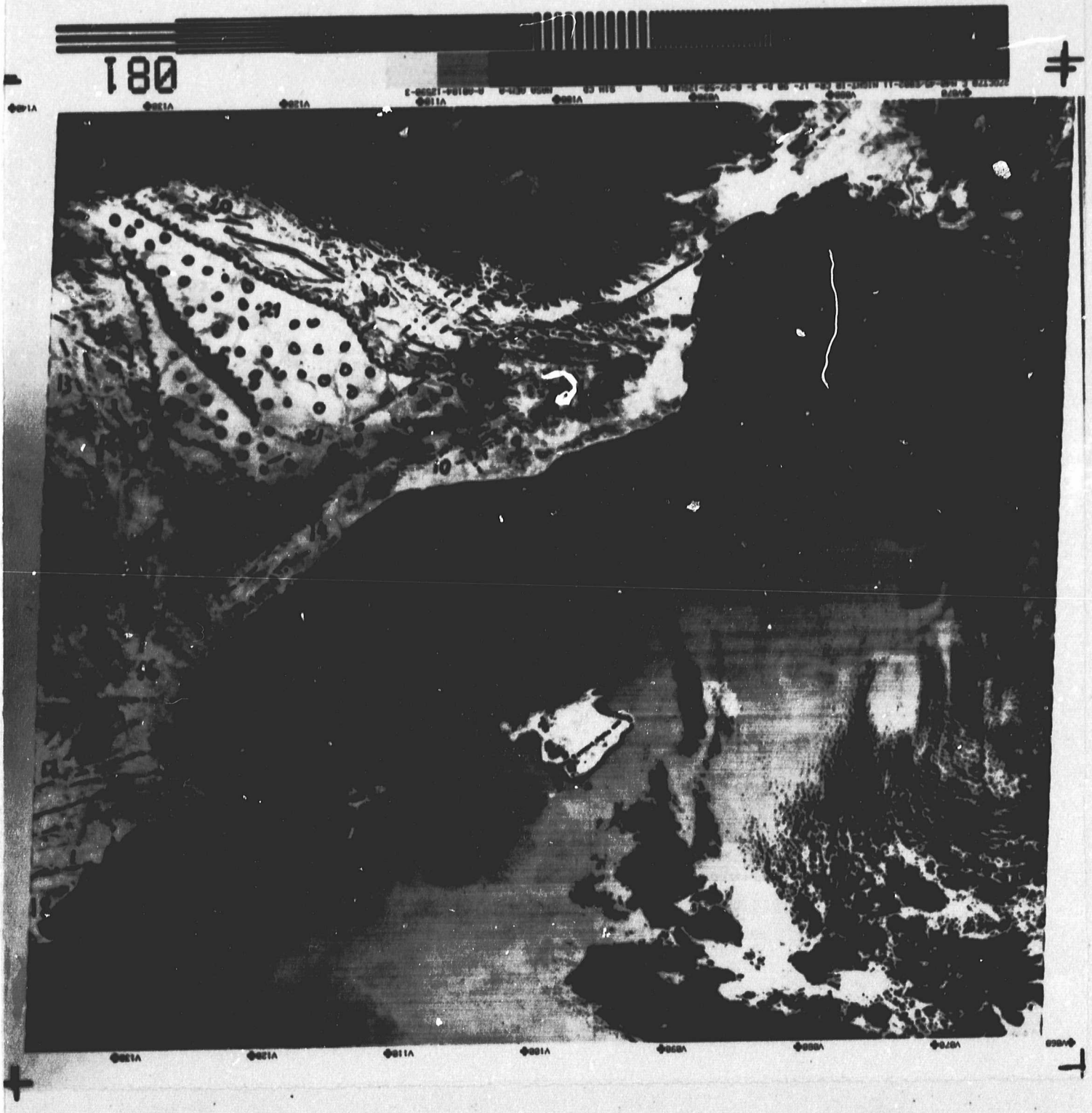

Fig. 7 Image 0184-12590-2&overlay
(This image is wrongly annotated as night-IR)

This visible image corresponds to the same area of the image A-A 0185-2 (108); therefore, it is possible to compare it with the geologic interpretation.

The border of clouds blocked by relief, which correspond to a situation of wind from the Levante, hinders the observation of the coast of the test-area. Nevertheless, the following morphostructural elements can be pointed out:

- The arched border of the Guadix-Baza depression of land (Granada) limited by the Sierra de Baza and the Sierra Nevada and what is possibly a NW-SE fracture.
- Tectonic contact between two subbetic units: The Sierra de Cazorla and the one located to the SW (it doesn't have a specific regional name) (2).
- Prebetic of the region that borders Murcia-Albacete-Alicante; in this area the most important fractures of "Betic direction" (generally inverted with vergency to the NW), are clearly distinguishable as well as other conjugated fractures whose direction is almost perpendicular, with a tangental component.

  It is possible to distinguish intramontane basins of the late Tertiary Period or of the Quaternary, which give medium gray tones (3).
  In this area, both the lithological changes (basically between limestones and marls) and the local structures lie under the resolution power of the image.

The tectonic depression of land of the medium course of the Júcar River (4) lies to the North of the cretacic massif of Carcelén (Albacete) and is filled by Tertiary continental materials; the depression of land appears even with more sharpness than in Landsat images.

The massive of El Caroch (5), whose structure is pentagonal and irregular, has a tectonic which is still problematic, because of its grinder structure, which is jagged due to complicated fractures. This massif is surrounded by strongly foldened mesozoic materials and is composed basically of cretacic limestones, though the dark tonality which is tronger to the W, corresponds to the dense forest which was destroyed by fire after this image was taken.

The whole Cordillera Ibérica-Maestrazgo (6) has only one clear separation: Forested areas (pinewood and mediterranean forest) and cultivated areas plus pastures.

The criterion for this division isn't geologic but topographic and morphologic: therefore areas with a high altitude or "abrupt relief" are considered "forest" or "woodland" as they are not profitable to cultures.

The wrentch faults of the East Coast of Almería (7) can be clearly observed.However its prolongation into the arch of Aguilas-Mazarrón (murcia) is covered by clouds.

The tertiary basin of Tajo-La Mancha (8), the depression of land Calatayud-Teruel (9), and the montaineous paleozoic whole, Sierra Morena-Montes de Toledo don't introduce anything new; the uniformity of gray tones of the stripe of La Mancha that goes from Ciudad Real to Albacete (of about 30-50 km wide and 220 km long), should be stressed.
After studying the area on the field, we suppose that this is due to the following reasons:

- The central area of La Mancha has a lower relief: the surface of finitertiary filling remained horizontal as it was not affected by erosion.
On the other hand, debris flow of the surrounding mesozoic and paleozoic areas, which provide fans of quaternary materials do not reach the zone of La Mancha.

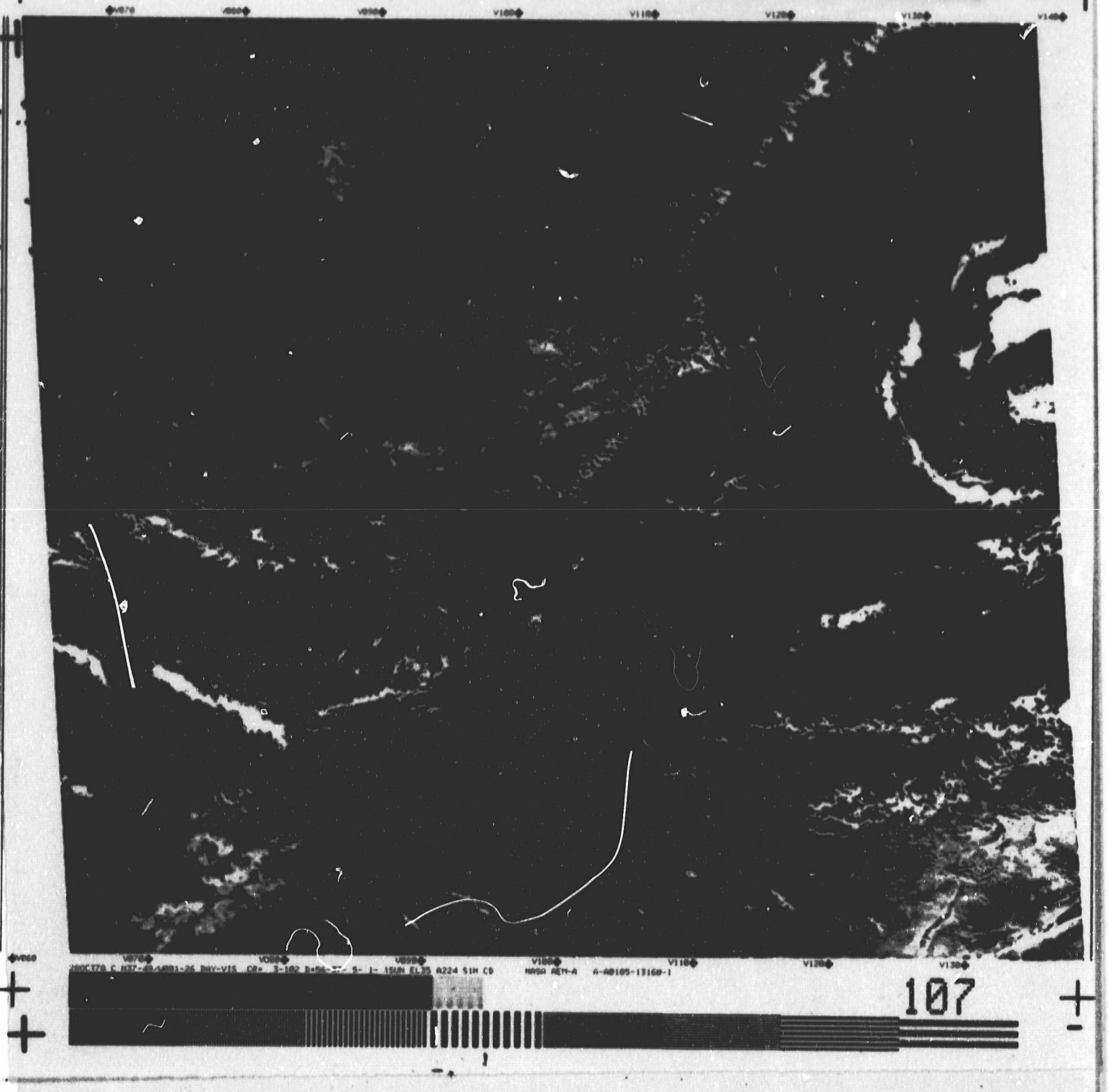

Fig. 8 Image 0185 - 13160 - 1 & overlay

This is a very interesting image in spite of the presence of stem clouds related to an area of low atmospheric preassures (which stake out the first interior reliefs of the levantine coast) and of the instrumental fault in the Southern half.

It corresponds to the visible image A-A-135-B160-1 (107).The alternation of lithologies (basically slates and quarzites in the Paleozoic and limestones and marls of the Mesozoic) produces changes in the spontaneous vegetation and also determines an inevitable selection of woods and cultures which appear in this images much clearer than in all other images, studied to the present.In some cases. its sharpness is superior to the results of the different Landsat bands, in spite of its greater definition and resolution power.

No new structural elements can be distinguished in the test area, although already known elements are observed more clearly:
Northern fractures of the cretaceous massive Chinchilla-Carcelén (1), Cretaceous grinder of El Caroch (2), Prebetic arch of Alcaraz (3), Structural "V" of Hellín of a complicated genesis (4) and many fractures and folds in the Iberic Southeast Cordillera, as well as in the Prebetic of Murcia and Alicante.

Really unpublished data however, appear in the Montes de Toledo and part of the Siarra Morena.Here, the directrixes of the hercynian megastructures, marked by the ordovician series with its nucleus in the armorican quarzites.These produced elongated and wild reliefs; dense mediterranean wood grows in its slope deposits.In this image, the dark tone of the mediterranean wood contrasts with the precambrian, schale-greywacke substratum (predominance of pastures and cereals) and with the teriary and quaternary covers (cereals, grapewine, etc.) which have a higher reflectnacy in infrared. A Second Phase of deformation can be observed: It folds previous structures of a typical hercynian direction, whith a strain which is almost at right angle to the previous ones.

The macrostructural units have been defined long ago though data on the field, are confirmed in these images:
e.i.Anticlinal Peraleda-Montoro (5), Batholit of Los Pedroches (6), Anticlinorium of Cáceres-Alcudia (7), Syniclinorium of Herrera del Duque (8), Synclinorium of Almadén, Anticlinorium of Guadalupe (10), Synclinal of Guadarranque (11) Anticlinorium of Agudo-Valdemanco (12), Syniclinorium de Puebla de Don Rodrigo (13), Anticlinorium of Navalpino (14), Anticlinorium of Valde-

lacasa (15), Synclinal of Navas de Estena (16), Anticlinal of Los Cortijos (17), Anticlinal of Las Guadalerzas (18), Syncline of Los Yébenes (19) and the complex structure of Los Montes.- (20)

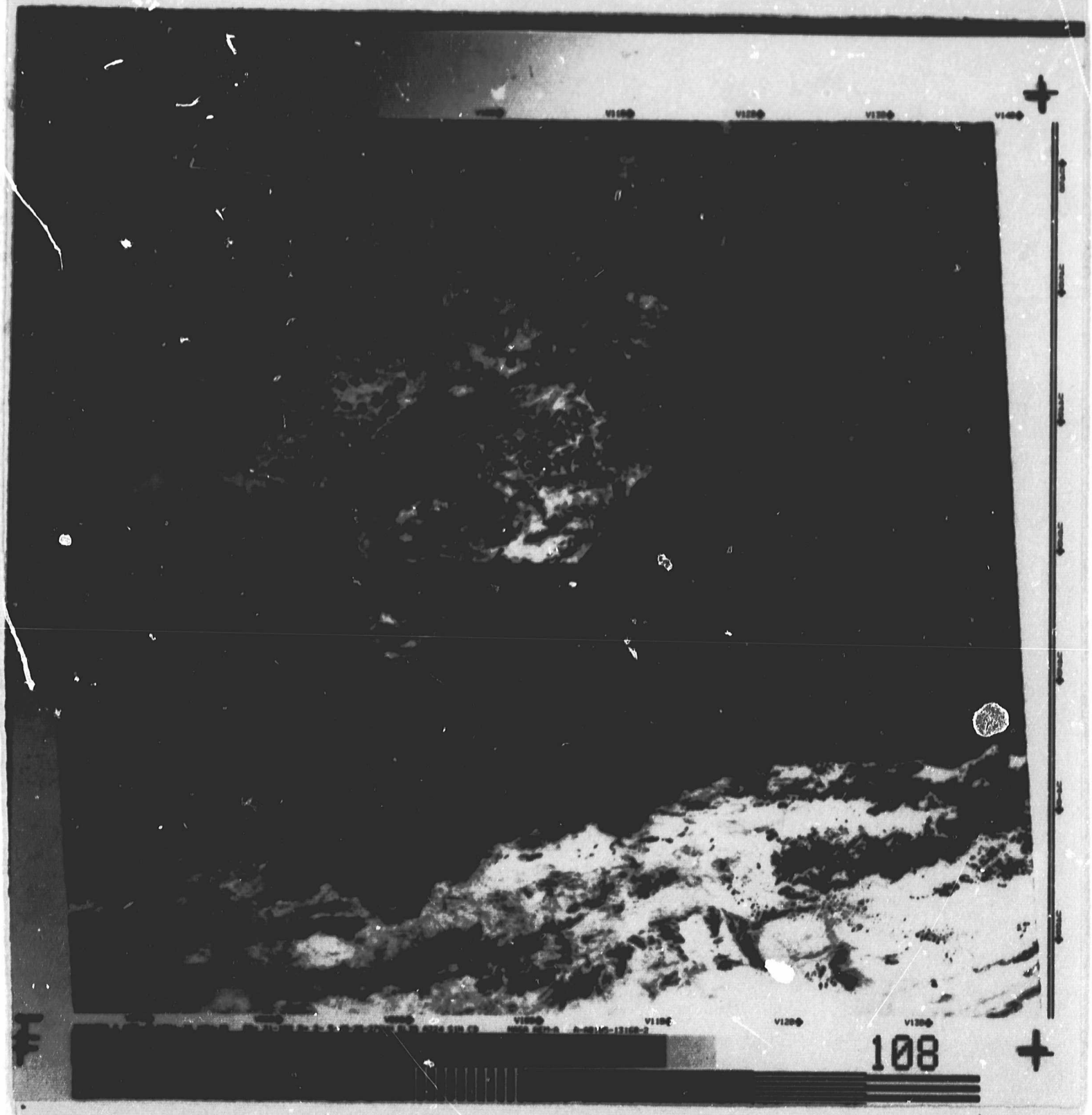

Fig.9 Image 0185 - 13160 - 2 & overlay

E D A P H O L O G Y

F.- EDAPHOLOGY

- "Interpretation of HCMM Imagery on the ERMAN-II System"
  (Reproduced from the Second Progress Report)
  José L.Labrandero
  Instituto de Edafología y Biología Vegetal

- "Results of the Interpretation of HCMM Images Applied to Soils"
  José L. Labrandero
  Instituto de Edafología y Biología Vegetal

INTERPRETATION OF HCMM IMAGERY ON THE ERMAN-II SYSTEM *

José L. Labrandero

Instituto de Edafología y B. Vegetal
(C.S.I.C.)

INTRODUCTION

The applications of remote sensing from satellite data to soil studies were initiated in Spain in 1975: first in the central region of Spain with Lansat-2 data, then with particular experiences for pedological investigation, and now using thermal infrared data from Heat Capacity Mapping Mission (HCMM) satellite.

The HCMM satellite data allows the measurement of surface temperatures by means of a two channel scanning radiometer. One spectral channel covers the visible and nearinfrared band (0.5 - 1.1 micrometers); the other channel covers the thermal infrared band (10.5 - 12.5 micrometers). These atmospheric spectral windows allow propagation of both radiations with least attenuation or interference. Environmental factors can produce anomalies on the images and the interpreter has to know the conditions under which they have been obtained, specially the thermal imagery.

The main objective in our study is the evaluation of HCMM data for pedological purposes: mapping soil units, supplementary information to the study of soils, and establish relationship between geological features and soil development.- Authors who have investigated thermal data in order to facilitate the interpretation of thermal infrared data, recommend making temperature measurements at the time of the HCMM satellite's overpass.

Our research program requires ground-truth data obtained on barren test areas at the time of the satellite's overpass. Regretfully, soil parameters were not available on the ground. Therefore the interpretation and analysis of HCMM data has been made without ground-truth data.

* Reproduced from HCM-034 Second Progress Report

II. MATERIALS AND METHODS

HCMM data available for our study were computer compatible tapes of calibrated and geometrically corrected data.These data correspond to scenes covering an area from Madrid to Valencia, and were gathered on the following dates:

October 28, 1978. Visible and near infrared (See page 154)

October 28, 1978. Daytime thermal infrared (See page 157)

The digital analysis of visible and thermal imagery from HCMM satellite was performed on the interactive system ERMAN-II, which provides gray-level display, on a CRT, of the digital data contained on the HCMM computer compatible tapes.

We produced gray-level subimages at different scales with the purpose of comparing results derived from the analyisis of HCMM data and reference information such as

1) Soil map of Spain at a 1.1.000.000 scale
2) Forestry map of Spain at a 1:400.000 scale
3) Geologic map at a 1:1.000.000 scale

III. INTERPRETATION OF CCT's ON THE ERMAN-II SYSTEM

In order to examine the main patterns of visible and thermal imagery, in this study we only considered the specific features of the land. Three typical aspects were used in the photointerpretation of the images. These were the following: soils, forestry and hydrography.

Soil Interpretation

In relation to this aspect, we can point out that delimitation of phisiographical soil units was very difficult in the daytime visible image and it was only possible in specific regular intervals along lines.

The HCMM daytime visible image shows, in general, similar characteristics to Landsat images though particular details are better defined in the latter because of its much greater resolution.

On the thermal day-imagery, soils appear warm and present different shades of gray.The diurnal surface temperature is affected by changes in local slope and the topographic effects can produce anomaloius cold spots.

The most noticeable feature on the thermal images was the detection of a soil unit characterized by superficial stones and gravel, according to the soil map.

Forestry Interpretation

Vegetation on the daytime thermal infrared image appears cold, with dark tones.

Two main forestry species are to be found in the study area of our image: Pinus Pinaster and Pinus Halepensis, both highly correlated with the mountain's relief.It is very important to point out the excellent discrimination of barren areas inside the areas with vegetation.

The information obtained from the visible image is only useful for sketching the forest areas.Delineating these areas could introduce some problems, due to shadow effects.

Hydrography Interpretation

Detection of hidrographic features is very easy on the images when we just distinguish main rivers, dams, lakes and other major hydrographic characteristics.Generally, water is less reflective than the adjacent soils, in the visible portion of the spectrum, and appears darker on visible imagery , but sometimes the detection presents serious difficulties in areas with high relief and dense forestry.

The creeks are easier to distinguish on daytime thermal infrared imagery than on the visible images, mainly because insolation (major source of surface heating) is minimal and therefore the contrast is stronger.

IV. PRELIMINARY RESULTS

The study has been carried out on two HCMM images for pedological purposes.The results presented here, show that the information obtained by visible and daytime thermal infrared imagery is not an important source of data for the increased identification of soil and terrain conditions. That the scale was too small and the ground resolution was too poor, might be the factors responsible for these results.

Our analysis of the HCMM Imagery on the interactive system ERMAN-II showed that the information provided was only partially useful for the soil mapping purposes.Results could probably be improved using excellent quality data from different dates of the year..

RESULTS OF THE INTERPRETATION OF HCMM IMAGES APPLIED TO SOILS

José L. Labrandero

Instituto de Edafología y Biología Vegetal

FOREWORD

In the previuos report submitted to NASA, we participated in the HCMM project, by interpreting two images corresponding to October 28, 1978.
For this task, we used the ERMAN-II interactive system of the UAM-IBM Research Center at the Madrid Autonomous University (Universidad Autónoma de Madrid) .The principal objective was to evaluate the thermal data obtained by the Heat Capacity Mapping Mission from an edaphological point of view.
In this first stage, great difficulties arose in marking the soil physiographical units from HCMM images.We have to point out the scale limitations and the lack of information available from this new data source, when using HCMM for the study of soils.

The results could have been improved had we disposed of a greater number of better quality images distributed throughout the year.

HCMM IMAGES AVAILABLE

We received new images in order to go with our investigation.The different types of images used in the interpretation were the following:

HCMM Image	- Day visible
" "	- Day infrared
" "	- Night infrared
Color Composite	- of HCMM visible,day IR and Night IR
HCMM Image	- Day-night difference of temperature
" "	- Apparent Thermal Inertia

All the images belong to the same date: July 7, 1978.

We have photo-analyzed the different kinds of images with the principal objective of using the results as a complement to studies of lithological formations and soils in the eastern part of Spain.

Based on the HCMM images identified by the numbers 007213170 (day) and 007202230 (night), the National Geographical Institute (Instituto Geográfico Nacional) has elaborated different false color composite images at a 1: 2,000,000 scale.The images have been registered in the IBM Research Center of the Madrid Autonomous University.

INTERPRETATION METHOD

The method of research has been the same in the photo-interpretation of all the HCMM images.It is based on the differences in the tones of the image as a function of temperature or the apparent thermal inertia of the objects represented in the image.We delimitate the principal areas corresponding to specific soil formations and lithologies by means of differences in tones (from black to white), differences in the false color, and shades within the same tones of colors.

We have already indicated that the photographical products of the HCMM have been modified in order to obtain images to the scale of 1: 2,000,000. The information about the terrain has been taken from different thematic maps (soils, geology, orography, crops, land use, etc.), drawn to the same scale.We marked the mayor boundaries in both the HCMM photographs and the thematic maps, with the object of making comparisons and studying the relationship between similar areas.

ANALYSIS OF THE HCMM IMAGE - DAY VISIBLE (Fig.1)

The HCMM image - day visible- is taken between 0.5 and 1.1 microns, that is, it encompasses the visible zone and a portion of the near infrared of the electromagnetic spectrum.The surface phenomena observed are the expression of the total sum of the spectral responses integrated in the whole range.The main change observed in comparison with the Landsat images is the enlargement of the range and the consequent reduction from four bands to only one band.

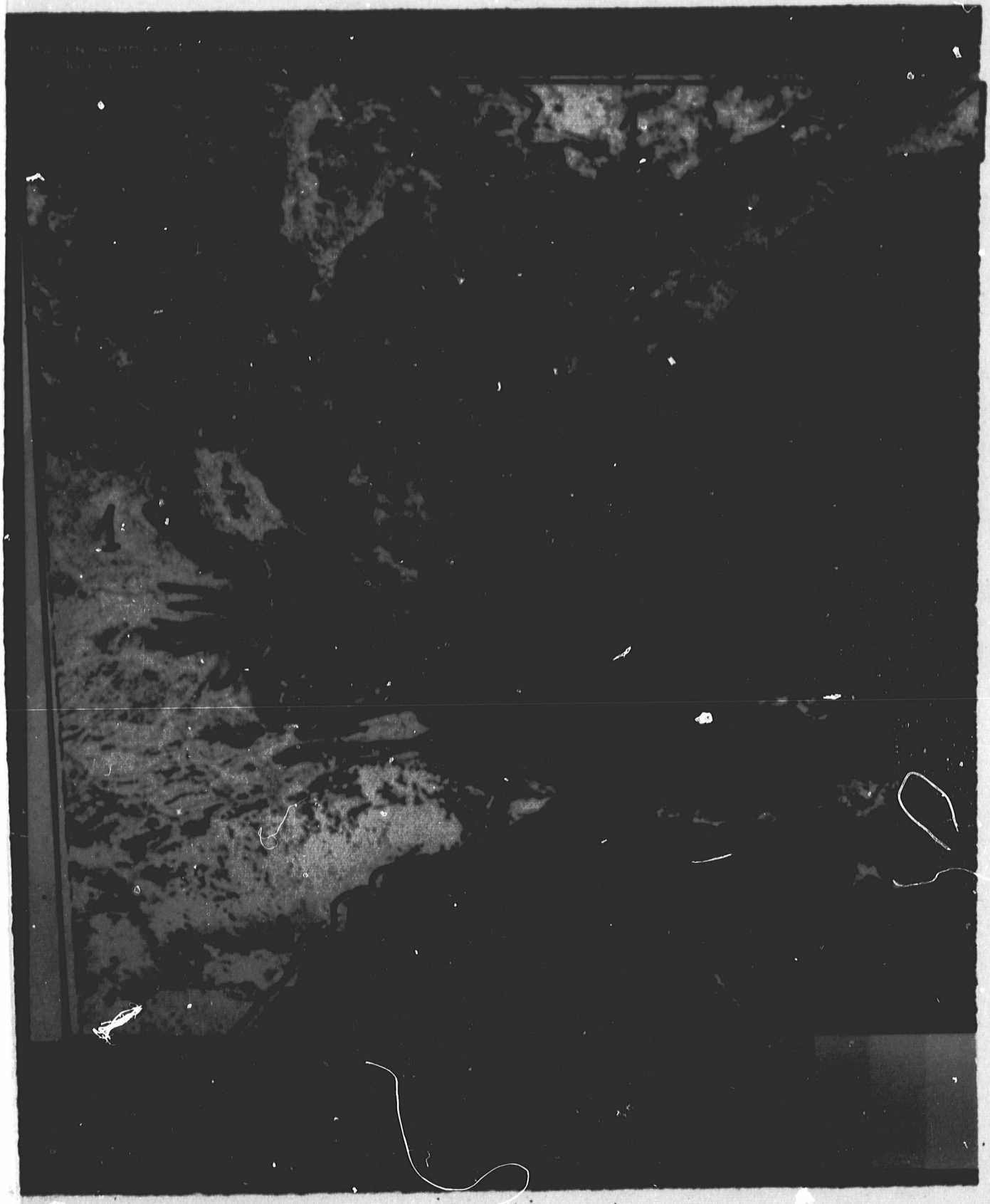

Fig. 1 Image 0072 - 13170 - 1 & overlay;
Visible-Day, 7-7-78

Generally, it is difficult to follow to their entirety the boundaries of the lithological formations and soils.We will point out the most important characteristics that could help us to evaluate the images from the geological point of view.

In the northern and western portions of figure 1 appear the lightest tones of the image. These tonalities correspond to continental marl formations alternating with sandstones and calcareous conglomerates (1).
Upon these sediments appear: soils of the Entisol and Ardisol orders in the depression of the Ebro River and soils of the Entisol and Ardisol orders in the La Mancha zone, between the provinces of Albacete and Cuenca.
The boundary or separation between this formation and the limestone formation alternating with marl and sandstone, (2) and (3), is very well defined and can be followed without much difficulty.

The Sierra de Albarracín (4) as well as the Sierra de Jalambre (5) and the Sierra de Grossa (6) show dark tonalities which correspond not only to the predominance of the lithological limestone with an abundance of soils of the Mollisol and Inceptisol orders, but rather to the relationship of these formations and the forest vegetation.In these mountains the marl and clay formations (7) that serve as original material for soils of the profile type A/ (B) / C stand out because of the contrast of their light tones.

Along the coastal Mediterranean strip, the alluvial deposits (8), the deposits permanently or temporarily covered with water (9) near the delta of the Ebro River, and the calcareous gravel bars (10) are well defined.
These formations serve as a support for the development of Entisol and Inceptisol type soils.

ANALYSIS OF THE HCMM IMAGE - DAY INFRARED (Fig.2)

The first remarkable fact of this infrared image is a better definition of the phenomena indicating the presence of water.Rivers, marshes and flooded areas stand out with very dark or black tones (since they correspond to cold areas) in the photograph of figure 2.

The precision of the boundaries that can be observed from the picture is only zonal, but these boundaries constitute the outline of the different lithological formations with which different soil units are associated.

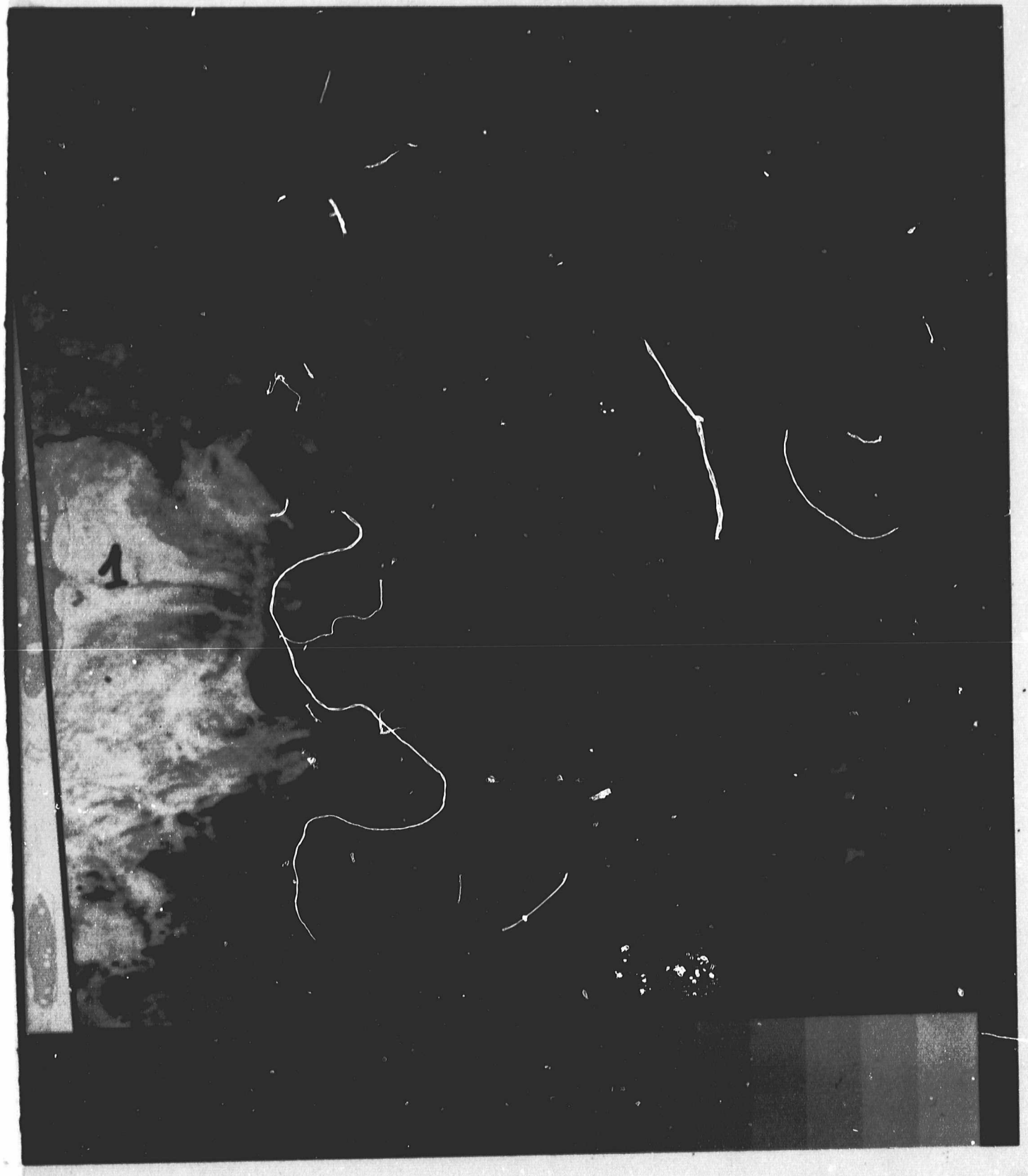

Fig.2 HCMM Image 0072 - 13170 - 2 & overlay;
IR-DAY, 7-7-78

The light tones (hotter during the day) basically correspond to calcareous gravel and continental marl formations.The dark areas of the photograph (colder ones) are related to the lithological formations of massive limestones sometimes alternating with sandstones.The medium tones mean areas where there is a predominance of marls associated with sandstones.

We shall define more concretely the interrelationship between the numbers of figure 2 and the lithological and edaphological formations.
The areas marked with (1) (very hot in the solar midday) show the lightest tones of the image and coincide with the existence of calcareous gravel and continental marls which are basic materials for the development of Inceptisol order soils.
The limestone formation alternating with marls and sandstones (2) exists in the so-called Sierra de Jabalambre where the dark tones stand out as a result of the low temperature and the existence of vegetal covering. Its tone is confused with that of other areas (3) whose dominant lithology is the massive limestone covered by Mollisol order soils, and with the lithology of the Sierra de Albarracín (4), basically surrounded by the same lithological formation.

The marl and clay formations present the same tone as the major part of the alluvial surfaces marked with the number 5, especially in those areas that are not covered by sheets of water.When the above mentioned occurs, the color of the photograph becomes black (6) because it corresponds to the deltaic deposits of River Ebro and to the zones reserved for the cultivation of rice.

Which are the significant coincidences observed between the visible and infrared images taken at noon? The limestone formations of the Sierra de Albarracín, Grossa and Jabalambre present similar features with dark and black tones.The same occurs with the calcareous gravels formations which show identical tones but closer to the white color.

In the visible image, the presence of forest vegetation darkens the corresponding area and in the day-infrared image it acts as an insulating element, preventing the temperature of the limestone to rise; wherever this vegetation is non-existent, areas of higher temperature are observed.

ANALYSIS OF THE HCMM IMAGE - NIGHT INFRARED (Fig.3)

The night infrared image clearly shows the existing distribution of temperature in terms of the altitude. There are three zones that can be perfectly differentiated with tones from light to dark, which mark the state of the temperatures of the soil and the rocks.The cooling of the earth crust as one moves from sea level to the peaks of the mountains is evident and is marked in the night-infrared image by three levels (fig.3 overlay)

The first level (1), which goes from the coastal line to the level curve indicating 1,000 meters in altitude is the hottest one; this is due to two factors:

1.- The direct influence of the sea as a smoother of the nocturnal temperature decrease, and

2.- Low elevation levels, ranging as stated before between 0 - 1,000 meters. In this first level some colder islands appear when the altitudes of the mountainous zones surpass 1,000 meters.

The second level (2) can be limited to those zones whose altitudes range between 1,000 and 1,500 meters above sea level. They correspond to the cold zones of Chinchilla and Ayora (both in the province of Albacete), part of the Serranía de Cuenca and foothills of the Gudar and Jabalambre Sierras.

The colder areas are restricted to the higher level (3), with an altitude of over 1,500 meters. These areas coincide with those of the Sierra de Albarracín, the central part of the Gudar and Jabalambre Sierras, and the summits.

It is suitable to remember that the picture was taken during summer (7/7/78), the year-time in which temperatures are pleasant in the whole territory included in the image.The variations in temperature in terms of altitude would be more apparent during winter. A night infrared image taken in winter would offer possibilities of outlining in a more precise way, the cold and hot zones.

Fig.3 HCMM Image 0072- 002230 - 3 & overlay;
Night-Infrared, July 7, 1978

ANALYSIS OF THE COLOR COMPOSITE DAY-IR / NIGHT IR (Fig.4.and pages 37 and 72)

The UAM-IBM Research Center has made the picture from two images: the day-infrared and the night-infrared.
We shall comment briefly the color composite of these two images.
In this image the information of two thermal images, taken at an interval of twelve hours is compiled.The result of this overlapping of information helps, in very specific cases, to outline areas which are not well defined in the original images when looked at separately.

Figure 4 corresponds to the interpretation of the color composite and in it the continental marls with clays and sandstones can be differentiated more clearly (1). The same can be said of the calcareous gravels (2), which clearly contrast with the massive limestone formations which alternate with marls of the alluvial materials (3) and of the deltaic sediments or of those covered with sheets of water (4).

The rest of the formations are more diffused and show shades ranging from red to green as a result of the overlapping of temperatures in a twelve hours interval.

ANALYSIS OF THE HCMM IMAGE. DAY-NIGHT TEMPERATURE DIFFERENCES (See fig.13. pg.51 and 72)

On interpreting this image, a general cooling tendency, going from the sea towards the center of the Peninsula, can be observed. It coincides with the change from the warm Mediterranean climate of the coast into the more harsh, dry and cold climate of the inland.The changes of tones which appear in the photograph range from dark tones (coast line) to light and even brilliant tones (interior of the Peninsula).

The hard and consolidated geological materials produce in the image lighter and brilliant tones as a logical result of their structure, porosity and minimum water content. The soils which cover these type of lithology do not modify the difference between day and night temperatures, since these are, generally speaking, of little depth so that they can hardly have an influence on the thermal behaviuor of the rocks.

Fig. 4. HCMM false color composite & overlay; Day IR/Night IR. July 7, 78 .

The limestone formations, predominantly cretaceous, constitute the principal lithological material of the coastal range of mountains; the soils developed in these formations serve as a support to the woodland which is quite predominant in these areas.The photograph shows little contrast in these zones indicating that the difference between day and night temperature is not very noticeable.This could be due mainly to the influence of the vegetation mass, which acts as a heat insulator.

The non-consolidated geological formations, i. e. those of a soft nature, generally appear in the picture with medium tones.The mosaic formed by light and dark tones is due to the association of non-consolidated ones (hard cretaceous limestone) with different types of soils.-
The vegetation mass implanted on them has also a great influence, which can't be forgotten.

In all the Quaternary formation which borders the coastal line, the soils are generally flooded for long periods of the year, during which rice is cultivated.Due to these rice cultivations, the day-night temperature of these zones is quite similar to that of the coast.

The cultivation of citrus fruits in this same coastal zone however, does not seem to have a clear influence on the tones of the photograph, which represents differences in day and night temperatures.

The different tones of the photography do not show the boundary between the consolidated cretaceous formations and the Quaternary, whose soils are intensively cultivated with irrigation systems.

The interaction between geological materials, vegetation and land use is probably the main reason for the absence of considerable variations in the difference of temperature.

A close relationship exists between the soils developed on limestone crust and difference in day and night temperature: these soils have a very small capacity for retaining water, therefore they can't regulate the changes of temperature.As a consequence we can observe higher brightness values or tones, which indicate a greater difference of temperature.

INTERPRETATION OF HCMM IMAGE-APPARENT THERMAL INERTIA (See fig. 15, pg.53 and 72)

On observating the image of apparent thermal inertia corresponding to July, 7, 1978, we have the impression that it identifies itself with the negative of the image which represents the day-night temperature differences of the same date.

The phenomena observed in the image of temperature differences can be observed in an analogous way but in an opposite sense.The existence of water swamps and lakes shows a very light tone in the image.The soils developed over a consolidated material (in our case, mainly limestone) appear with dark tones in the photograph and those soils developed over soft geological materials present lighter tones.

Is the image of thermal inertia indicative of specific phenomena? We must point out the scarce validity the information from this photograph has for this zone, which is geologically speaking, really complex; when reduced to a scale of about 1:2.000.000, it becomes even more complex.

We believe that the poor resolution is the main reason for this fault, or at least, for the difficulty of obtaining valid information applicable to the recognition of geological materials and soils.

FINAL CONCLUSIONS

In the eastern part of Spain, the soils are closely related to the rocks which constitute their original material.Due to this soil-rock relationship, the photo-interpretation of the HCMM images with edaphological objectives is also of a great geological use.

In HCMM images the drawing of boundaries between cartographical soil units can be performed only in very specific areas and even there, just partly; there are very few units whose outline can be drawn completely.
We have been able to outline without difficulty some soft and hard calcareous lithological formations, alluvia and permanently water-covered deposits over which develop soils that in the American taxonomy are included in the Entisol, Inceptisol, and Mollisol orders.

The geological materials which are best identified in the different types of analyzed HCMM images are the following:

- Calcareous gravel bars, Quaternary alluvium and hard limestone.

In the day-infrared image the course of rivers, marshy and swampy zones are clearly differentiated.The night-infrared image shows clearly three levels in relation to altitude and to land units of land (whether vegetation ot landscape).

A G R I C U L T U R E

G.- AGRICULTURE

- "Agricultural Report on the Photographic Images Provided by the HCMM Satellite".
  Fernando López de Sagredo
  Servicio de Fotogrametría y Fotointerpretación

REPORT ON THE PHOTOGRAPHICAL IMAGES PROVIDED BY THE HCMM SATELLITE

F. López de Sagredo
Servicio de Fotogrametría y Fotointerpretación
Universidad Politécnica
Madrid.

FOREWORD

We shall begin our report by giving a brief reminder of the inicial objectives, which were the following:

- Knowledge of surface temperatures of cultivated lands both with and without vegetation, comparing these temperatures with each other and also with those of forested and mountainous areas, both with and without vegetation .
- Study of modifying factors such as hidromorfism and also orientation and inclination of the soil surface.

Later on, a third objective was added to the above mentioned:

- To obtain any data about erosion, as it is closely related to vegetation, water content and soil temperature.

The studied area corresponds to the following sheets on the National Topographical Map: (1:50.000 scale): 668 (Sagunto), 722 (Valencia), 696 (Burjasot) and 747 (Sueca).

METHODOLOGY

The inicial data source consists of a series of black and white images of two bands: reflectance (0,55 to 1,1μm) and thermal infrared (10,5 to 12,5μm).These images were detailed on the Second Progress Report dated on December 1979.

In order to carry out the program as planned, we counted on the installation, on the field, of several data-gathering stations (Recording Thermometers).

These should have been installed in a series of determined locations according to the objectives: to obtain field data coinciding in time with the satellite's overpasses.
Regretfully, for reasons beyond our control, it was impossible to have these recording thermometers available; this caused a lack of basic information from the first moment on.

Our study has been carried out by comparing HCMM images with the thematic cartography this Fotogrammetry and Photographic Interpretation Service owns.

We have to point out that the previous studies performed by this Service proved the then existing cartography to be quite deficient.
This forced our Department to work out, on our own, an updated thematic cartography, which has been the basis of our comparisons.
It should be noted, however, that the area we have studied, shows enormous differences of soil occupation in short periods of time.

Later on, we thought of processing the images with a microdensitometer in order to determine zones with equal density.Thereby we tried to establish different areas and give them own denominations, according to their density.

In the end, a microdensitometer wasn't available either.
Recently, the possibility of handling information from digital processing of HCMM images was offered to us; at the time of writing we have not had yet the opportunity of doing so, though we place great hope on the use of this data.

CONCLUSIONS

The value of our conclusions is relative, as they have been conditioned by serious obstacles.

We have to admit that the results could have been very different had we had the opportunity of elaborating the information in a more tecnified way.

The conclusions which have been arrived at have both negative and positive aspects. Among the negative aspects, the most notable are the following:

- The lack of enough resolving power. The area shown in a pixel (600x600 m) includes in many cases a wide variety of croops, which means that it provides very poor information.

- The lack of periodically distributed images over time.- In many cases the sequence corresponding to one particular date was unavailable.

Due to these two points and to the lack of temperature data on the field at the time of the satellite's overpass, it was impossible to study temperature variations of soils and crops; consequently, the images just provide information about temperature gradients.

- We have to undeline that the atmospheric conditions over the zone have been particularly negative: in many images we can observe that tha presence of clouds hampers a clear view of the land.

- The relief obscures a great deal of information: the particular topographical configuration of the area is responsible for a temperature gradient which is directly related to altitude.

- Generally speaking, the thematic cartography referred to this area, owned by the Fotogtammetry and Photointerpretation Service is quite complete and its information apparently superior to that derived from HCMM images.

As positive aspects we have to point out the following:

- Information provided by HCMM is very general and therefore quite useful when large areas are under study.

For example, in the case of the studied area, which extends from Castellón to the Cape of San Antonio, one can clearly distinguish the spots that represent rice fields from those that indicate the cultivation of citric fruits and irrigated lands.

On the other hand, it is not easy to differentiate the limits be-between the cultivation of citric fruits from that of irrigated lands. In many cases this is due to the sensor's lack of resolution, as the density of cultivation in the area is very high.

- We have to point out another positive aspect, even if it lies beyond our objectives: We observed the possibility of locating, in the sea, sources of water, different in temperature from that of the sea, mainly near the coast.

- The night-infrared thermal images show water accumulations, such as dams, and free water courses.

- The day-infrared thermal images reveal most accurately the borders between non-irrigated and irrigated cultivations, in regions of low atmospheric humidity. This can be observed in the image of irrigated zones of Lérida and the Vega del Ebro, dated on July, 7 1978, which falls within the stated objectives in spite of lying outside the study area.

FINAL CONCLUSIONS

We believe HCMM photographic images to be of great value, specially if we apply the information they contain to large areas.
This information would be of particular interest if computer-aided analysis techniques were available.

We also believe that the study, in determined areas, of seasonal variations in the temperature of vegetation and soils, is quite promising. Therefore it would be necessary to employ an adequate methodology and technology (i.e. digital analysis, densitometry, etc.), in order to establish a relationship between these seasonal variations (of vegetation and soils) and productivity in general, so that we could consider the possibility of establishing harvest predictions.

Finally, we shall underline that we would like to continue our research in these fields, using the available materials and trying to employ the equipment which regretfully was not available for the present work.

HYDROLOGY

H .- HYDROLOGY

- "Application of the HCMM Satellite Data to the Study of the Subterranean Water Discharges on the Mediterranean Sea"
  (Reproduced from the First Progress Report)
  Jesús Paredes
  Centro de Estudios Hidrográficos

THE APPLICATION OF THE HCMM SATELLITE DATA TO THE STUDY OF THE SUBTERRANEAN WATER DISCHARGES IN THE MEDITERRANEAN SEA.

Jesús Paredes
Centro de Estudios Hidrográficos
M.O.P.U.

INTRODUCTION

In the tecnical proposal of HCMM investigation 034, "Thermal Mapping, Geothermal Source Location, Natural Effluents and Plant Stress in the Mediterranean Coast of Spain" dated September, 1, 1975, the collaboration of the Hidrographic Study Center in point number 3, was settled.

Until July 1979, this Center didn't receive any information from the HCMM satellite that would permit studying its usefulness to the proposed plan.From this date and from the available images, the following have been selected:

0184-12590-3	Night	IR	- 22 Oct. 78	(see pg.151)
190-13090-1	Day	IR	- 2 Nov. 78	(Figure 1)
190-13090-2	Day	VIS	- 2 Nov.78	(Figures 2 and 3)

These images include the Spanish Western Coast (figure 4) with its coast line free of clouds, from which we were able to study the tonality variations of the coast waters.

IMAGE ANALYSIS

The images have been analyzed on 37 x 39 cm. positive copies (1: 2.000.000 scale) and from the analysis of three of them, the following considerations have been made:

1) In the A0184-12590-3 and 190-13090-2 images,the thermal anomalies in the Rosas Gulf can be clearly seen, in which water appears darker inside the Gulf.This may be caused by marine currents.

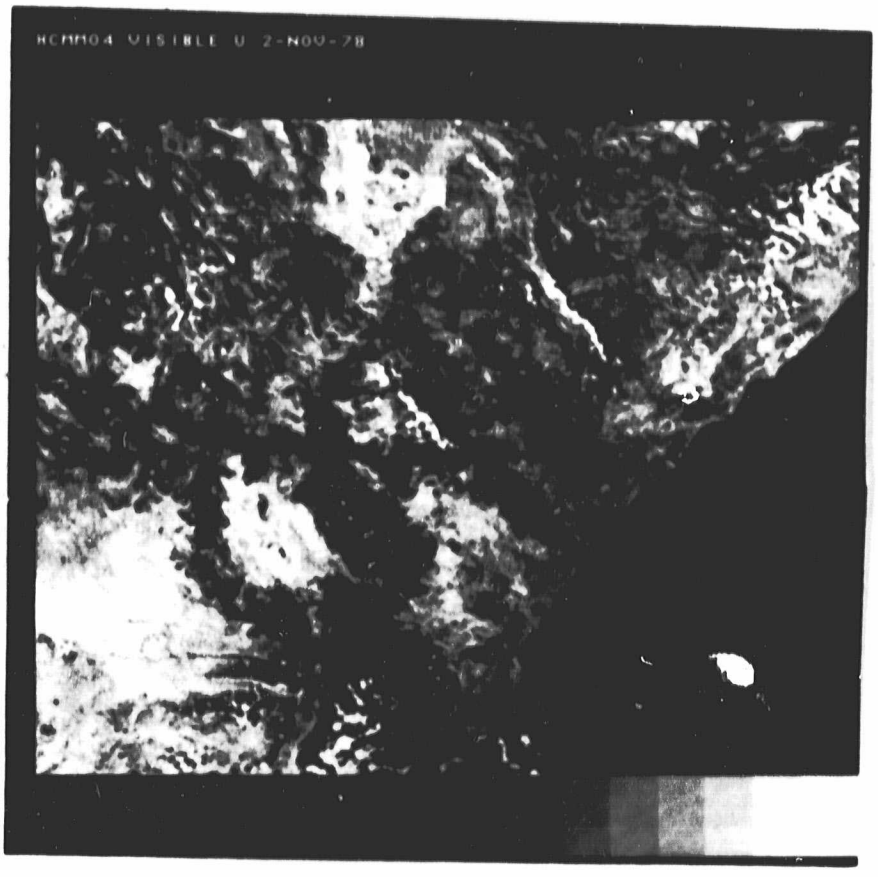

Fig. 1 Digitally (uniform) enhanced subscene, from image 190-13090-1 (area of Valencia)

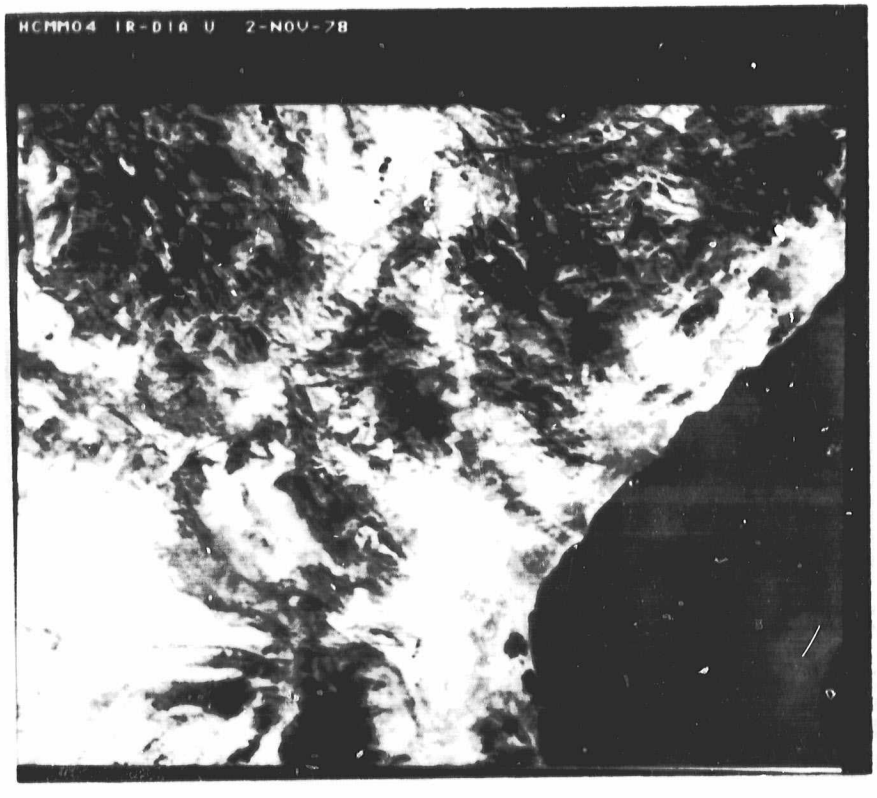

Fig. 2 Digitally (uniform) enhanced subscene from image 190-13090-2

Fig. 3
Original Day IR image A0190-13090-2, photographically enhanced

ORIGINAL PAGE
BLACK AND WHITE PHOTOGRAPH

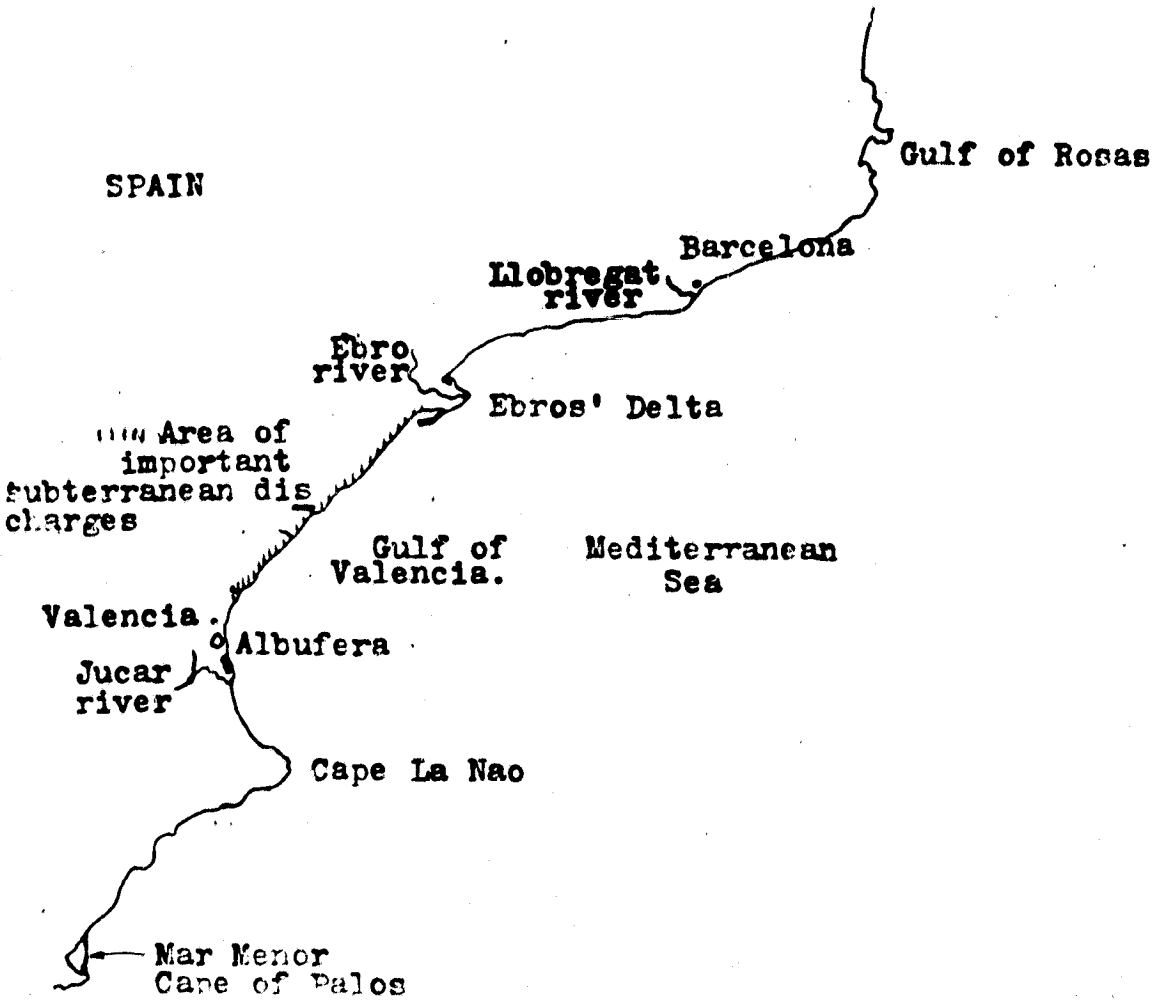

Figure 4 Geographic Location overlay
(scale 1/4.000.000)

2) A slightly dark tonality is appreciated on the zones where the Llobregat (near Barcelona), the Ebro (in the delta) and the Júcar rivers flow into the sea. This allows us to affirm that the river temperatures were inferior to those of the sea, at the moment the images were gathered.

3) The anomalies observed on the South of Cape Nao, image 184-12590-3, seems to be only the rush of two marine currents.

4) None of these images allows us to identify the anomalies in the coastal points where there are the most important submarine discharges (in the coast from Vinaroz to Benicasim and from Burriana to Sagunto).
In some zones a slightly darker tonality can be seen, but the ground resolution of the HCMM sensor does not allow us to assume that these anomalies are the result of the discharges, because they are punctual and have a discharge of only several hundred liters per second of water.

5) On the original 190-13090-1 image (visible) the water is completely black and it is not possible to see any anomaly.

CONCLUSIONS

The image scale and the resolution of the HCMM detector are inadequate for the study of subterranean discharges into the sea in the test area.

Nevertheless it can be expected that with an enhacement of some partial zones, we may obtain better results in their analysis.

C-3

PATTERN RECOGNITION

I.- PATTERN RECOGNITION

- "Numerical Analysis of HCMM Data"
  (Reproduced from the Second Progress Report)
  Ramón Bermúdez de Castro
  Instituto Geográfico Nacional (under contract)

NUMERICAL ANALYSIS OF HCMM DATA *

Ramón Bermúdez de Castro * *
Sección de Teledetección
I.G.N.

INTRODUCTION

Radiometric enhacement of HCMM images leads to acceptable results when trying to perform a visual analysis of that imagery but, because of the presence of a band containing information in the thermal infrared portion of the spectrum and due to the poor experience in the interpretation of such information, it was considered convenient to perform the analysis in a numerical way.

Pattern recognition tecniques applied to the bidimensional data space, will enable us to obtain natural grouping of pixels (classes), each class represented by a statistical distribution defined by certain parameters (mean and covariance matrix).

* * Work performed under contract with Instituto Geográfico Nacional, Madrid.

* REPRODUCED FROM HCM-034 SECOND PROGRESS REPORT

DESCRIPTION OF THE WORK

The present work was performed using ERMAN-II image processing system at UAM-IBM Scientific Center.

In order to perform a numerical analysis of the data set, it was considered convenient to obtain scatter diagrams of these data for the study areas as it is shown in figure (1). These diagrams give a priori knowledge of every possible distribution of interest within the selected area.

A further application of a cluster algorithm to the area enables us to observe the distribution of the different spectral classes in the bidimensional data space.A first inspection of the data shows several highly populated areas that will correspond to a particular natural phenomena present at the scene.

At the same time it was considered interesting to know the spectral characteristics of certain natural features as clouds and haze and their possible influence on image analysis.Several fields within the selected images were chosen, all of them associated with known natural features. Among them, clouds and haze have been chosen as being representative fields in this kind of data.

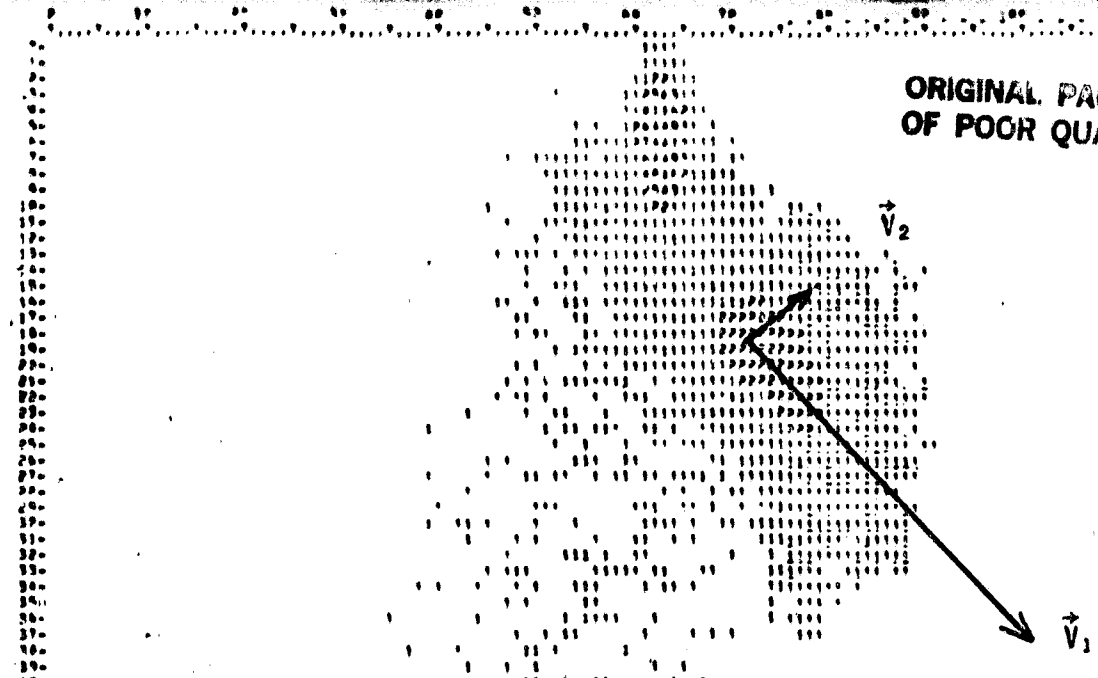

Correlation matrix

1.0000

0.7825 1.0000

$\vec{V}_1$ = first principal component

$\vec{V}_2$ = second principal component

Character				
1	0	-	100	pixels
2	101	-	200	"
3	201	-	300	"
4	301	-	400	"
5	401	-	500	"
6	501	-	600	"
7	601	-	700	"
8	701	-	800	"
9	801	-	900	"
:	901	-	1000	"
A	1000	-	2000	"

Fig. 1.- Scatter diagram of study area (located between lines 700 to 923, and pixels 899 to 1094 of image A 0190-13090).

FIELD 1 : WATER

As shown in photograph 1 (Image A0036-13440), this field contains a portion of Mediterranean Sea located on the south east of Spain. By looking at the histograms of this field (visible band) two maximums were observed, both of them with low reflectance; the one with the highest population has a minimum response.It can be deduced that there are two different spectral classes both of them with low spectral response.Analysis of the distribution of statistical parameters (μ,σ) reveals a high standard deviation in the visible band.

IR band histogram is unimodal with medium response.Statistical parameters show a normal distribution with a small standard deviation, though, it is higher than that of zones without haze.From the observation of both bands one can deduce the high probability of coexistence of water and low haze with approximately the same temperature.

Every characteristic formerly described is reasonable when considering the semi-transparency of thin clouds and haze.When either thin clouds or haze are located above the water, mean and standard deviation of the distribution increases their value in the visible portion of the spectrum, with regard to water.This increment in the statistical parameters is lower in the IR because of the low altitude of haze (in this particular case),that forces the temperature to be similar to that of water (see Fig.3).

FIELD 2: CLOUDS

Within the same image (A0036-3.40, photography 1) a group of clouds named ANUBIS has been selected.Histograms are shown in figure (2).

In the visible band, these distributions show high values in both mean and standard deviation.It is reasonable to think that the visible sensor is not saturated by upwelling radiation coming from these clouds.

In the infrared band, radiation arriving to the sensor is a function of the temperature of cloud's upper layers, as this temperature is a function of the cloud's altitude.Summarizing, clouds will be easily identifiable, spectrally speaking, by the following characteristics:

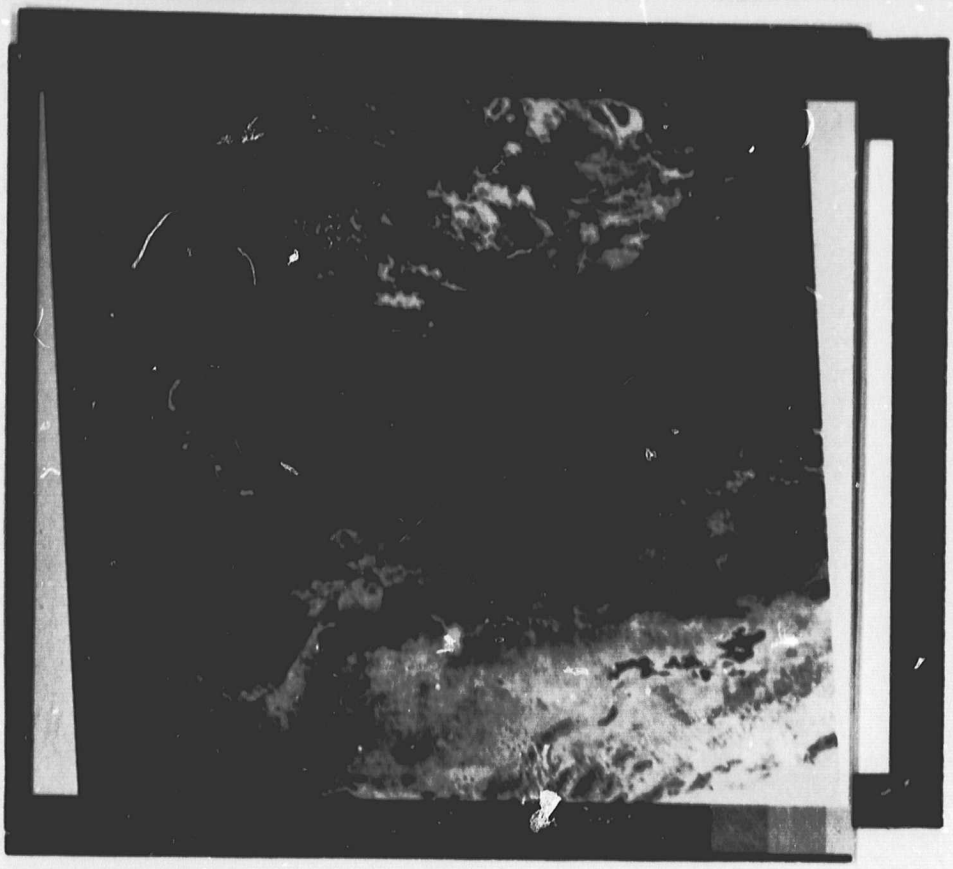

Photograph 1: visible band of image A0036-13440. ANUBIS and CAMP1 belong to this image.

ORIGINAL PAGE
BLACK AND WHITE PHOTOGRAPH

Photograph 2: color composite of the study area (located between lines 700 to 923, and pixels 899 to 1094 of image A0190-13090).(Visible green, IR red).

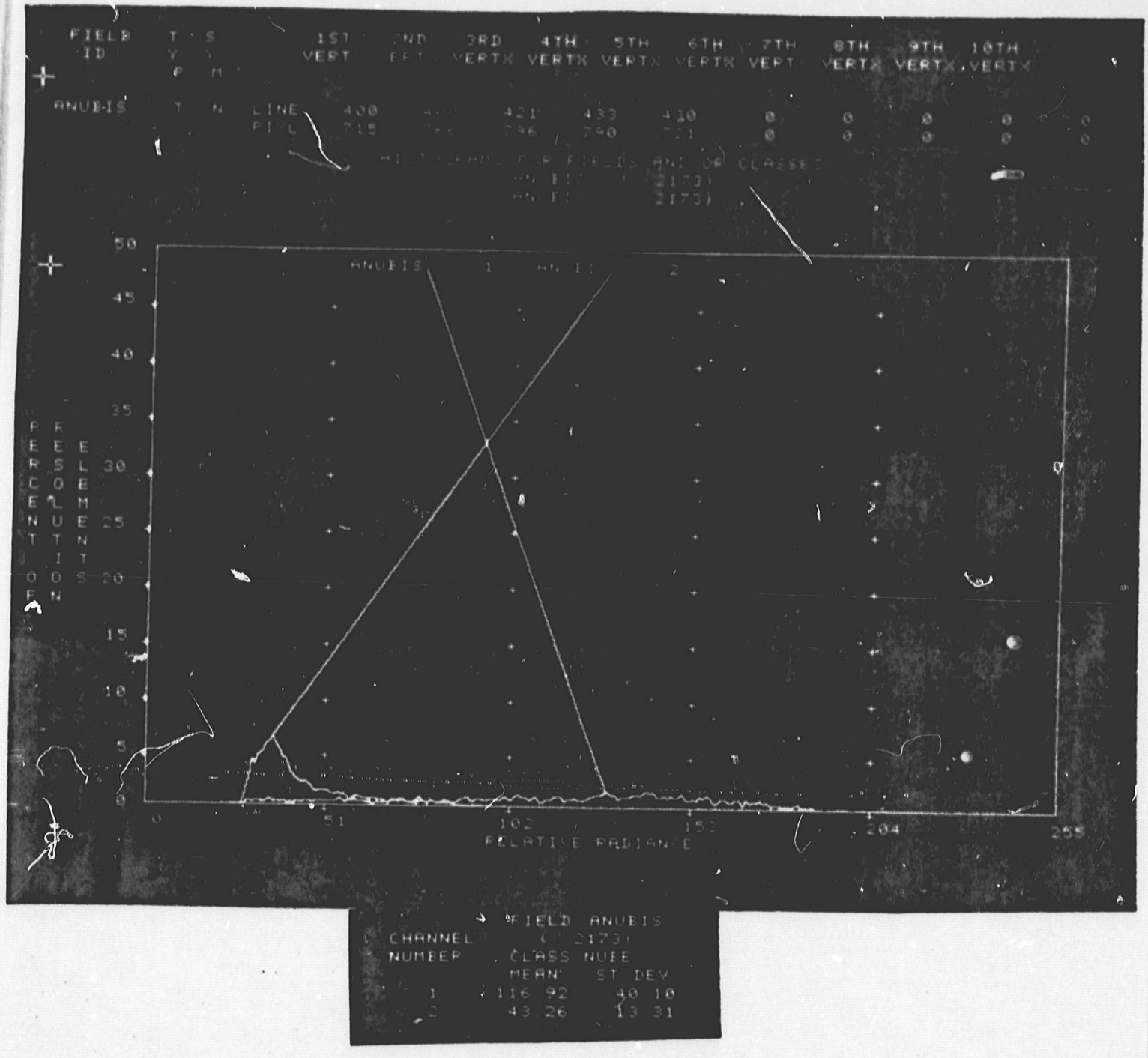

FIG.2: LOCATION, HISTOGRAMS AND STATISTICAL PARAMETERS OF ANUBIS.

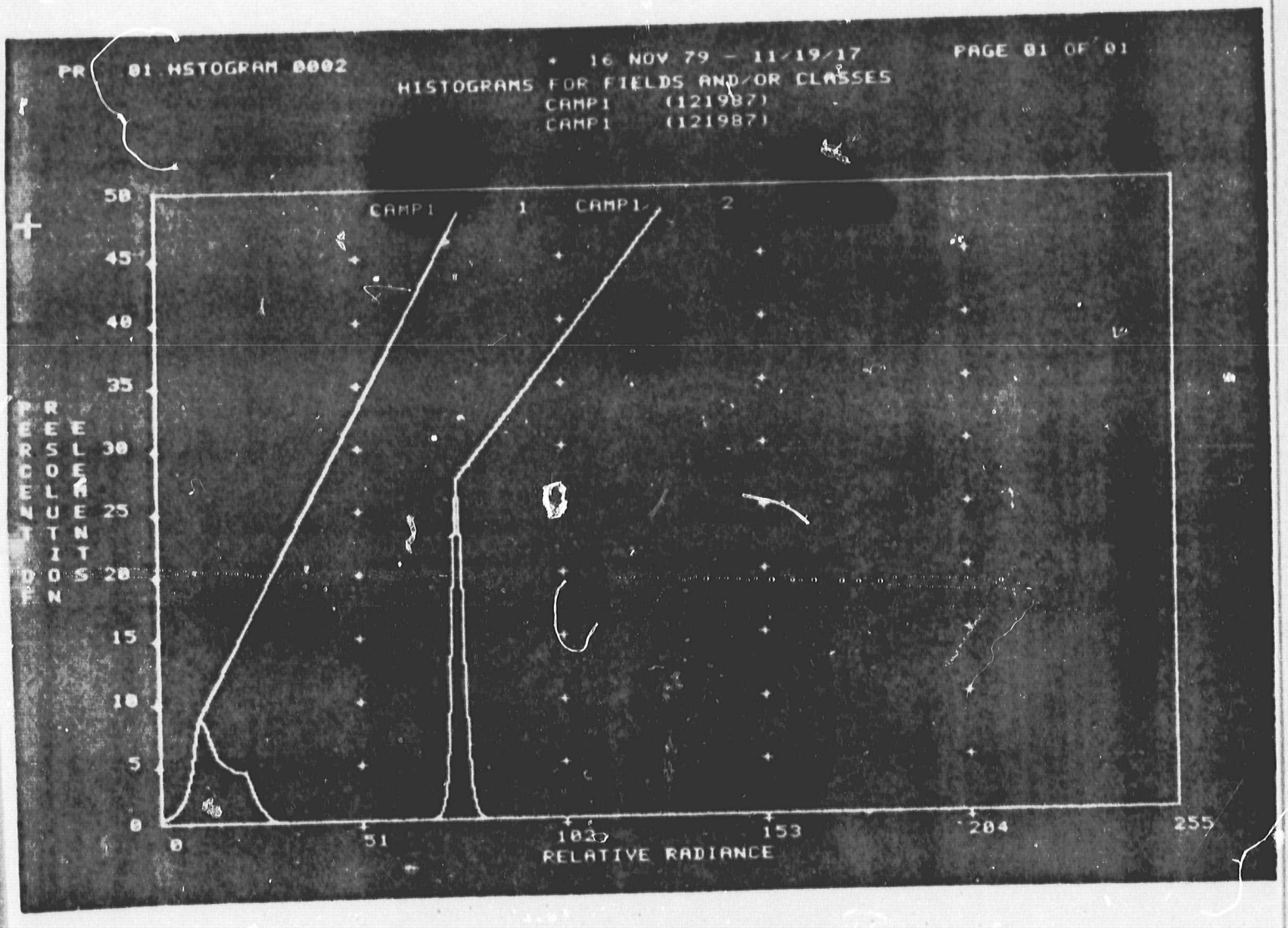

CHANNEL NUMBER	FIELD CAMP1 (121987) CLASS AGUA MEAN	ST DEV
1	14 02	5 77
2	74 97	1 63

Fig. 3: Location, histograms and statistical parameters of CAMP 1.

a) Mean value is generally low in the IR and high in the visible.

b) High standard deviation in both bands.

c) The correlation coefficients between bands is negative.

The former conclusions are shown in figures 2, 4 & 5.

Summarizing again, clouds characteristics can negatively affect radiommetric corrections of images because of the broadness of cloud histograms. These histograms occupy a very broad region within the dinamic range of an image.

CLUSTER ANALYSIS

For the purpose of this task, a clustering algorithm contained in the ERMAN-II image processing package was used. This algorithm is a modification from the ISODATA of Ball and Hall (1967). The algorithm is governed by two routines termed "SPLIT" and "COMBINE".

The routine "SPLIT" divides every class with standard deviation higher than a threshold "SDMAX" (specified by the user) in any channel.

The routine "COMBINE" merges two classes if their distance is lower than a threshold also specified by the user.

Two different approaches were followed in order to initialize the cluster centers.

In the first way the overall distribution that represents the zone to cluster is considered as an initial class. This class is successively split in further interactions, by means of the "SPLIT" routine, up to a specified maximum number of clusters.

Because of the large number of parameters that the user has to specify and considering the reduced knowledge of these parameters in this kind of data, a second option has been taken. This option minimizes the influence of these parameters.

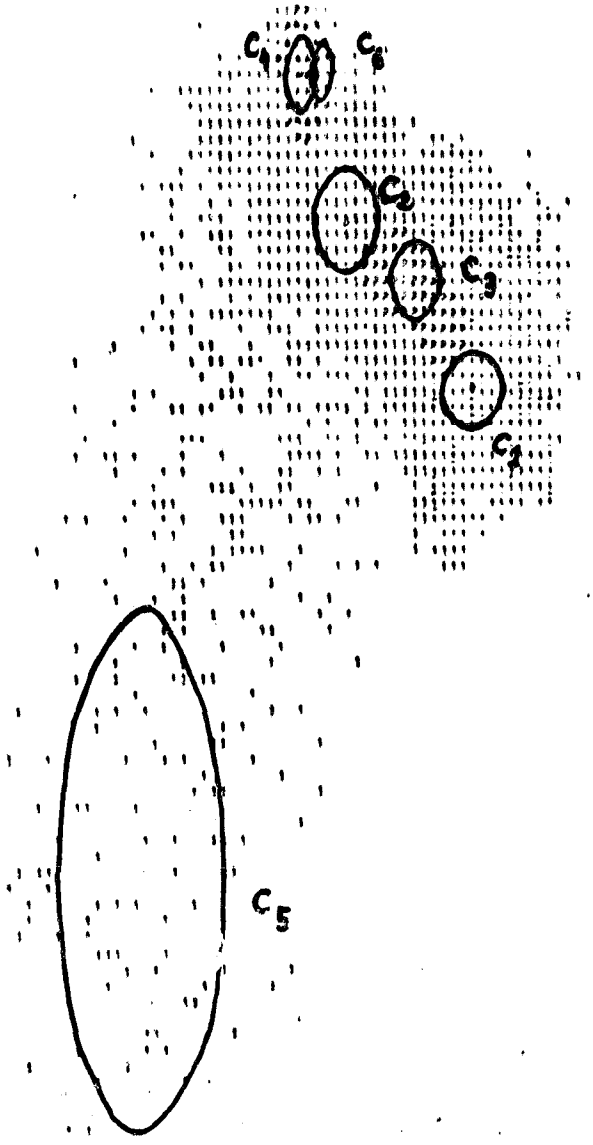

Fig. 4: Cluster centers obtained in photograph 3.
class 5 represents clouds.

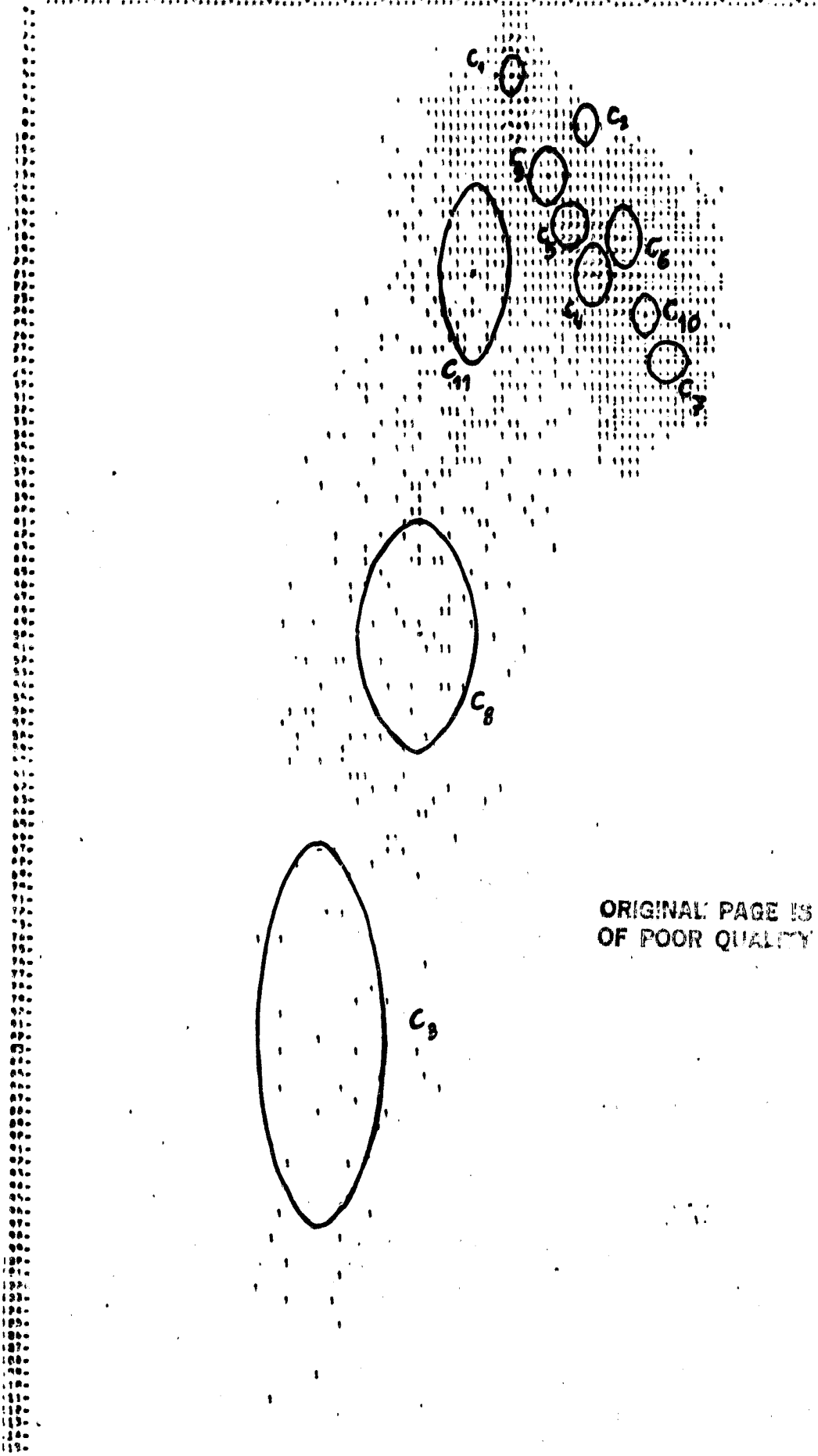

Fig. 5: Cluster centers obtained in photograph 4.

Classes 8, 3 represents clouds.

In this second method, initial cluster centers are fixed in number to the maximum number of cluster specified to the clustering algorithm; with this option, an inhibition of the "SPLIT" routine is expected.

The initial cluster centers are chosen to be uniformly distributed along the diagonal of the rectangle with coordinates $\mu \pm \sigma$ on each axis. This diagonal matchs approximately the principal component of the distribution. The diagonal will be fixed by the distribution of the data in the sampling space as shown by the scatter diagram (figure 3).

Further interactions perform a migration of the cluster centers until an estabilization in cluster evolution is reached. "COMBINE" routine has been used in both cases.

RESULTS

The clustering algorithm has been applied to several areas located in several images.

Some of the results are shown in figures 4 through 7. Tables showing mean and standard deviation for each channel are shown for the resulting classes.

BIBLIOGRAPHY

- ERMAN II USER"S GUIDE. IBM Federal Systems Division, HOUSTON, TEXAS.
- ARTHUR G. WACKER. "A cluster approach to finding spactral boundaries in multispectral images". LARS information note 122969, Purdue University. WEST LAFAYETTE, IN.
- "Remote Sensing, the cuantitative approach". P.H. SWAIN, S.M. DAVIS (LARS, Purdue University). 1978 Mc Graw-Hill, Inc.
- BALL, G.M. and D.J. HALL. "A clustering technique for summarizing multivariate data". Behavioral Science, 12, 153-155 (March 1967).

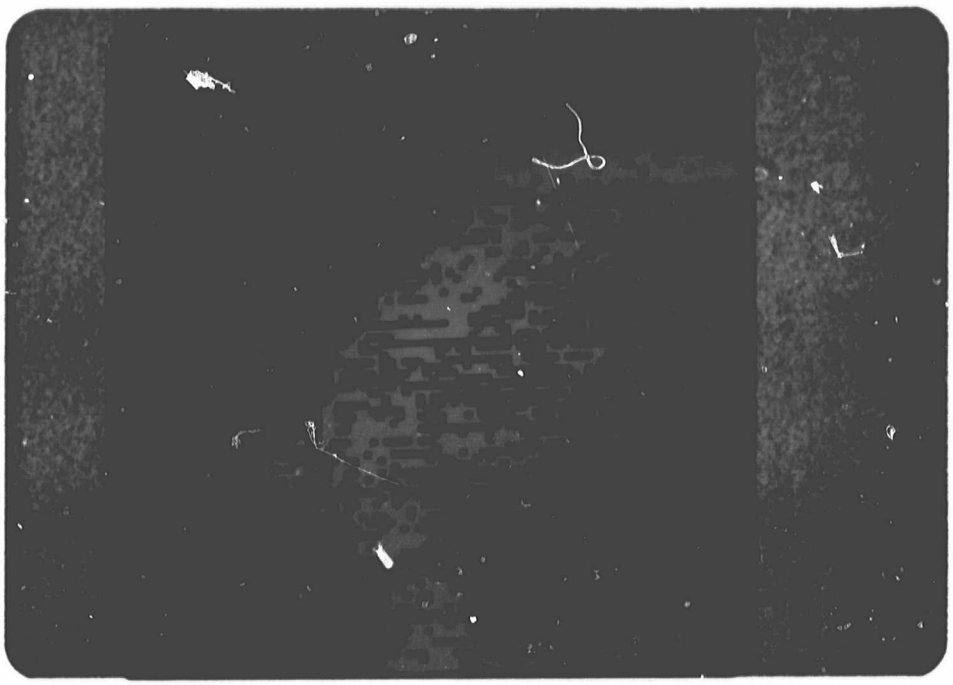

Photograph 3: Cluster map of the study area obtained with "seli generating vectors" option and maximum number of clusters = 12.

Fig. 6: Mean and standard deviation of six classes represented in photograph 3.

	CHANNEL 1		CHANNEL 2		COLOR
	μ	σ	μ	σ	
CLASS 1	24.83	2.69	79.79	3.06	BLUE
CLASS 2	15.76	3.06	67.10	3.28	GREEN
CLASS 3	19.15	2.30	74.07	2.77	MAGENTA
CLASS 4	5.98	1.95	62.15	1.05	RED
CLASS 5	56.84	18.21	46.40	9.04	CYAN
CLASS 6	5.88	1.78	64.20	0.75	YELLOW

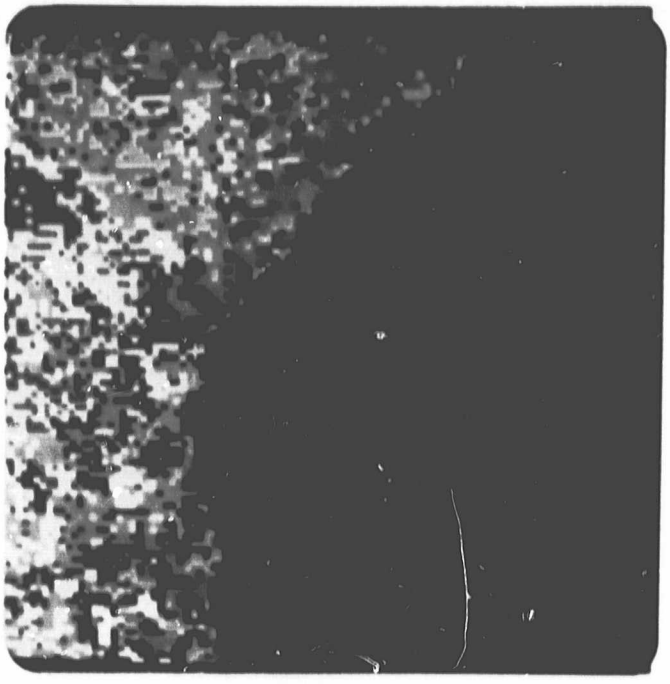

Photograph 4: Cluster map of the study area obtained with "external vectors" option, skip factor = 2 and maximum number of clusters = 15

Photograph 5: Classification map of the study area using maximum likelyhood classifier. Same classes as in photograph 4.

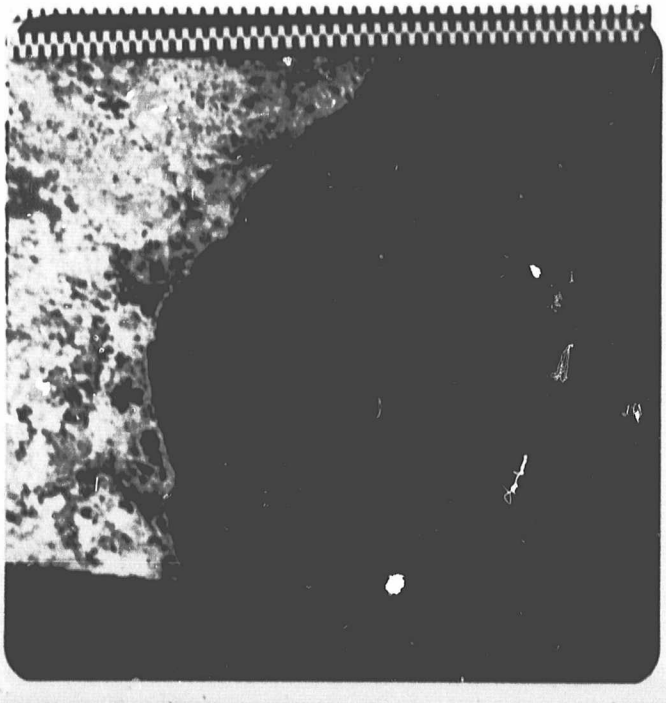

Fig. 7. Mean and standard deviation of eleven classes represented in photograph 4.

	CHANNEL 1		CHANNEL 2		COLOR	TYPE
	μ	σ	μ	σ		
CLASS 1	5.28	1.43	62.76	1.22	BLACK	WATER
CLASS 2	8.78	1.42	62.47	1.59	BLACK	WATER
CLASS 3	82.17	15.30	36.83	8.23	WHITE	CLOUDS
CLASS 4	21.59	1.86	73.43	2.05	BLUE	NI (1)
CLASS 5	17.31	1.64	70.35	2.30	GREEN	NI
CLASS 6	18.43	1.98	77.22	2.12	CYAN	NI
CLASS 7	27.87	1.64	82.65	2.40	RED	FOREST
CLASS 8	50.00	8.90	49.67	7.89	WHITE	CLOUDS
CLASS 9	13.43	1.80	67.06	2.55	MAGENTA	VEGETATION
CLASS 10	23.80	1.70	79.24	2.12	YELLOW	NI
CLASS 11	20.80	6.64	56.49	4.08	WHITE	CLOUDS

(1) NOT IDENTIFIED.

EXECUTIVE SUMMARY

HCM-034 "THERMAL MAPPING, GEOTHERMAL SOURCE LOCATION, NATURAL EFFLUENTS AND PLANT STRESS IN THE MEDITERRANEAN COAST OF SPAIN".-

This has been the Final Report of NASA Investigation HCM-034, "Thermal Mapping, Geothermal Source Location, Natural Effluents and Plant Stress in the Mediterranean Coast of Spain", performed for NASA/Goddard Space Flight Center.Heretofore, the joint work of different groups of investigators has been presented.

The objective of this work has been to evaluate the suitability of HCMM data for obtaining information on several relevant areas.
In order to do this, HCMM data from the test area (S.E. Spain), have been geometrically processed to match a geographical grid of reference, thus making possible its overlay, as well as with other available data; they have been radiometrically corrected and enhanced, making it possible to have almost absolute values for albedo and temperature on one hand, and to increase their interpretability on the other.HCMM data have also been compared to ancillary information and ground-truth data.We found similarities and differences and we attempted to find an explanation for the latter.
We tried to obtain as much information as possible from HCMM data and then we compared it to the existing data.

Research areas and main findings are summarized below:

- Data Management: The delays in the distribution of the data, which in some cases amounted to 1.5 years, as well as the irregularities in the shipping of the data, placed severe constraints on the investigators, forcing them to change the original project and consequently its planning.

  Of the end products delivered by NASA's Image Processing Facility, namely Thermal Inertia and Differences of Temperatures digital data, only one set, corresponding to one single date, was received in time.

- Image Analysis: The influence of natural effects (meteorological, atmospheric transmittance, topographical, shadows, altitude,...) as well as those caused by HCMM (Dynamic range, effective NE T and NE , transmission and quantification of the data, noise,.....) was evaluated.
  A statistical analysis of the best HCMM image received was performed, transforming it to its principal components, with an increase in the discrimination power of the data.

- Image Preprocessing: Registration procedures have been developed, which allow one to superimpose day and night images taken on the same or different dates.HCMM images have been registered to Landsat ones.

- Image Processing: Several digital enhancement techniques have been applied to HCMM data, delivering the processed images to the coinvestigators for their evaluation.A simple procedure for reducing the noise present in the images has been implemented.Differences of temperature and Apparent Thermal Inertia images over the test area were produced, starting from the registered HCMM images delivered by the UAM-IBM Scientific Center.

- Oceanography: A qualitative comparison has been made between HCMM thermal data and oceanographic measurements on the Alboran Sea (W.Mediterranean), mainly on its anticyclonic gyre.A strong resemblance was found, that suggests the high potential of satellite data in oceanographic studies.
  Another area of extreme interest, because of its strong dynamics, as shown in HCMM summer imagery, is the Balearic Islands, near to the Sardinia Stripe (see image A0081-01510-3).

- Geology: Although the test area was not very adequate, given its complex geological structure, an evaluation of the images and a geologic interpretation was performed on most of them.Day-visible images were found to be of limited value, especially when compared to Landsat.Day-IR allows the discrimination of different vegetated covers.
  Summer and Fall Night IR images provide most information from a geological point of view. New interesting findings are:

  1) A better demarcation of the main continental tertiary basins in Spain (Duero, Ebro and Tajo Rivers),ending the dispute concerning demarcation by fractures.

  2) A good perspective of the megastructures that affect the Iberian Peninsula has been achieved, giving us a deeper insight of their importance.

  3) The edges of the hercynian megafolds of the Toledo Mountains were traced without discontinuities.

  4) A suggested earlier course of the Ebro river appears well differentiated. No geothermal anomalies nor hot springs, which exist in the test area, could be located, possibly because of their small size, and the high temperatures and strong relief of the area.

- Edaphology: In the test area, soils are closely related to the rocks that constitute their original material.The outline of definite soil units on HCMM images has been possible only in part.
Differentiable soil units in the area correspond to soft and hard calcareous formations and to the alluvia and waterlogged sedimentary deposits. Best identified geological materials are calcareous gravel bars, quaternary alluvia and limestone.

Day IR enables us to differentiate rivers, marshy and swampy zones. Night IR masks altitude and large land-use units.Day-IR temperature differences were only useful to discriminate between soils on crusty limestone. Tha available thermal inertia image appeared to be very similar in value to that of temperature differences.

The complex geology and land use pattern of the test area, given the HCMM resolution, hurt the analysis.

- Agriculture: Rice fields could be discriminated from irrigated land and orchards, while these two latter areas could not be differentiated.
Day IR imagery marks clearly the border between irrigated and non-irrigated areas; water shows up very well at night.The main problems were the low resolution of the sensor, lack of image sequences, strong atmospheric and topographical effects in the area.The analysis of seasonal variations is the most promising methodology.

- Hydrology: Given the resolution (both spectral and spacial) of HCMM data and the characteristics of the submarine discharges in the area, it was impossible to detect any anomaly of submarine origin.
The mixture of water between that of the most important rivers and sea water is very interesting in HCMM thermal images: In the Delta of the Ebro River, the zone of mixture of both surface and subfluvial waters of the river with the Meditarranean Sea, can be clearly observed, as well as its dynamic.Zones of surgency are visible specially in the southern part of the delta.

- Pattern Recognition: After an analysis of the HCMM data by means of histograms, scatter plots and statistics, a clustering algorithm based on ISODATA was applied. Water, clouds and haze are clearly distinguishable. Land areas form a huge cluster, and although it is easy to differentiate forest, irrigated areas and barren land, highly populated mixture classes appear.

Clustering of the principal components gives somewhat better results, though there is not a great difference.The low discrimination power of the HCMM data is partly due to the causes presented under "Image Analysis".

- Land Use: The characteristics of the HCMM and those of the test area, forced us to reject "a priori" these kind of studies in the present project.-

Having at sight the data delivered by NASA, the techniques developped and the results achieved, it's now when we can begin a serious work, based on the selection and adequate processing of the data,on the applicability of HCMM data to the obtention of information on the subjects we have mentioned, with guarantees of success and completion in time.

From tha aforesaid, we think the present research project has fulfilled its principal objective; to evaluate the real interest of the HCMM data in a well studied zone whose characteristics are critical in relation to tha data.

Antonio Martínez de Aragón

HCM-034 Coordinator

INDEX

"THERMAL MAPPING, GEOTHERMAL SOURCE LOCATION, NATURAL EFFLUENTS AND PLANT STRESS IN THE MEDITERRANEAN COAST OF SPAIN" .

FINAL REPORT

INDEX